tified as ca. 99% unreacted DEM-3 dimer by ^{1}H NMR (vide supra). The components of the aqueous phase were identified by ^{1}H NMR as paraquat (δ 4.35 (s, 3 H), 8.37 (d, J = 7, 2 H), 8.90 (d, J = 7, 2 H)) and 2-(ethylamino)-2-methylpropanol hydrochloride (spectrum identical to that described above). Integrals of the NMR signals for paraquat and the amino alcohol indicated a 2.5% conversion of DEM-3 dimer to the amino alcohol.

B. Buffered Methanol Medium. The reaction was performed in pH 7, Tris-buffered methanol. This time the reaction mixture turned dark blue. Again, the residue from solvent evaporation was extracted into 1 mL of D_2O and 1 mL of $CDCl_3$. The components of the organic phase were identified by ^{1}H NMR as DEM-3 dimer and 2-(ethylamino)-2-methylpropanol (δ 1.06 (s, 6 H), 1.07 (t, J = 7.2, 3 H), 2.44 (q, J = 7.2, 2 H), 3.33 (s, 2 H)). The components of the aqueous phase were identified as paraquat and a small amount of 2-(ethylamino)-2-methylpropanol hydrochloride, also from the ^{1}H NMR spectrum. Integrals of the NMR signals indicated a 41% conversion of DEM-3 dimer to amino alcohol.

Attempted Reduction of Daunomycin with DEM-3 Dimer. The reaction vessel was a 9 mm × 20 cm Pyrex tube equipped with a 2.5-cm side arm. The side arm was charged with 2.65×10^{-6} mol of DEM-3 dimer dissolved in methylene chloride, and the methylene chloride was evaporated with a stream of nitrogen. The main tube was charged with 2 mL of 2×10^{-3} M 1:1 Tris/Tris·HCl buffered methanol containing 2.66×10^{-6} mol of daunomycin. The methanol solution was freeze-thaw-degassed, and the tube was sealed with a torch. After mixing the reagents, the solution was heated at 36 °C for 18 h. C-18 reverse-phase HPLC analysis as described earlier[35] showed no formation of 7-deoxydaunomycinone.

Acknowledgment. The authors thank Edward King for assistance with the kinetic analysis of approach to equilibrium and many helpful suggestions. Giorgio Gaudiano for critical reading of the manuscript, and A. R. Ravishankara for use of his copy of the numerical integration program FACSIMILE. The authors also thank Chan Sangsurasak for the measurement of the *meso/dl* ratio for TM-3 dimer in methanol-d_4. Financial support from the NSF in the form of Grant CHE-8903637, from the University of Colorado Council on Research and Creative Work in the form of a Faculty Fellowship to T.H.K., and the University of Colorado Undergraduate Research Opportunity Program in the form of a grant to P.A.F. is gratefully acknowledged.

(35) Bird, D. M.; Gaudiano, G.; Koch, T. H. *J. Am. Chem. Soc.* **1991**, *113*, 308.

Molecular Meccano. 1. [2]Rotaxanes and a [2]Catenane Made to Order

Pier Lucio Anelli,[†] Peter R. Ashton,[†] Roberto Ballardini,*[,⊥] Vincenzo Balzani,*[,‡] Milagros Delgado,[§] Maria Teresa Gandolfi,[‡] Timothy T. Goodnow,[§] Angel E. Kaifer,*[,§] Douglas Philp,[†] Marek Pietraszkiewicz,[†] Luca Prodi,[‡] Mark V. Reddington,[†] Alexandra M. Z. Slawin,[∥] Neil Spencer,[†] J. Fraser Stoddart,*[,†] Cristina Vicent,[†] and David J. Williams*[,∥]

Contribution from the Department of Chemistry, The University, Sheffield S3 7HF, UK, Istituto FRAE-CNR, I-40126 Bologna, Italy, Dipartimento di Chimica "G. Ciamician", Università degli Studi di Bologna, I-40126 Bologna, Italy, Department of Chemistry, University of Miami, Coral Gables, Florida 33124, and Chemical Crystallography Laboratory, Department of Chemistry, Imperial College, London SW7 2AY, UK. *Received February 6, 1991. Revised Manuscript Received June 24, 1991*

Abstract: A new synthetic strategy for the elaboration of supramolecular species and molecular compounds containing noncovalently interacting components is described, with the long-term objective of constructing highly ordered, wholly synthetic assemblies from readily available starting materials. These could serve as a basis for the future development of mechanoelectrical and photoelectrical communication systems and devices capable of storing and processing information. The approach was conceived against a background of a quarter of a century's experience in supramolecular, alias host–guest, chemistry. It is based on the use of irreversibly interlocked molecular systems that take the form of catenanes and rotaxanes. Such compounds are seen to be the ideal vehicles through which to transfer from supramolecular and host–guest chemistry the knowledge and experience gained from studying complexes between small chemical entities to very much larger molecular assemblies. Once we know how to interlock molecular components irreversibly and efficiently, we shall have a very much clearer idea on how to intertwine related polymer chains reversibly. A number of template-directed syntheses of [2]rotaxanes and a [2]catenane is discussed. They illustrate that *there are inherently simple ways of making apparently complex unnatural products from appropriate substrates without the need for reagent control or catalysis.* The noncovalent bonding interactions that are used to self-assemble the 1:1 complexes, which serve as precursors to the rotaxanes and the catenane, as well as to the [2]rotaxanes and the [2]catenane themselves, "live on" in their structures and superstructures after the self-assembly process is complete. A variety of methods, including X-ray crystallography, fast atom bombardment mass spectrometry, ultra violet–visible, luminescence, nuclear magnetic resonance, and electron spin resonance spectroscopies, and electrochemistry, demonstrate the high structural order that is incorporated into these new molecular assemblies in both the solid and solution states.

The living world is made up of molecular compounds that interact physically and react chemically with each other, often in rather specific and selective ways. The phenomenon of molecular recognition has evolved around the principles of self-organization, self-assembly, and self-synthesis to the extent that participating molecules must not only be blessed with a reasonably precise chemical form but they also usually perform a particular biological function. One of the most exciting and potentially rewarding challenges the chemist faces today is to devise and realize wholly synthetic systems[1] that function like their biological

[†] University of Sheffield.
[⊥] Istituto FRAE-CNR, Bologna.
[‡] Università di Bologna.
[§] University of Miami.
[∥] Imperial College.

(1) Lehn, J.-M. *Angew. Chem., Int. Ed. Engl.* **1988**, *27*, 89–112. *J. Inclusion Phenom.* **1988**, *6*, 351–396. *Angew. Chem., Int. Ed. Engl.* **1990**, *29*, 1304–1319. In *Frontiers in Supramolecular Organic Chemistry and Photochemistry*; Schneider, H.-J.; Dürr, H., Eds.; VCH: Weinheim, Germany, 1991; pp 1–28.

0002-7863/92/1514-193$03.00/0

counterparts by storing and transferring information at a molecular level. The manufacture and manipulation of materials on this nanometer scale raises[2] the prospect of being able to perform physical feats with microscopic devices reminiscent of the automatic control units comprising the nervous system and the brain. The fundamental investigation of the chemical science that will enable the future development of mechanoelectrical and photoelectrical communication systems and devices is a challenging field of research—one that could be referred to as *molecular cybernetics*.[3]

The question is how to construct materials that express their properties at a molecular level and how to gain access to these properties. While the problems associated with the successful development of electronic[4a] and photonic[4b] molecular device systems are numerous, the most pressing fundamental ones are those of synthesis and fabrication. What is required is the development of a modular chemical approach in which molecular-size fragments are incorporated into a polymolecular array in a highly controlled and totally precise manner. As stated by Carter,[5] "this challenge will probably only be mastered when we have learned the principles of self-organization and self-synthesis from the biological world and have applied them more broadly to both organic and inorganic chemistry".

The answers will probably emerge from the new fields of supramolecular[6] and host–guest[7] chemistry that have been developing with such vigor ever since Pedersen announced[8] his discovery[9] of the so-called crown ethers. This contemporary area[10] of chemistry has focussed the attention of the synthetic chemist[11-32] on the nature of the noncovalent bond as never before. In particular, template effects[13,31,33,34] have been observed during the course of

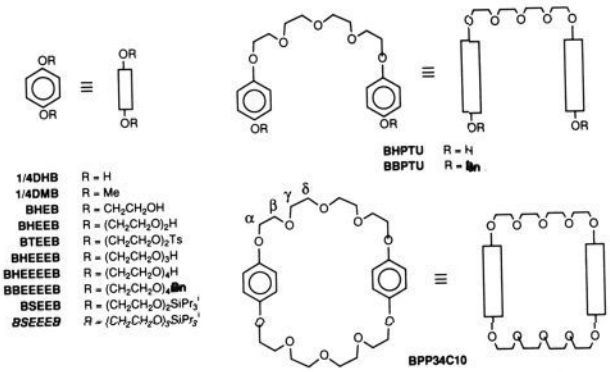

Figure 1. Acronyms and cartoons employed with the neutral compounds.

Scheme I

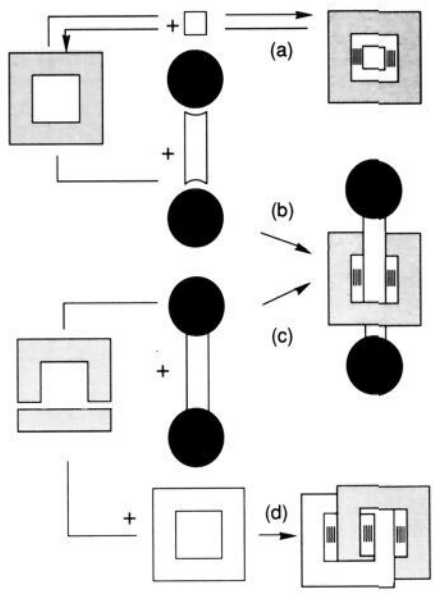

(2) Stoddart, J. F.; Mathias, J. P.; Kohnke, F. H. *Angew. Chem. Adv. Mater.* **1989**, *101*, 1129–1136.

(3) Cybernetics (Gk. *kybernetes*: steersman, governor) can be defined as the study of the self-organizing machine or mechanical brain. See: *Webster's Third New International Dictionary*; G & C Merriam: Springfield, MA, 1976; pp 563.

(4) (a) *Molecular Electronic Devices*; Carter, F. L., Siatowski, R. E., Eds.; North Holland: Amsterdam, 1988. (b) Balzani, V.; Scandola, F. *Supramolecular Photochemistry*; Horwood: Chichester, England, 1991.

(5) Carter, F. L. *Physica* **1984**, *10D*, 175–194.

(6) (a) Lehn, J.-M. *Struct. Bonding (Berlin)* **1973**, *16*, 1–69. *Pure Appl. Chem.* **1977**, *49*, 857–870. **1979**, *51*, 979–997. **1980**, *52*, 2303–2319 and 2441–2459. *Acc. Chem. Res.* **1978**, *11*, 49–57. Leçon Inaugurale, Collège de France, Paris, 1980. *Science* **1985**, *227*, 849–856. In *Supramolecular Photochemistry*; Balzani, V., Ed.; Reidel: Dordrecht, The Netherlands, 1987; pp 29–43. (b) Popov, A. I.; Lehn, J.-M. In *Coordination Chemistry of Macrocyclic Compounds*; Melson, G. A., Ed.; Plenum: New York, 1979; pp 537–584. (c) Potvin, P. G.; Lehn, J.-M. *Prog. Macrocyclic Chem.* **1987**, *3*, *167–239*.

(7) (a) Cram, D. J.; Cram, J. M. *Science* **1974**, *183*, 803–809. *Acc. Chem. Res.* **1978**, *11*, 8–14. In *Selectivity, A Goal for Synthetic Efficiency*; Bartman, W., Trost, B. M., Eds.; Verlag Chemie: Weinheim, Germany, 1983; pp 42–64. (b) Cram, D. J.; Helgeson, R. C.; Sousa, L. R.; Timko, J. M.; Newcombe, M.; de Jong, F.; Gokel, G. W.; Hoffman, D. H.; Domeier, L. A.; Peacock, S. C.; Kaplan, L. *Pure Appl. Chem.* **1975**, *43*, 327–349. (c) Cram, D. J.; Trueblood, K. N. *Top. Curr. Chem.* **1981**, *98*, 43–106. In *Host Guest Chemistry/Macrocycles*; Vögtle, F., Webber, E., Eds.; Springer-Verlag: Berlin, 1985; pp 125–188. (d) Cram, D. J. In *Applications of Biomedical Systems in Chemistry*; Jones, J. B., Sih, C. J., Perlman, D., Eds.; Wiley Interscience: New York, 1976; pp 815–873. *Science* **1983**, *219*, 1177–1183. **1988**, *240*, 760–767. *Angew. Chem., Int. Ed. Engl.* **1986**, *25*, 1039–1057. **1988**, *27*, 1009–1112. *CHEMTECH* **1987**, 120–125. *J. Inclusion Phenom.* **1988**, *6*, 397–413.

(8) Pedersen, C. J. *J. Am. Chem. Soc.* **1967**, *89*, 2495–2496 and 7017–7036. *Angew. Chem., Int. Ed. Engl.* **1988**, *27*, 1021–1027. *J. Inclusion Phenom.* **1988**, *6*, 337–350.

(9) (a) Pedersen, C. J. *Aldrichimia Acta* **1971**, *4*, 1–4. In *Selections from Aldrichimia Acta*: *Fifteen Years*, 1984; pp 15–18. (b) Pedersen, C. J.; Truter, M. R. *Endeavour* **1971**, *30*, 142–146. (c) Pedersen, C. J.; Frensdorff, H. K. *Angew. Chem., Int. Ed. Engl.* **1972**, *11*, 16–25. (d) Pedersen, C. J. In *Synthetic Multidentate Macrocyclic Compounds*; Izatt, R. M., Christensen, J. J., Eds.; Academic: New York, 1978; pp 1–51. In *Current Topics in Macrocyclic Chemistry in Japan*; Kimura, E., Ed.; Hiroshima University: Hiroshima, Japan, 1987; pp 1–4. See also the article: Schroder, H. E. *The Productive Scientific Career of Charles Pedersen* in the same publication, pp 5–13 and in *Pure Appl. Chem.* **1988**, *60*, 445–449.

(10) (a) Truter, M. R. *Chem. Br.* **1987**, *23*, 1149. (b) Milgrom, L. *New Scientist* 22 Oct 1987, No. 1538, pp 31–32. (c) Stoddart, J. F. *Nature* **1988**, *334*, 10–11. (d) Dietrich, B.; Sauvage, J.-P. *New J. Chem.* **1988**, *12*, 725–728. (e) See also feature articles in *Chem. Eng. News* 19 Oct 1987, pp 4–5 and 30–33. *Chem. Ind.* **1987**, 731. *Chem. Br.* **1988**, *24*, 752–753.

(11) See review articles: (a) *Synthetic Multidentate Macrocyclic Compounds*; Izatt, R. M., Christensen, J. J., Eds.; Academic: New York, 1978. (b) *Progress in Macrocyclic Chemistry*; Izatt, R. M., Christensen, J. J., Eds.; Wiley: New York, 1979, Vol. 1; 1981, Vol. 2; 1987, Vol. 3. (c) *Coordination Chemistry of Macrocyclic Compounds*; Melson, G. A., Ed.; Plenum: New York, 1979. (d) *The Chemistry of the Functional Groups. Supplement E. The Chemistry of Ethers, Crown Ethers, Hydroxyl Groups, and their Sulphur Analogues*; Patai, S., Ed.; Wiley: Chichester, England, 1980; Part 1. (e) *Cyclophanes*; Keehn, P. M., Rosenfield, S. M., Eds.; Academic: New York, 1983; Vols. I and II. (f) *Inclusion Compounds*; Atwood, J. L., Davies, J. E. D., MacNicol, D. D., Eds.; Academic: London, 1984; Vols. 1-3. (g) *Host Guest Complex Chemistry/Macrocycles*; Vögtle, F., Webber, E., Eds.; Springer-Verlag: Berlin, 1985. (f) *Current Topics in Macrocyclic Chemistry in Japan*; Kimura, E., Ed.; Hiroshima University: Hiroshima, Japan, 1987. (g) *Macrocyclic and Supramolecular Chemistry in Italy*; Andretti, G. D., Pochini, A., Ungaro, R., Eds.; University of Parma, Parma, Italy, 1988. (h) *Crown Ethers and Analogs*; Patai, S., Rappoport, Z., Eds.; Wiley: Chichester, England, 1989. (i) *Supramolecular Assemblies*: *New Developments in Biofunctional Chemistry*; Murakami, Y., Ed.; Mita Press: Tokyo, 1990. (j) *Bioorganic Chemistry Frontiers*; Dugas, H., Ed.; Springer Verlag: Berlin, 1990, Vol. 1; 1991, Vol. 2. (k) *Cation Binding by Macrocycles*: *Complexation of Cationic Species by Crown Ethers*; Inoue, Y., Gokel, G. W., Eds.; Marcel Dekker: New York, 1990. (l) *Inclusion Phenomena and Molecular Recognition*; Atwood, J. L., Ed.; Plenum: New York, 1990. (m) *Frontiers in Supramolecular Organic Chemistry and Photochemistry*; Schneider, J.-J., Dürr, H., Eds.; VCH: Weinheim, Germany, 1991.

(12) Hiraoka, M. *Crown Compounds*; Elsevier: New York, 1982.

(13) Gokel, G. W.; Korzeniowski, S. H. *Macrocyclic Polyether Synthesis*; Springer-Verlag: Berlin, 1982.

(14) Prelog, V. *Pure Appl. Chem.* **1978**, *50*, 893–904.

(15) Cornforth, J. W. *Proc. R. Soc. London, Ser. B* **1978**, *203*, 101–117.

(16) MacNicol, D. D.; McKendrick, J. J.; Wilson, D. R. *Chem. Soc. Rev.* **1978**, *7*, 65–87.

many chemical reactions that yield complexing macrocycles and molecular receptors as products, often with remarkable efficiencies and selectivities. Alkali metal and alkaline earth metal cations play[35] an important role as noncovalently bound templates during

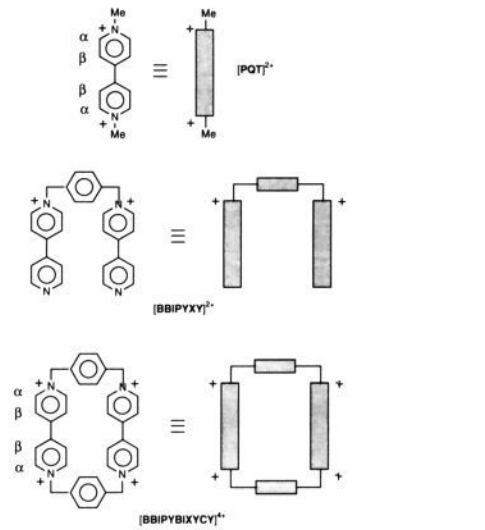

Figure 2. Acronyms and cartoons employed with the charged compounds.

Scheme II

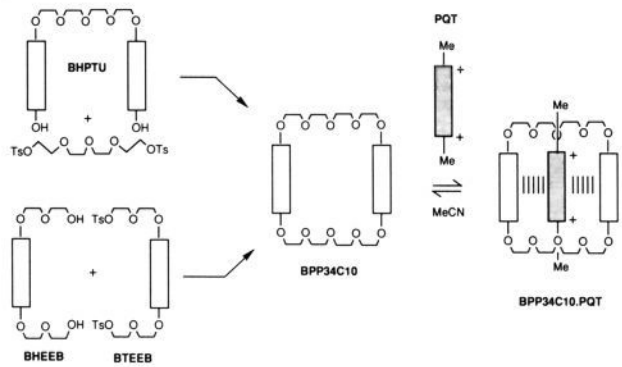

the preparation of many oxygen- and nitrogen-containing macrocyclic compounds. The template effect not only speeds up reaction rates but it also leads to much higher yields of products; i.e., the evidence for it is both kinetic and thermodynamic. Organic cations can also act[36] as noncovalently bound templates during crown ether syntheses. In the case of transition metals,[37] covalent bonds are invariably formed during templated syntheses of nitrogen-, sulfur- and phosphorus-containing macrocycles, and so it is much more difficult to release by demetalation the covalently bound template from within the macrocyclic compound. Nonetheless, in the hands of Sauvage and his co-workers,[38] numerous

(17) (a) Stoddart, J. F. *Chem. Soc. Rev.* **1979**, *8*, 85–142. *Lectures in Heterocyclic Chemistry*; Castle, R. N., Schneller, S. W., Eds.; Hetero Corp.: Orem, UT, 1980; Vol. 5, pp S47–S60. *R. Soc. Chem., Annu. Rep. Sect. B* **1984**, 353–378. In *The Chemistry of Enzyme Action*; Page, M. I., Ed.; Elsevier: Amsterdam, 1984; pp 529–561. In *Enzyme Mechanisms*; Page, M. I., Williams, A., Eds.; RSC Special Publication: London, 1987; pp 35–55. *Biochem. Soc. Trans.* **1987**, *15*, 1188–1191. *Top. Stereochem.* **1987**, *17*, 207–288. *Pure Appl. Chem.* **1988**, *60*, 467–472. *R. Soc. Chem., Annu. Rep., Sect. B* **1989**, 353–386. (b) Colquhoun, H. M.; Stoddart, J. F.; Williams, D. J. *New Scientist* 1 May 1986, No. 1056, pp 44–48. *Angew. Chem., Int. Ed. Engl.* **1986**, *25*, 487–507.

(18) (a) de Jong, F.; Reinhoudt, D. N. *Adv. Phys. Org. Chem.* **1980**, *17*, 279–433. (b) Reinhoudt, D. N. *J. Coord. Chem.* **1988**, *18*, 21–43.

(19) (a) Bradshaw, J. S.; Stott, P. E. *Tetrahedron* **1980**, *36*, 461–510. (b) Jolley, S. T.; Bradshaw, J. S.; Izatt, R. M. *J. Heterocycl. Chem.* **1982**, *19*, 3–19. (c) Izatt, R. M.; Bradshaw, J. S.; Nielsen, S. A.; Lamb, J. D.; Christensen, J. J. *Chem. Rev.* **1985**, *85*, 271–339.

(20) Tabushi, I. *Acc. Chem. Res.* **1982**, *15*, 66–72. *Tetrahedron* **1984**, *40*, 269–292. *Pure Appl. Chem.* **1986**, *58*, 1529–1534.

(21) Hayward, R. C. *Chem. Soc. Rev.* **1983**, *12*, 285–308.

(22) Pierre, J.-L.; Baret, P. *Bull. Soc. Chim. Fr.* **1983**, 367–380.

(23) (a) Hamilton, A. D. In *Comprehensive Heterocyclic Chemistry*; Katritzky, A. R., Rees, C. W., Eds.; Pergamon: Oxford, 1984; Vol. 7, Part 5, pp 731–761. (b) Hamilton, A. D. *J. Chem. Educ.* **1990**, *67*, 821–828. (c) Hamilton, A. D.; Pant, N.; Muehldorf, A. *Pure Appl. Chem.* **1988**, *60*, 533–538.

(24) Kellogg, R. M. *Angew. Chem., Int. Ed. Engl.* **1984**, *23*, 782–794.

(25) (a) Gutsche, C. D. *Acc. Chem. Res.* **1983**, *16*, 161–170. *Top. Curr. Chem.* **1984**, *123*, 1–47. *Pure Appl. Chem.* **1988**, *60*, 483–488. Calixarenes. In *Monographs in Supramolecular Chemistry*; Stoddart, J. F., Ed.; Royal Society of Chemistry: Cambridge, England, 1989. (b) Gutsche, C. D.; Alain, I.; Iqbal, M.; Mangiafico, T.; Nam, K. C.; Rogers, J.; See, K. A. *J. Inclusion Phenom.* **1987**, *7*, 61–72.

(26) Sutherland, I. O. *Chem. Soc. Rev.* **1986**, *15*, 63–91. *J. Inclusion Phenom.* **1989**, *7*, 213–226. *Pure Appl. Chem.* **1989**, *61*, 1547–1554.

(27) Diederich, F. *Angew. Chem., Int. Ed. Engl.* **1988**, *27*, 362–386. *J. Chem. Educ.* **1990**, *67*, 813–820.

(28) Schneider, H.-J.; Busch, R.; Kramer, R.; Schneider, U.; Theis, I. *Adv. Chem. Ser.* **1987**, *215*, 457–489.

(29) Rebek, J., Jr. *Science* **1987**, *235*, 1478–1484. *J. Mol. Recog.* **1988**, *1*, 1–8. *J. Inclusion Phenom.* **1989**, *7*, 7–17. *Pure Appl. Chem.* **1989**, *61*, 1517–1522. *Angew. Chem., Int. Ed. Engl.* **1990**, *29*, 245–255.

(30) Hosseini, M. W. *La Recherche* January 1989, No. 206, Vol. 20, pp 24–32.

(31) Lindoy, L. F. *The Chemistry of Macrocyclic Ligand Complexes*; Cambridge University Press: Cambridge, England, 1989.

(32) Vögtle, F. *Supramoleculare Chemie*; Teubner: Stuttgart, Germany, 1989.

(33) Laidler, D. A.; Stoddart, J. F. In *The Chemistry of the Functional Groups. Supplement E. The Chemistry of Ethers, Crown Ethers, Hydroxyl Groups, and their Sulphur Analogues*; Patai, S., Ed.; Wiley: Chichester, England, 1980; Part 1, pp 1–57. In *Crown Ethers and Analogs*; Patai, S., Rappoport, Z., Eds.; Wiley: Chichester, England, 1989; pp 1–57.

(34) Krakowiak, K. E.; Bradshaw, J. S.; Zamecka-Krakowiak, D. J. *Chem. Rev.* **1989**, *89*, 929–972.

(35) (a) Greene, R. N. *Tetrahedron Lett.* **1972**, 1793–1796. (b) Chastrette, M.; Chastrette, F. *J. Chem. Soc., Chem. Commun.* **1973**, 534–535. (c) Cook, F. L.; Caruso, T. C.; Byrne, M. P.; Bowers, C. W.; Speck, D. H.; Liotta, C. L. *Tetrahedron Lett.* **1974**, 4029–4032. (d) Dale, J.; Daasvatn, K. *J. Chem. Soc., Chem. Commun.* **1976**, 295–296. (e) Reinhoudt, D. N.; Gray, R. T. *Tetrahedron Lett.* **1975**, 2105–2108. (f) Gray, R. T.; Reinhoudt, D. N.; Smit, C. J.; Veenstra, I. *Recl. Trav. Chim. Pays-Bas* **1976**, *95*, 258–263. (g) Reinhoudt, D. N.; Gray, R. T.; Smit, C. J.; Veenstra, I. *Tetrahedron* **1976**, *32*, 1161–1169. (h) Reinhoudt, D. N.; de Jong, F.; Tomassen, H. P. M. *Tetrahedron Lett.* **1979**, 2067–2070. (i) Mandolini, L.; Masci, B. *J. Am. Chem. Soc.* **1977**, *99*, 7709–7710. *Synth. Commun.* **1979**, *9*, 851–856. *J. Am. Chem. Soc.* **1984**, *106*, 168–174 and 3706. (j) Mandolini, L. *Pure Appl. Chem.* **1986**, *58*, 1485–1492. (k) Vitali, C. A.; Masci, B. *Tetrahedron* **1989**, *45*, 2201–2212 and 2213–2222. (l) Desvergne, J.-P.; Bouas-Laurent, H. *J. Chem. Soc., Chem. Commun.* **1978**, 403–404. (m) Rasshofer, W.; Vögtle, F. *Liebigs Ann. Chem.* **1978**, 552–558. (n) Ping-Lin, K.; Miki, M.; Okahara, M. *J. Chem. Soc., Chem. Commun.* **1978**, 504–505. (o) Nakatsuji, Y.; Nakamura, T.; Yonetani, M.; Yuga, H.; Okahara, M. *J. Am. Chem. Soc.* **1988**, *110*, 531–538. (p) Yamawaki, J.; Ando, T. *Chem. Lett.* **1979**, 755–758. **1980**, 533–536. (q) Newkome, G. R.; Kawato, T.; Benton, W. H. *J. Org. Chem.* **1980**, *45*, 626–628. (r) Kulstad, S.; Malmsten, L. A. *Tetrahedron Lett.* **1980**, *21*, 643–646. (s) Gokel, G. W.; Dishong, D. M.; Schultz, R. A.; Gatto, V. J. *Synthesis* **1982**, 997–1012. (t) Pietraszkiewicz, M.; Jurczak, J. *J. Chem. Soc., Chem. Commun.* **1983**, 132–133. (u) Bogatsky, A. V.; Lukyanenko, N. G.; Basok, S. S.; Ostrovskaya, L. K. *Synthesis* **1984**, 138. (v) Biernat, J. F.; Luboch, E. *Tetrahedron* **1984**, *40*, 1927–1929. (w) Schultz, R. A.; White, B. D.; Dishong, D. M.; Arnold, K. A.; Gokel, G. W. *J. Am. Chem. Soc.* **1985**, *107*, 6659–6668.

(36) (a) Madan, K.; Cram, D. J. *J. Chem. Soc., Chem. Commun.* **1975**, 427–428. (b) Kyba, E. P.; Helgeson, R. C.; Madan, K.; Gokel, G. W.; Tarnowski, T. L.; Moore, S. S.; Cram, D. J. *J. Am. Chem. Soc.* **1977**, *99*, 2564–2571.

(37) (a) Curtis, N. F. *J. Chem. Soc.* **1960**, 4409–4417. (b) Curtis, N. F.; Curtis, Y. M.; Powell, H. K. J. *J. Chem. Soc. A* **1966**, 1015–1018. (c) Hay, R. W.; Lawrance, G. A.; Curtis, N. F. *J. Chem. Soc., Dalton Trans.* **1975**, 591–593. (d) Curtis, N. F.; Einstein, F. W. B.; Willis, A. C. *Inorg. Chem.* **1984**, *23*, 3444–3449. (e) Comba, P.; Curtis, N. F.; Lawrance, G. A.; Sargeson, A. M.; Skelton, B. W.; White, A. H. *Inorg. Chem.* **1986**, *25*, 4260–4267. (f) Thompson, M. C.; Busch, D. H. *J. Am. Chem. Soc.* **1964**, *86*, 3651–3655. (g) Melson, G. A.; Busch, D. H. *J. Am. Chem. Soc.* **1965**, *87*, 1706–1710. (h) Busch, D. H.; Farmery, K.; Goedken, V.; Katovic, V.; Melnyk, A. C.; Sperati, C. R.; Tokel, N. *Adv. Chem. Ser.* **1971**, *100*, 44–78. (i) Melson, G. A.; Funke, L. A. *Inorg. Chim. Acta* **1984**, *82*, 19–25. (j) Nelson, S. M. *Pure Appl. Chem.* **1980**, *52*, 461–476. (k) Drew, M. G. B.; Esho, F. S.; Lavery, A.; Nelson, S. M. *J. Chem. Soc., Dalton Trans.* **1984**, 545–546.

(38) For a comprehensive review, see: Dietrich-Buchecker, C. O.; Sauvage, J.-P. *Chem. Rev.* **1987**, *87*, 795–810. The terms *catenand* and *catenate* are defined in this article. A transition metal complex involving interlocking rings as the coordinating ligand has been named a *catenate*. The name *catenand* has been proposed to describe this new class of coordinating ligand. For a more recent review, see: Sauvage, J.-P.; Dietrich-Buchecker, C. O. In *Bioorganic Chemistry Frontiers 2*; Dugas, H., Ed.; Springer-Verlag: Berlin, 1991; pp 195–248.

metallocatenanes[39] have been isolated and characterized by following a synthetic strategy based on a three-dimensional template effect induced by a transition metal[40,41] to afford a so-called *catenate*,[38] which can be demetalated to yield the related *catenand*.[38]

The relevant background information is now available within the research fields identified above to allow us to start evolving a completely new synthetic methodology for the modular construction of large, discrete, and ordered molecular assemblies from prefabricated molecular components.[42] The approach, we would argue, should appeal to the self-assembly aspects of the template effect involving not covalently bonded species, but weak noncovalently bonded components that do not implicate, in the beginning at least, relatively strong coordinate interactions with (transition) metal ions. The bond-forming processes should then occur easily within the ordered environment of the noncovalent templating forces in such a way as to retain the order originally imposed by the weak interactions. Finally, the molecular fragments, which are organized in this manner, should subsequently be unable to dissociate from each other for simple mechanical reasons after the reactions are complete. The usual host–guest relationship (Scheme I) involves (a) rapid association between host and guest to form a (1:1) complex. In this situation, dissociation of the complex into its molecular components occurs, albeit less rapidly, i.e., a reversible process ensues. If, however, the guest is trapped mechanically within or around the associated host, then dissociation is prevented and the process becomes an irreversible one. There are several ways[43] of achieving this end. One is to form *rotaxanes*[44] by either (b) threading or (c) clipping processes; another is (d) to use the clipping process to make *catenanes*.[44] Although both of these molecular forms are already well-documented[45] in the literature,[39,46] they have rarely been regarded as

Scheme III

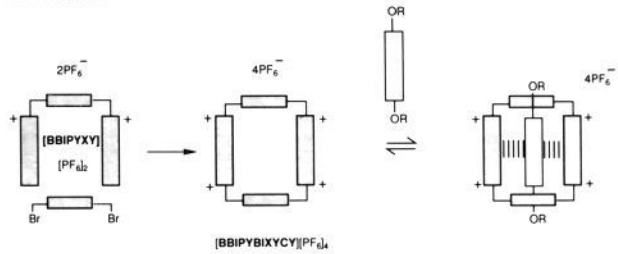

Scheme IV

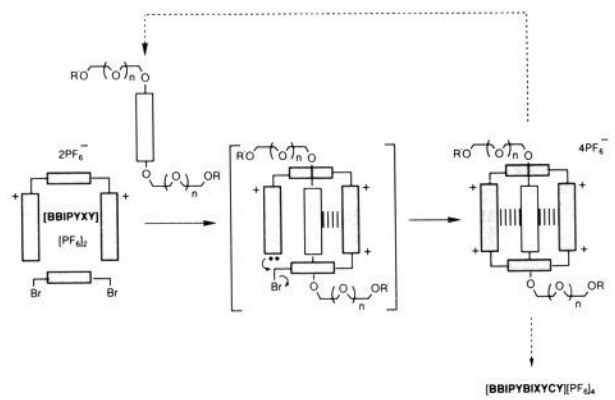

(39) (a) Dietrich-Buchecker, C. O.; Sauvage, J.-P.; Kintzinger, J.-P. *Tetrahedron Lett.* **1983**, *24*, 5095–5098. (b) Dietrich-Buchecker, C. O.; Sauvage, J.-P.; Kern, J.-M. *J. Am. Chem. Soc.* **1984**, *106*, 3043–3045. (c) Albrecht-Gary, A. M.; Saad, Z.; Dietrich-Buchecker, C. O.; Sauvage, J.-P. *J. Am. Chem. Soc.* **1985**, *107*, 3205–3209. (d) Sauvage, J.-P.; Weiss, J. *J. Am. Chem. Soc.* **1985**, *107*, 6108–6110. (e) Dietrich-Buchecker, C. O.; Sauvage, J.-P.; Weiss, J. *Tetrahedron Lett.* **1986**, *27*, 2257–2260. (f) Dietrich-Buchecker, C. O.; Khemiss, A.; Sauvage, J.-P. *J. Chem. Soc., Chem. Commun.* **1986**, 1376–1378. (g) Dietrich-Buchecker, C. O.; Guilheim, J.; Pascard, C.; Sauvage, J.-P. *Angew. Chem., Int. Ed. Engl.* **1987**, *26*, 661–663. (h) Dietrich-Buchecker, C. O.; Edel, A.; Kintzinger, J.-P.; Sauvage, J.-P. *Tetrahedron* **1987**, *43*, 333–344. (i) Mitchell, D. K.; Sauvage, J.-P. *Angew. Chem., Int. Ed. Engl.* **1988**, *27*, 930–931. (j) Albrecht-Gary, A.-M.; Dietrich-Buchecker, C. O.; Saad, Z.; Sauvage, J.-P. *J. Am. Chem. Soc.* **1988**, *110*, 1467–1472. (k) Guilheim, J.; Pascard, C.; Sauvage, J.-P.; Weiss, J. *J. Am. Chem. Soc.* **1988**, *110*, 8711–8713. (l) Dietrich-Buchecker, C. O.; Hemmert, C.; Khemiss, A.; Sauvage, J.-P. *J. Am. Chem. Soc.* **1990**, *112*, 8002–8008. (m) Sauvage, J.-P. *Acc. Chem. Res.* **1990**, *23*, 319–327.

(40) For the recently reported synthesis and properties of a molecular trefoil knot, see: Dietrich-Buchecker, C. O.; Sauvage, J.-P. *Angew. Chem., Int. Ed. Engl.* **1989**, *28*, 189–192.

(41) It should be noted in passing that double-stranded helicates with oligobipyridine ligands wrapped around tetrahedrally coordinated Cu(I) ions are produced by a self-assembly process that exhibits positive cooperativity (complexation of one metal ion facilitates binding of the next and so on) and self–self recognition (preferential pairing to the same ligand in the presence of a mixture). See: Lehn, J.-M.; Rigault, A.; Siegel, J.; Harrowfield, J.; Chevier, B.; Moras, D. *Proc. Natl. Acad. Sci. USA* **1987**, *84*, 2565–2569. Lehn, J.-M.; Rigault, A. *Angew. Chem., Int. Ed. Engl.* **1988**, *27*, 1095–1097. Koert, U.; Harding, M. M.; Lehn, J.-M. *Nature* **1990**, *346*, 339–342. The preparation and structural characterization of double helical binuclear complexes of copper, nickel, and silver with the open-chain pentadentate ligand, quinquepyridine, have also been reported recently. See: (a) Constable, E. C.; Drew, M. G. B.; Ward, M. D. *J. Chem. Soc., Chem. Commun.* **1987**, 1600–1601. (b) Barley, M.; Constable, E. C.; Corr, S. A.; McQueen, R. C. S.; Nutkins, J. C.; Ward, M. D.; Drew, M. G. B. *J. Chem. Soc., Dalton Trans.* **1988**, 2655–2662. (c) Constable, E. C.; Ward, D. W.; Tocher, D. A. *J. Am. Chem. Soc.* **1990**, *112*, 1256–1258. (d) Constable, E. C.; Elder, S. M.; Healy, J.; Ward, M. D.; Tocher, D. A. *J. Am. Chem. Soc.* **1990**, *112*, 4590–4592.

(42) We used to build houses—the walls, brick-by-brick, the roofs, tile-by-tile, the floors, plank-by-plank of wood, the windows, pane-by-pane of glass—in such a way that it could take a year or more. Now, houses come prefabricated and can be erected inside a week. A similar transformation awaits the art of synthetic chemistry. We have already learned how to synthesize molecular compounds atom-by-atom, group-by-group, often employing highly sophisticated reagents and catalysts to make and break covalent bonds and so manipulate functional groups with incredible efficiency and awe-inspiring elegance. Now, we need to learn how to assemble molecular compounds, molecule-by-molecule, spontaneously from molecular components with use of the stabilizing and ordering properties of noncovalent bonds between the substrate molecules, thus avoiding wherever possible, the use of reagents and catalysts, however exotic. We have referred to this type of control as structure-directed synthesis in order to draw attention to the importance of the structures of the substrates and/or of the products—rather than of any reagents or catalysts—in directing the course of some chemical reactions. Previously, it has been recorded that "there are inherently simple ways of making apparently complex unnatural products from appropriate substrates without the need for reagent control or catalysis". See: Ashton, P. R.; Isaacs, N. S.; Kohnke, F. H.; Mathias, J. P.; Stoddart, J. F. *Angew. Chem., Int. Ed. Engl.* **1989**, *28*, 1258–1261. We have emphasized the importance of this concept in connection with repetitive Diels–Alder reactions that proceed with very high multiple diastereoselectivities; see: (a) Ellwood, P.; Mathias, J. P.; Stoddart, J. F.; Kohnke, F. H. *Bull. Soc. Chim. Belg.* **1988**, *97*, 669–678. (b) Kohnke, F. H.; Mathias, J. P.; Stoddart, J. F. In *Molecular Recognition: Chemical and Biochemical Problems*; Roberts, S. M., Ed.; RSC Special Publication No. 78: Cambridge, England, 1989; pp 241–269. It has also been addressed in the field of biomolecules and natural product synthesis; see: Echenmoser, A. *Angew. Chem., Int. Ed. Engl.* **1988**, *27*, 5–39. In analyzing the specific structural elements of vitamin B_{12}, Eschenmoser has observed that "these outwardly complex structural elements are found to 'self assemble' with surprising ease under structurally appropriate preconditions; the amount of 'external instruction' required for their formation turns out to be surprisingly small in view of the complexity and specificity of these structural elements".

(43) One way is to imprison small molecules inside large, rigid, spherical container molecules. If the small molecule trapped inside these so-called *carcerands* cannot escape short of rupturing some covalent bonds on the surface of the molecular container, then complexation is mechanically associated with an irreversible process. For a discussion of the new phase of matter provided within the interiors of these molecular container compounds, see: (a) Cram, D. J.; Karbach, S.; Kim, Y. H.; Baczynskyj, L.; Kalleymeyn, G. W. *J. Am. Chem. Soc.* **1985**, *107*, 2575–2576. (b) Cram, D. J.; Karbach, S.; Kim, Y. H.; Baczynskyj, L.; Marti, K.; Sampson, R. M.; Kalleymeyn, G. W. *J. Am. Chem. Soc.* **1988**, *110*, 2554–2560. (c) Sherman, J. C.; Cram, D. J. *J. Am. Chem. Soc.* **1989**, *111*, 4527–4528. (d) Bryant, J. A.; Blanda, M. T.; Vincenti, M.; Cram, D. J. *J. Chem. Soc., Chem. Commun.* **1990**, *112*, 1403–1405. (e) Sherman, J. C.; Knobler, C. B.; Cram, D. J. *J. Am. Chem. Soc.* **1991**, *113*, 2167–2172. (f) Bryant, J. A.; Blanda, M. T.; Vincenti, M.; Cram, D. J. *J. Am. Chem. Soc.* **1991**, *113*, 2194–2204. (g) Quan, M. L. C.; Knobler, C. B.; Cram, D. J. *J. Chem. Soc., Chem. Commun.* **1991**, 660–662. (h) Cram, D. J.; Tanner, M. E.; Knobler, C. B. *J. Am. Chem. Soc.* **1991**, *113*, 7717–7727. (i) Cram, D. J.; Tanner, M. E.; Thomas, R. *Angew. Chem., Int. Ed. Engl.* **1991**, *30*, 1024–1027.

(44) The generic names *rotaxane* (Latin: *rota* = wheel, *axis* = axle) and *catenane* (Latin: *catena* = chain) have now gained wide acceptance. The number of molecular components comprising these compounds that include "topological", as well as covalent bonds, is given in square brackets as a prefix before the name; e.g., [2]rotaxanes and [2]catenanes are the simplest examples.

much more than academic curiosities. Generally speaking, they have been prepared[39] in relatively low yields by using the concept of statistical threading or by directed synthesis through temporary covalent bonding to a central core, which is subsequently dissected out to release the rotaxane or catenane.

Examples of the use of noncovalent bonding to direct the syntheses of rotaxanes and catenanes are rare. Here, we describe[47] how such noncovalent bonding can be used to template their syntheses and demonstrate by a variety of methods, including X-ray crystallography, fast atom bombardment mass spectrometry, UV–visible, luminescence, NMR, and ESR spectroscopies, and electrochemistry, the high structural order that is incorporated automatically into these new molecular assemblies.

Scheme V

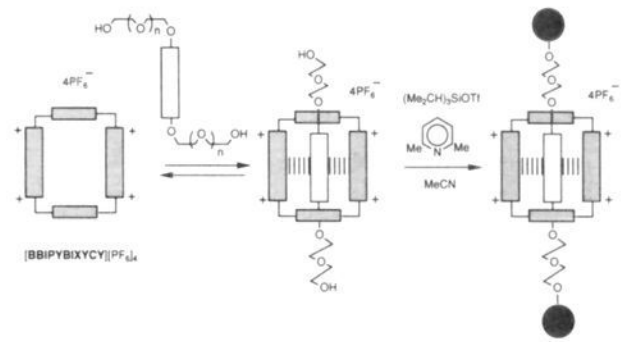

Scheme VI

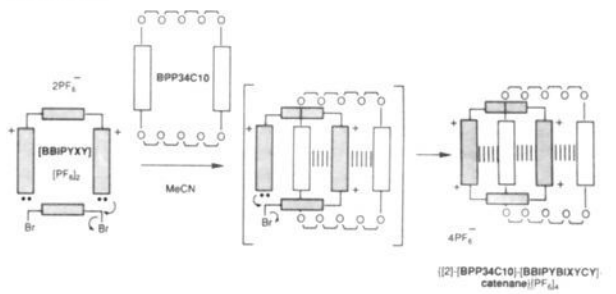

Results and Discussion

Names and Cartoons. It will be convenient in presenting the results to employ acronyms composed of letters, and occasionally numbers, to identify the neutral and charged compounds displayed in Figures 1 and 2, respectively. Thus, 1,4-dihydroxybenzene and 1,4-dimethoxybenzene are abbreviated to 1/4DHB and 1/4DMB, respectively, and bis-*p*-phenylene-34-crown-10 to BPP34C10. The other acronyms employed in Figure 1 can be deduced on the basis of the following definitions: B stands for bis when at the beginning, for benzyloxy when in the middle, and benzene when at the end of the name. E, H, P, S, and T stand for ethoxy, hydroxy, phenoxy, triisopropylsilyloxy, and tosyloxy, respectively. CY, TU, XY, and BIXY represent cyclophane, trioxaundecane, xylylene, and bisxylylene units, respectively. In addition, in Figure 2, BIPY stands for a bipyridinium ring system, with the formal charges being indicated in the usual manner; e.g., paraquat is represented by $[PQT]^{2+}$. In the cartoon versions of the structural formulas displayed in Figures 1 and 2, smaller rectangles represent para-disubstituted benzene rings, whereas the larger ones represent bipyridinium ring systems. In neutral molecules (Figure 1), the rectangles are unshaded, whereas they are shaded in the case of the positively charged organic species (Figure 2), with the formal

(45) (a) Schill, G. *Catenanes, Rotaxanes and Knots*; Academic Press: New York, 1971. In *Conformational Analysis*; Chiurdoglu, G., Ed.; Academic Press: New York, 1971; pp 229–239. (b) Boeckmann, J.; Schill, G. *Tetrahedron* **1974**, *30*, 1945–1957. (c) Rouvray, D. H. *Educ. Chem.* **1971**, *8*, 134–137. (d) Sokolov, V. I. *Russ. Chem. Rev. (Engl. Transl.)* **1973**, *42*, 452–463.

(46) The first successful synthesis of a [2]catenane (composed of two 34-membered rings) was based on statistical threading and was reported in 1960; see: Wasserman, E. *J. Am. Chem. Soc.* **1960**, *82*, 4433–4434, and subsequently (a) Frisch, H. L.; Wasserman, E. *J. Am. Chem Soc.* **1961**, *83*, 3789–3795. (b) Wasserman, E. *Sci. Am.* **1962**, *207* (5), 94–102. The extremely low yields of catenanes obtained by this approach were improved considerably when a polymer-bound macrocycle containing 32 carbon atoms was subjected to 70 successive statistical threading reactions to give a [2]rotaxane in 7% yield following its release from the polymer; see: Harrison, I. T.; Harrison, S. *J. Am. Chem. Soc.* **1967**, *89*, 5723–5724. The statistical threading approach was subsequently developed [see: (c) Harrison, I. T. *J. Chem. Soc., Perkin Trans. 1* **1974**, 301–304. (d) Schill, G.; Beckmann, W.; Schweickert, N.; Fritz, H. *Chem. Ber.* **1986**, *119*, 2647–2655] in the laboratories of Harrison and Schill, and yields of [2]rotaxanes in the region of 10% have been achieved. Of particular significance, with respect to the present investigation, is that heterogeneous [2]rotaxanes and [2]catenanes have also been prepared by statistical threading of polyethylene glycols prior to their tritylation through dibenzo crown ether macrocycles; see: (e) Agam, G.; Graiver, D.; Zilkha, A. *J. Am. Chem. Soc.* **1976**, *98*, 5206–5214. (f) Agam, G.; Zilkha, A. *J. Am. Chem. Soc.* **1976**, *98*, 5214–5216. Statistical threading via a [2]rotaxane also provided a means of synthesizing the first hydrocarbon catenane; see: Schill, G.; Schweickert, N.; Fritz, H.; Vetter, W. *Angew. Chem., Int. Ed. Engl.* **1983**, *22*, 889–891. Another novel route to [2]catenanes relies on the so-called semistatistical principle; see: Lüttringhaus, A.; Isele, G. *Angew. Chem., Int. Ed. Engl.* **1967**, *6*, 956–957. This approach combines the characteristics of the statistical threading method with those of the directed syntheses of precatenanes, i.e., triansa compounds, from which catenanes can be unambiguously generated by cleavage of the appropriate covalent bonds; see: Schill, G.; Lütteringhaus, A. *Angew. Chem., Int. Ed. Engl.* **1964**, *3*, 546–547. Since 1964, Schill's group have been very active in using the directed synthesis approach to prepare numerous [2]rotaxanes, [2]catenanes, and [3]catenanes; see: (g) Schill, G.; Zollenkopf, G. *Liebigs Ann. Chem.* **1969**, *721*, 53–74. (h) Schill, G.; Zürcher, C. *Chem. Ber.* **1977**, *110*, 2046–2066. (i) Rissler, K.; Schill, G.; Fritz, H.; Vetter, W. *Chem. Ber.* **1986**, *119*, 1374–1399. (j) Schill, G.; Schweickert, N.; Fritz, H.; Vetter, W. *Chem. Ber.* **1988**, *121*, 961–970. Although the approach is elegant, the multistep character of the directed synthesis of rotaxanes and catenanes renders it a time-consuming and low-yielding approach. The possibility of harnessing weak noncovalent bonding interactions between the molecular components of interlocking systems and so encourage threading processes was first proposed in 1958; see: Lütteringhaus, A.; Cramer, F.; Prinzbach, H.; Henglein, F. M. *Liebigs Ann. Chem.* **1958**, *613*, 185–198. However, following their unsuccessful attempt to prepare a catenane from an inclusion complex of α-cyclodextrin, more than 20 years elapsed before rotaxanes consisting of α- and β-cyclodextrin threaded by polymethylene-bridged dinuclear cobalt(III) complexes were reported; see: (k) Ogino, H. *J. Am. Chem. Soc.* **1981**, *103*, 1303–1304. (l) Ogino, H.; Ohata, K. *Inorg. Chem.* **1984**, *23*, 3312–3316. (c) Yamanari, K.; Shimura, Y. *Bull. Chem. Soc. Jpn.* **1983**, *56*, 2283–2289. More recently, organometallic rotaxanes involving 18-crown-6 and related crown ethers as coordinating ligands for zinc and magnesium have been characterized by X-ray crystallography; see: (m) Pajerski, A. D.; BergStresser, G. L.; Parvez, M.; Richey, H. G., Jr. *J. Am. Chem. Soc.* **1988**, *110*, 4844–4845. (n) Markies, P. R.; Nomoto, T.; Akkerman, O. S.; Bickelhaupt, F.; Smeets, W. J. J.; Spek, A. L. *J. Am. Chem. Soc.* **1988**, *110*, 4845–4846. The introduction of templated syntheses by Sauvage and his associates in 1983 represented a major breakthrough; see refs 38 and 39. Seizing upon the very special topography of the pseudotetrahedral complex formed when two 2,9-disubstituted 1,10-phenanthroline ligands fit around a copper(I) ion, they have prepared several [2]catenates—some of them chiral—and [3]catenates, their derived catenands following demetalation, and, very recently, a molecular trefoil knot. Although synthetically derived examples of catenanes, rotaxanes, and trefoil knots are still relatively rare, it is surely not without significance that the common occurrence in nature's laboratory of duplex circular DNAs in supercoiled, catenated, and knotted forms is well-established; see (o) Wang, J. C. *Acc. Chem. Res.* **1973**, *6*, 252–256. (p) Krasnow, M. A.; Stasiak, A.; Spengler, S. J.; Dean, F.; Koller, T.; Cozzarelli, N. R. *Nature* **1983**, *304*, 559–560. An intellectually satisfying synthetic route into catenanes is the Möbius strip approach; see: (q) Wasserman, E.; Ben-Efraim, D. A.; Wolovsky, R. *J. Am. Chem. Soc.* **1968**, *90*, 3286–3287. (r) Wolovsky, R. *J. Am. Chem. Soc.* **1970**, *92*, 2132–2133. (s) Ben-Efraim, D. A.; Batich, C.; Wasserman, E. *J. Am. Chem. Soc.* **1970**, *92*, 2133–2135. (t) Walba, D. M.; Richards, R. M.; Haltiwanger, R. C. *J. Am. Chem. Soc.* **1982**, *104*, 3219–3221. (u) Walba, D. M. *Tetrahedron* **1985**, *41*, 3161–3212.

(47) Some of the results discussed in this paper have been mentioned in abbreviated formats in preliminary communications; see: (a) Allwood, B. L.; Spencer, N.; Shahriari-Zavareh, H.; Stoddart, J. F.; Williams, D. J. *J. Chem. Soc., Chem. Commun.* **1987**, 1061–1064. (b) Allwood, B. L.; Spencer, N.; Shahriari-Zavareh, H.; Stoddart, J. F.; Williams, D. J. *J. Chem. Soc., Chem. Commun.* **1987**, 1064–1066. (c) Ashton, P. R.; Slawin, A. M. Z.; Spencer, N.; Stoddart, J. F.; Williams, D. J. *J. Chem. Soc., Chem. Commun.* **1987**, 1066–1069. (d) Slawin, A. M. Z.; Spencer, N.; Stoddart, J. F.; Williams, D. J. *J. Chem. Soc., Chem. Commun.* **1987**, 1070–1072. (e) Odell, B.; Reddington, M. V.; Slawin, A. M. Z.; Spencer, N.; Stoddart, J. F.; Williams, D. J. *Angew. Chem., Int. Ed. Engl.* **1988**, *27*, 1547–1550. (f) Ashton, P. R.; Odell, B.; Reddington, M. V.; Slawin, A. M. Z.; Stoddart, J. F.; Williams, D. J. *Angew. Chem., Int. Ed. Engl.* **1988**, *27*, 1550–1553. (g) Ashton, P. R.; Goodnow, T. T.; Kaifer, A. E.; Reddington, M. V.; Slawin, A. M. Z.; Spencer, N.; Stoddart, J. F.; Vicent, C.; Williams, D. J. *Angew. Chem., Int. Ed. Engl.* **1989**, *28*, 1396–1399.

charges positioned appropriately.

Synthesis. 1/4DHB was alkylated with 2-(2-chloroethoxy)-ethanol (K_2CO_3, DMF) and 2-[2-(2-chloroethoxy)ethoxy]ethanol (*t*-BuOK, *t*-BuOH) to give BHEEB and BHEEEB, respectively. Tosylation (TsCl, Et_3N, CH_2Cl_2) of BHEEB afforded BTEEB. Alkylation (*t*-BuOK, *t*-BuOH, THF) of 1/4DHB with 2-[2-[2-[2-(benzyloxy)ethoxy]ethoxy]ethoxy]ethyl tosylate,[48] followed by de-O-benzylation (H_2, Pd/C, CH_2Cl_2–MeOH) of the product (BBEEEEB), yielded BHEEEEB. The bis(silyl ethers) BSEEB and BSEEEB were obtained by silylation (*i*-Pr_3SiOTf, imidazole, CH_2Cl_2) of BHEEB and BHEEEB, respectively. Reaction (NaH, DMF) of 4-(benzyloxy)phenol with tetraethylene glycol bistosylate followed by de-O-benzylation (H_2, Pd/C, $CHCl_3$–MeOH) gave BHPTU. BPP34C10 was obtained (Scheme II) in very similar yields (25 and 28%, respectively) by two different routes: (i) cyclization (NaH, THF) of BHPTU with tetraethylene glycol bistosylate and (ii) cyclization (NaH, THF) of BHEEB with its derived bistosylate, BTEEB. The cyclophane [BBIPYBIXYCY][PF_6]$_4$ was prepared initially in two steps, the second of which is shown in Scheme III. Reaction (MeCN under reflux) of 4,4′-bipyridine and 1,4-bis(bromomethyl)benzene yielded, after anion exchange (NH_4PF_6, H_2O), the known[49] [BBIPYXY][PF_6]$_2$, which was cyclized (again, MeCN under reflux) with 1 molar equiv of 1,4-bis(bromomethyl)benzene to give, once again after anion exchange (NH_4PF_6, H_2O), the tetracationic cyclophane as its hexafluorophosphate in 12% yield. This low yield was reproducible and could only be improved substantially by one of a number of interesting procedural variations. One moderately successful procedure was to perform the reaction *at room temperature* in the presence of a 3 molar excess of the template (Scheme IV). Among the many potential neutral molecule templates that were evaluated, BHEEB and BHEEEB increased the yields of the tetracationic cyclophane to 35 and 23%, respectively. By contrast, 1/4DMB and BHEB were both totally ineffectual as templates. Under the template-directed procedure, the product, which is isolated in the beginning, is the deep orange 1:1 complex formed between the diol and the tetracationic cyclophane. Decomplexation is easily achieved by continuous liquid–liquid extraction of an aqueous solution of the complex with CH_2Cl_2. The separation, which can be followed conveniently by the gradual disappearance of the orange color from the aqueous layer, takes several days. The templating diol is recovered almost quantitatively from the organic phase, and the aqueous phase contains almost pure tetracationic cyclophane. Next, it was discovered that, by replacing MeCN by DMF as solvent[50] and adding a catalytic amount of NaI, the template-directed synthesis of [BBIPYBIXYCY][PF_6]$_4$ could be increased in its overall efficiency, giving a 45% yield of the same product. On carrying out the same reaction at ultrahigh[51] pressure (10 kbars), the yield of the tetracationic cyclophane was raised even further to 62%. When either BHEEB or BHEEEB was treated (Scheme V) with *i*-Pr_3SiOTf in MeCN containing [BBIPYBIXYCY][PF_6]$_4$ and a suitably hindered base (lutidine), the [2]rotaxanes (n = 1 and 2) incorporating BSEEB and BSEEEB threads were both isolated in 22% yields following anion exchange (NH_4PF_6, H_2O); i.e., both {[2]-[BSEEB]-[BBIPYBIXYCY]rotaxane}[PF_6]$_4$ and {[2]-[BSEEEB]-[BBIPYBIXYCY]rotaxane}[PF_6]$_4$ can be prepared by the threading procedure. Although it was not possible to prepare the [2]rotaxane incorporating BSEEEB by a clipping procedure, {[2]-[BSEEEB]-[BBIPYBIXYCY]rotaxane}[PF_6]$_4$ was obtained (Scheme IV with n = 2 and R′ = *i*-Pr_3Si) in a modest 14% yield by reacting [BBIPYXY][PF_6]$_2$ and 1,4-bis(bromomethyl)benzene in MeCN in the presence of 3 molar equiv of

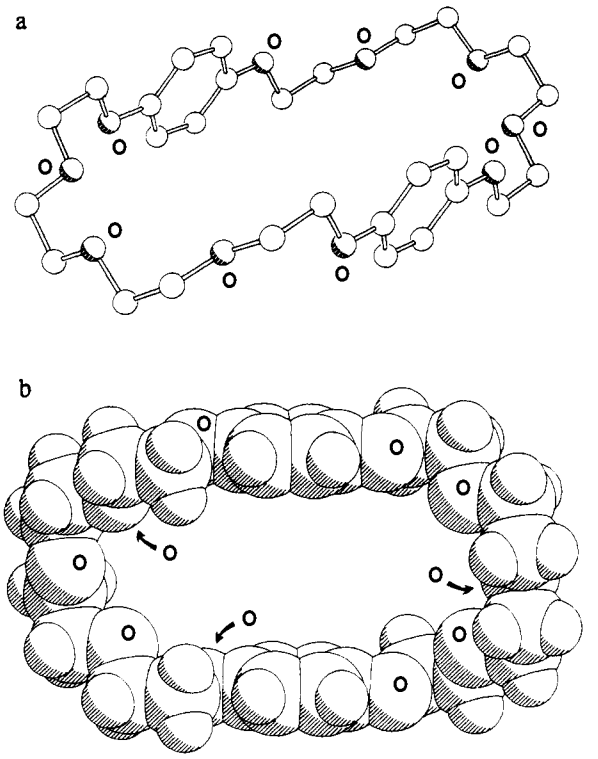

Figure 3. Ball-and-stick (a) and space-filling (b) representations of the solid-state structure of BPP34C10.

BSEEEB, followed by anion exchange (NH_4PF_6, H_2O) in the usual manner. By pursuing a similar clipping procedure, this time in the presence of 3 molar equiv of BPP34C10 (Scheme VI) rather than BSEEEB and employing the familiar workup routine, {[2]-[BPP34C10]-[BBIPYBIXYCY]catenane}[PF_6]$_4$ was isolated in a remarkable 70% yield.

Since the [BBIPYXY]$^{2+}$ dication appears *not*[52] to be complexed by BPP34C10, we are led to propose tentatively (Scheme VI) a mechanism for the formation of the [2]catenane that involves the production of a tricationic intermediate[53] in free solution, which then threads its way through the BPP34C10 macrocyclic ring, thus forming an intermediate 1:1 complex. The nature of the reaction template is such that entropically, and possibly even enthalpically,[54] the final intramolecular cyclization to give {[2]-[BPP34C10]-[BBIPYBIXYCY]catenane}[PF_6]$_4$ is highly favored. It is intriguing that the molecular assembly containing the tetracationic macrocycle is a lot easier to synthesize than is [BBIPYBIXYCY][PF_6]$_4$ by itself. Contrast the 70% and 12% yields, respectively, in MeCN and reflect on the fact that the [2]catenane is formed in good yield at room temperature, whereas the tetracationic macrocycle is only isolated in poor yield after heating under reflux in MeCN. The clipping process to form (Scheme IV) the {[2]-[BSEEEB]-[BBIPYBIXYCY]rotaxane}-[PF_6]$_4$ is understandably less efficient (14% yield) than it is in the case of the preparation of the [2]catenane. Whatever the detailed reasons for the better yields of these molecular assemblies compared with the tetracationic macrocycle, the influence of the template directing factors during the synthesis of these molecular assemblies is profound. The efficiencies of reactions can also be controlled by a variety of means, e.g., by opting for highly polar solvents such as DMF, by introducing a template into the reaction

(48) Beadle, J. R.; Korzenoiski, S. H.; Rosenberg, D. E.; Garcia-Slauge, B. J.; Gokel, G. W. *J. Org. Chem.* **1984**, *49*, 1594–1603.

(49) (a) Geuder, W.; Hünig, S.; Suchy, A. *Angew. Chem., Int. Ed. Engl.* **1983**, *22*, 489–490. (b) *Tetrahedron* **1986**, *42*, 1665–1677.

(50) Pietraszkiewicz, M.; Salanski, P.; Ostaszewski, R.; Jurczak, J. *Heterocycles* **1986**, *24*, 1203–1204.

(51) Jurczak, J.; Ostaszewski, R.; Pietraszkiewicz, M.; Salanski, P. *J. Inclusion Phenom.* **1987**, *5*, 553–561. For a review of the use of ultrahigh pressures in chemical synthesis, see: Isaacs, N. S.; George, A. V. *Chem. Br.* **1987**, *23*, 47–54.

(52) When solutions of [BBIPYXY][PF_6]$_2$ and BPP34C10 in MeCN are mixed together, there is no orange coloration associated with charge transfer nor is there any appreciable change in the ^{1}H NMR spectrum of the equimolar mixture compared with the spectra of the two separate components.

(53) The [PQT]$^{2+}$ dication is a good model for this trication. Its bis(hexafluorophosphate) forms a strong 1:1 complex (K_a = 730 M^{-1}) with BPP34C10 in Me_2CO.

(54) It is not unlikely that the nucleophilicity of the nitrogen lone pair in the intermediate is enhanced by the π-donating ability of the stacked hydroquinol residue.

Table I. Distances[a] (Angstroms) and Angles[a] (Degrees) Characterizing the Molecular and Supramolecular Geometries of [BBIPYBIXYCY][PF_6]$_4$ and its 1:1 Complexes with 1/4DMB, BHEEB, BHEEEB, BHEEEEB, {[2]-[BSEEB]-[BBIPYBIXYCY]-Rotaxane}[PF_6]$_4$, {[2]-[BSEEEB]-[BBIPYBIXYCY]Rotaxane}[PF_6]$_4$, and {[2]-[BPP34C10]-[BBIPYBIXYCY]Catenane}[PF_6]$_4$

compound or complex	θ[b]	ψ[c]	ϕ[d]	τ[e]	O(a)[f]	O(b)[f]	O(c)[f]	O(d)[f]	O(e)[f]	Z···Z[g]	X···Y[h]	H···Y[i]	X–Y···Y[j]
[BBIPYBIXYCY][PF_6]$_4$	19	23	14							6.8			
[1/4DMB·BBIPYBIXYCY][PF_6]$_4$	4	24	13	45	3.94					6.9	4.8	2.9	156
[BHEEB·BBIPYBIXYCY][PF_6]$_4$	20	30	8	52	4.07	4.39	3.79			7.2	5.0	2.8	165
[BHEEEB·BBIPYBIXYCY][PF_6]$_4$	4	22	11	47	3.93	4.28	3.90	3.36		7.0	5.1	2.8	159
[BHEEEEB·BBIPYBIXYCY][PF_6]$_4$	12	25	12	50	4.06	4.38	3.87	3.25	3.40	6.9	5.1	2.8	165
{[2]-[BSEEB]-[BBIPYBIXYCY]rotaxane}[PF_6]$_4$[k,l]	6	32	4	80	*m*	*m*	*m*	*m*	*m*	7.5	5.0	*m*	*m*
	26	29	5	72	*m*	*m*	*m*	*m*	*m*	7.4	5.0	*m*	*m*
{[2]-[BSEEEB]-[BBIPYBIXYCY]rotaxane}[PF_6]$_4$[n]	19	26	10	46	4.06	4.28	3.99	6.53		7.1	5.1	2.9	160
{[2]-[BPP34C10]-[BBIPYBIXYCY]catenane}[PF_6]$_4$	6	24	10	47	3.98	4.42	4.16	3.34	3.88	7.1	5.1	2.8	166
	6	26	14		4.25	4.51	4.00	4.20	4.57		5.2	2.9	157

[a] The distances and angles can be appreciated more easily by reference to diagrams A, B, and C below:

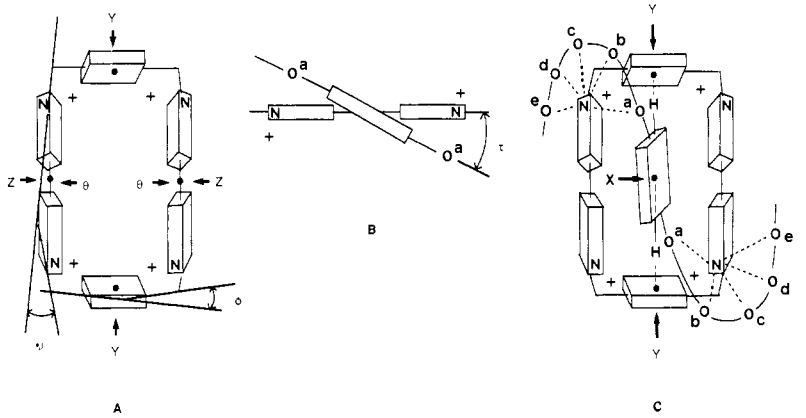

A B C

[b] The twist angle θ is defined as the average of the moduli of the four C–C–C–C torsional angles about the central C–C bond within the bipyridinium residues, the anti torsional angles being reduced to 180° − α. [c] The bowing of the *p*-xylylene residues is expressed by the angle ϕ, subtended by the two C–CH_2 bonds emanating from the *p*-phenylene rings. [d] The bowing of the paraquat residues is expressed by the angle ψ, subtended by the two N^+–CH_2 bonds emanating from the bipyridinium rings. [e] The twist angle τ is defined as the angle between the O^a–O^a and N^+–N^+ vectors. [f] Distances from N^+ in the pyridinium ring encircled by the polyether chain. [g] Width of the tetracationic cyclophane. [h] Centroid–centroid distance. [i] H–centroid distance. [j] Angle at the H atom involved in the edge-to-face interaction. [k] There are two sets of data for {[2]-[BSEEB]-[BBIPYBIXYCY]rotaxane}[PF_6]$_4$ because there are two independent molecules in the unit cell. [l] The Si···Si distances in the two independent molecules are 15.9 and 16.2 Å. [m] Because of the near-normal arrangement of the hydroquinol residues with respect to the bipyridinium units, it would not be meaningful to quote these distances. [n] The Si···Si distance is 22.8 Å.

flask (Scheme IV), and by running reactions at ultrahigh pressures. Nowhere in the final step, however, is there a need for reagent or catalyst control. The substrate molecules are "intelligent" enough by themselves to dictate the outcome of their reactions. This is a concept that is now set to undergo rapid development as new synthetic methodologies are developed for the construction of supramolecular and polymolecular structures.

X-ray Crystal Structures. In the solid state, BPP34C10 exists (Figure 3) in two crystallographically independent conformations, both possessing centers of symmetry and both displaying unusually open conformations. The two opposite hydroquinol residues are approximately in register with respect to each other and separated by ca. 7.2 Å between their mean planes. The plane described by each hydroquinol residue extends to include not only the phenoxymethylene units as expected[55] but also the "next" carbon atom in each direction along the polyether chains. The resulting free pathway of ca. 10.6 × 4.7 Å through the center of the macrocycle is of suitable dimensions to permit the insertion of a π-electron-deficient aromatic ring system between the two π-electron-rich hydroquinol units.

The solid-state structure (Figure 4) of the 1:1 complex formed between the $[PQT]^{2+}$ dication and BPP34C10 showed that the π-electron-deficient bipyridinium ring system is indeed inserted through the center of the macrocycle with retention of a centrosymmetric geometry, the terminal methyl groups of the $[PQT]^{2+}$ dication protruding above and below the periphery of the macrocyclic ring in a pseudorotaxane-like manner (Figure 4a). The interplanar separation between each of the bipyridinium rings and the hydroquinol units is 3.7 Å. Despite this slightly large separation for a π-stacking interaction, a key feature of both the solution- and solid-state complexes is a deep red coloration, demonstrating the presence of significant charge-transfer interactions between host and guest. Along with other dispersive and electrostatic forces, including weak [C–H···O] hydrogen bonding, these interactions combine together with van der Waals interactions to stabilize this 1:1 complex.

The interactions observed in the $[BPP34C10{\cdot}PQT]^{2+}$ complex dication suggested (Figure 4) the possibility of reversing the host–guest roles by creating a cyclophane-like receptor for neutral and π-electron-rich hydroquinol units incorporating two bipyridinium units separated by ca. 7 Å. This led to the identification of the tetracationic cyclophane $[BBIPYBIXYCY]^{4+}$ as a potential host. The single-crystal X-ray structure (Figures 5a and 6a) revealed this cyclophane to have an open centrosymmetric shape of overall dimensions ca. 6.8 × 10.3 Å. A notable feature of both the bipyridinium and *p*-xylylene units is the significant distortion from normal planar geometry involving both twisting (θ = 19°) and bowing (ψ, ϕ = 23, 14°) of the aromatic rings (see Table I). These are almost certainly occasioned by the desire of each of the four methylene links to retain their near-tetrahedral geometries (108 and 109°).

The extension of the host–guest role concept is demonstrated convincingly by the 1:1 complexes formed between the tetracationic cyclophane $[BBIPYBIXYCY]^{4+}$ and 1/4DMB (Figures 5b, 6b, and 7a), BHEEB (Figures 5c, 6c, and 7b), BHEEEB (Figures 5d, 6d, and 7c), and BHEEEEB (Figures 5e, 6e, and 7d). In all

(55) This geometry favors delocalization of oxygen lone pairs into the π-system of the aromatic ring. Cf. Makriyannis, A.; Fesik, S. *J. Am. Chem. Soc.* **1982**, *104*, 6462–6463. Kruse, L. I.; Cha, J. K. *J. Chem. Soc., Chem. Commun.* **1982**, 1329–1331. Mersch, J. D.; Sanders, J. K. M.; Matlin, S. A. *J. Chem. Soc., Chem. Commun.* **1983**, 306–307.

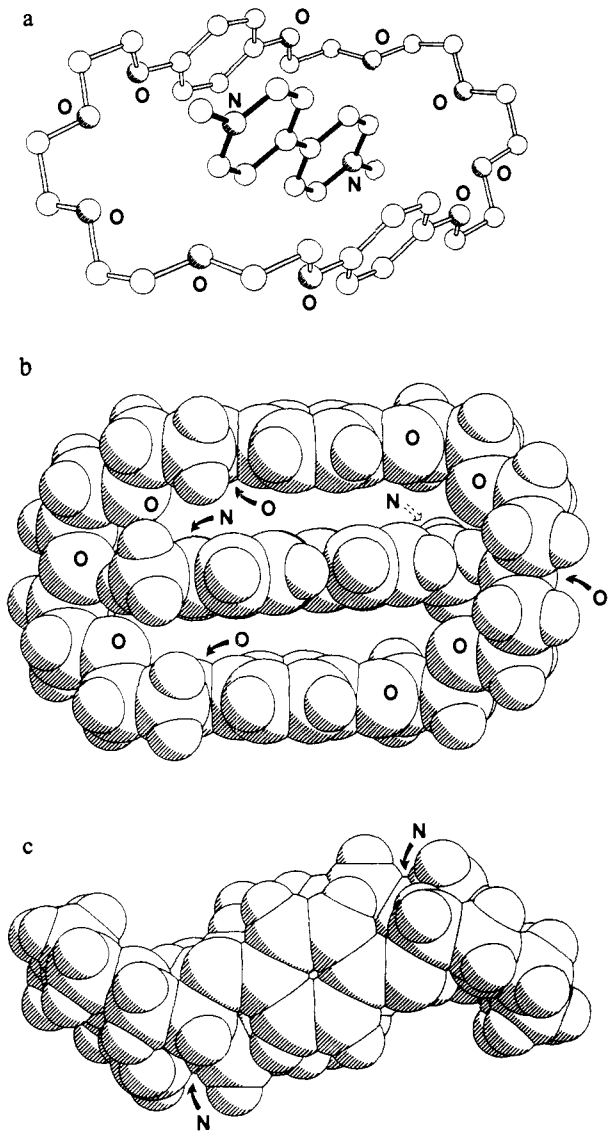

Figure 4. Ball-and-stick (a) and space-filling (b and c) representations of the solid-state structure of $[PQT{\cdot}BPP34C10]^{2+}$.

of these complexes, the neutral guest can be inserted rotaxane-like centrosymmetrically through the center of the tetracationic cyclophane with interplanar separations between the π-electron-rich and π-electron-deficient aromatic rings in the range 3.4–3.6 Å (see Table I).[54] There is a remarkable degree of consistency in the tilt (τ = 45–52°) of the O–C_6H_4–O axis of the guest threads relative to the bipyridinium N^+–N^+ vector in the host's beads. There is no immediately obvious correlation between the degrees of distortion (Table I) in the geometries of the tetracationic cyclophane beads and the size of the threads. The bipyridinium units are distorted from the normal planar geometries, involving both twisting (θ = 4–20°) and bowing (ψ = 22–30°) of their aromatic rings. The *p*-xylylene units also experience bowing (ϕ = 8–13°). After emerging from the centers of the tetracationic cyclophane beads, the polyether tails of the neutral threads are directed over and around two diametrically opposite corners of the macrocycle. Within the series, there is a reasonable degree of consistency in the separation of the oxygen atoms in the tails of the threads and a nitrogen atom carrying a formal positive charge on the bead. These reach a maximum for O(b) at ca. 4.4 Å and a minimum for O(d) at ca. 3.3 Å.

The natural progression to the actual rotaxanes themselves entails the incorporation of bulky (triisopropylsilyl)oxy terminal groups on both ends of a thread. In the single-crystal X-ray structure of {[2]-[BSEEEB]-[BBIPYBIXYCY]rotaxane}$^{4+}$, it is demonstrated (Figures 8a, 9a, and 10a) that the bead is still positioned as expected around the central hydroquinol unit of the thread, in a geometry not too dissimilar from that of the 1:1 complex, [BHEEEB·BBIPYBIXYCY]$^{4+}$, itself. As previously noted for the 1:1 complexes, the polyether tails are similarly disposed at opposite corners of the tetracationic macrocycle. With respect to the nitrogen atoms carrying the formal charges on the bead, they reach a maximum of ca. 6.5 Å for O(e)—the oxygen atoms bonded directly to the silicon atoms—and achieve a minimum for O(d) at ca. 4.0 Å. Clearly, the terminal triisopropylsilyl groups are of sufficient size to prevent unthreading from taking place. Reduction in the length of the polyether tails by one bis(methylenoxy) unit results (Figures 8b, 9b, and 10b) in a dramatic change in the structure of this smaller rotaxane, {[2]-[BSEEB]-[BBIPYBIXYCY]-rotaxane}$[PF_6]_4$, for which there are two independent molecules found to be present in the crystal. In both molecules, the central hydroquinol residues are oriented to give near-normal tilt angles with respect to the planes of the macrocycles, and the polyether chains are folded over the central regions of the bipyridinium units. This gross change in overall shape of this rotaxane is presumably forced upon it by the significant reductions in the distances separating the balls at the termini of the threads (Si···Si, 15.9 and 16.2 Å). It is interesting to recall that, whereas {[2]-[BSEEEB]-[BBIPYBIXYCY]rotaxane}$[PF_6]_4$ may be synthesized by using either a threading or a clipping mechanism, only the threading mechanism successfully led to the preparation of {[2]-[BSEEB]-[BBIPYBIXYCY]rotaxane}$[PF_6]_4$. The values for the twist angle (θ) and for those angles (ψ and ϕ) associated with the bowing of the aromatic residues in the beads are similar to the values quoted previously for the 1:1 complexes. However, the interplanar separations of ca. 3.7–3.8 Å between the π-electron-rich and π-electron-deficient aromatic rings in the smaller and atypical rotaxane are the largest observed (Table I) in the series so far.

The single-crystal X-ray structure (Figures 11–13) of {[2]-[BPP34C10]-[BBIPYBIXYCY]catenane}$[PF_6]_4$ reveals the expected alternating π-donor/π-acceptor stacking interactions in the molecule as a consequence of the threading of the BPP34C10 macrocyclic polyether through the [BBIPYBIXYCY]$^{4+}$ tetracationic macrocycle and vice versa. The mean plane separations of 7.0 Å between the two hydroquinol rings and of 7.1 Å between the two bipyridinium rings equate with interplanar separations of ca. 3.5 Å between the π-donors and π-acceptors. Clearly, one hydroquinol is "inside" and the other is "alongside" the [BBIPYBIXYCY]$^{4+}$ tetracationic macrocycle, while, of course, one bipyridinium unit is "inside" and the other is "alongside" the BPP34C10 macrocyclic polyether. Whereas the "inside" hydroquinol ring has an anti geometry associated with the conformation of the phenoxymethylene units, as in BPP34C10 (Figures 3a and 4a) and the $[BPP34C10{\cdot}PQT]^{2+}$ complex dication (Figures 3b and 4b), the "alongside" hydroquinol unit adopts a conformation with syn geometry. The distances of the oxygen atoms in the polyether chains from the closest nitrogen atom with its formal positive charge vary between 3.34 and 4.57 Å. The values for the twist angles (θ) and for those other angles (ψ and ϕ) associated with the bowing of the aromatic residues in the [BBIPYBIXYCY]$^{4+}$ tetracationic macrocycle are similar (Table I) to the values quoted previously for the 1:1 complexes and the [2]rotaxanes. As previously noted, these distortions reflect the desire of the four methylene links to retain near-tetrahedral geometries (N^+–C–C angles of 106, 107, 108, and 109°).

In all of the solid-state structures involving the [BBIPYBIXYCY]$^{4+}$ tetracationic macrocycle, with the exception of the atypical [2]rotaxane {[2]-[BSEEB]-[BBIPYBIXYCY]rotaxane}$[PF_6]_4$, there are weak edge-to-face interactions between the orthogonally aligned *p*-phenylene units in the tetracations and the included hydroquinol rings. The centroid–centroid distances (Table I) vary from 4.8 to 5.2 Å with the associated H–centroid distances of 2.8–2.9 Å for the electropositive hydrogen atoms on the included hydroquinol rings that are oriented more or less directly into the centers of the π-systems associated with the *p*-phenylene units; the angles subtended at these hydrogen atoms span from 156 to 165°. Examples of these electrostatic T-type

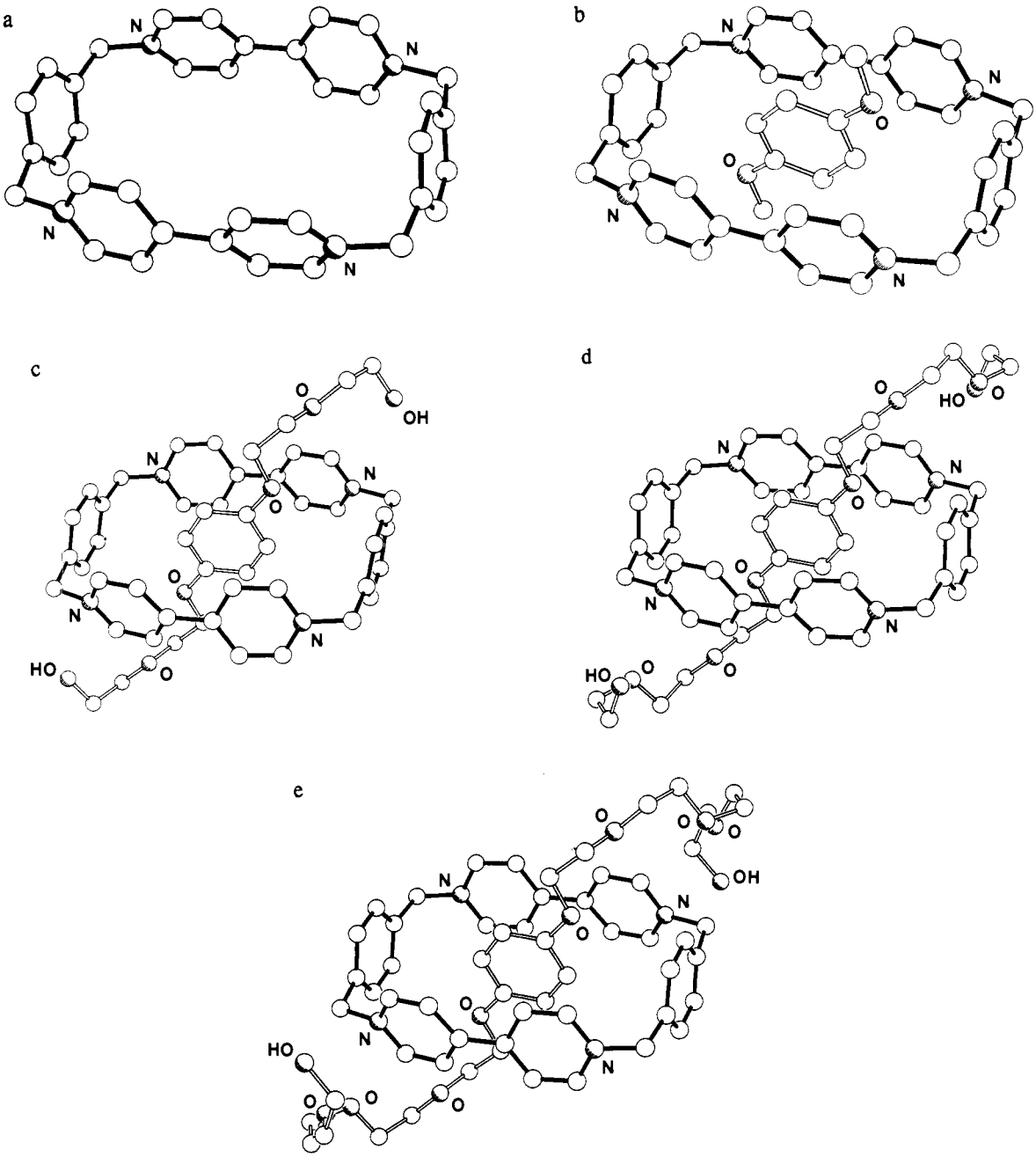

Figure 5. Ball-and-stick representations of the solid state structures of (a) $[BBIPYBIXYCY]^{4+}$, (b) $[1/4DMB\cdot BBIPYBIXYCY]^{4+}$, (c) $[BHEEB\cdot BBIPYBIXYCY]^{4+}$, (d) $[BHEEEB\cdot BBIPYBIXYCY]^{4+}$, and (e) $[BHEEEEB\cdot BBIPYBIXYCY]^{4+}$.

interactions, involving orthogonally disposed aromatic rings, are well-documented[56] in the literature in a broader context. They are undoubtedly responsible for conferring some additional modest stabilization upon the 1:1 complexes and are also presumably the source of a further moderately stabilizing influence, over and above that provided by the π-stacking,[57] upon the solid-state structures of the [2]rotaxanes and the [2]catenane.

FABMS. Although ions characteristic of the 1:1 complexes formed between $[BBIPYBIXYCY][PF_6]_4$ and 1/4DMB and BHEB were not observed by FABMS, peaks corresponding to $[M - 2PF_6]^+$ were observed (Table II) for the 1:1 complexes involving BHEEB, BHEEEB, and BHEEEEB. These observations correlate well with the relative stabilities (see Table III for K_a values) of these 1:1 complexes. Both [2]rotaxanes and the [2]catenane (Figure 14) produced ions characteristic of the successive loss of PF_6 units from the molecular ion. In all cases, ions were observed at m/z 955, 810, and 665 for the $[M - PF_6]^+$, $[M - 2PF_6]^+$, and $[M - 3PF_6]^+$ ions arising from $[BBIPYBIXYCY][PF_6]_4$.

Stability Constants. Table III lists the stability constants and derived free energies of complexation for the 1:1 complexes formed between $[BBIPYBIXYCY][PF_6]_4$ and 1/4DMB, BHEB, BHEEB, BHEEEB, and BHEEEEB, obtained spectrophotometrically in acetonitrile at 25 °C for the equilibrium $G + H \rightleftarrows G\cdot H$, where G is the guest (i.e., 1/4DMB, BHEB, BHEEB, BHEEEB, or BHEEEEB), H is the host (i.e., $[BBIPYBIXYCY][PF_6]_4$), and G·H is the 1:1 complex formed between them. As usual, the K_a and $-\Delta G°$ values are given by

$$K_a = [G\cdot H]/[G][H] \quad (1)$$

and

$$-\Delta G° = RT \ln K_a \quad (2)$$

(56) For discussions on edge-to-face interactions involving aromatic ring systems, see: Gould, R. O.; Gray, A. M.; Taylor, P.; Walkinshaw, M. D. *J. Am. Chem. Soc.* **1985**, *107*, 5921–5927. Burley, S. K.; Petsko, G. A. *J. Am. Chem. Soc.* **1986**, *108*, 7995–8001. Jorgensen, W. L.; Severance, D. L. *J. Am. Chem. Soc.* **1990**, *112*, 4768–4774.

(57) For a recent discussion of the nature of π–π interactions between aromatic rings, see: Hunter, C. A.; Sanders, J. K. M. *J. Am. Chem. Soc.* **1990**, *112*, 5525–5534.

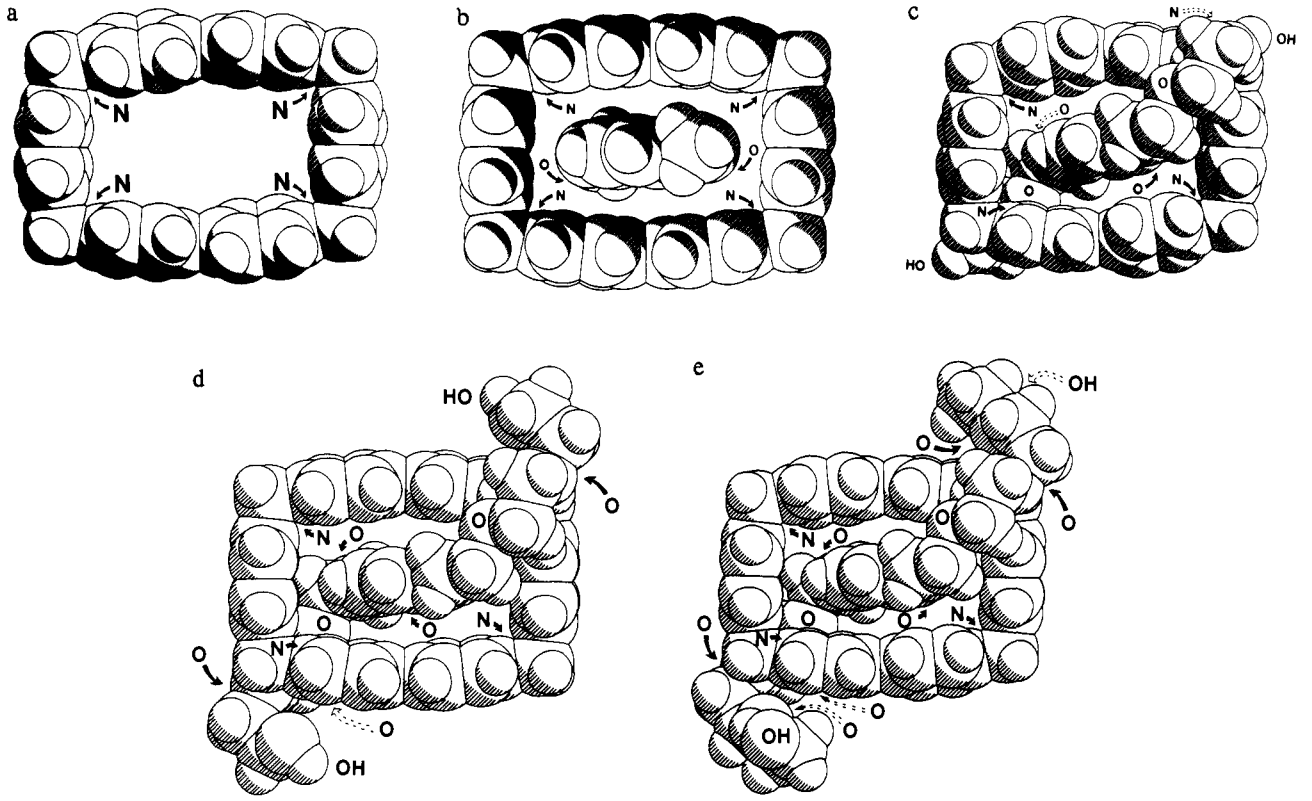

Figure 6. Plan views of the space-filling representations of the solid-state structures of (a) $[BBIPYBIXYCY]^{4+}$, (b) $[1/4DMB\cdot BBIPYBIXYCY]^{4+}$, (c) $[BHEEB\cdot BBIPYBIXYCY]^{4+}$, (d) $[BHEEEB\cdot BBIPYBIXYCY]^{4+}$, and (e) $[BHEEEEB\cdot BBIPYBIXYCY]^{4+}$.

Table II. FABMS[a] Data for $[BBIPYBIXYCY][PF_6]_4$ and its 1:1 Complexes with 1/4DMB, BHEB, BHEEB, BHEEEB, BHEEEEB, {[2]-[BSEEB]-[BBIPYBIXYCY]Rotaxane}$[PF_6]_4$, {[2]-[BSEEEB]-[BBIPYBIXYCY]Rotaxane}$[PF_6]_4$, and {[2]-[BPP34C10]-[BBIPYBIXYCY]Catenane}$[PF_6]_4$

compound or complex	M[b]	M − PF_6	M − $2PF_6$	M − $3PF_6$
$[BBIPYBIXYCY][PF_6]_4$	1100	955	810	665
$[1/4DMB\cdot BBIPYBIXYCY][PF_6]_4$	1238	(1093)[c]	(948)	(803)
$[BHEB\cdot BBIPYBIXYCY][PF_6]_4$	1298	(1153)	(1008)	(863)
$[BHEEB\cdot BBIPYBIXYCY][PF_6]_4$	1386	(1241)	1096	(951)
$[BHEEEB\cdot BBIPYBIXYCY][PF_6]_4$	1474	(1329)	1184	(1039)
$[BHEEEEB\cdot BBIPYBIXYCY][PF_6]_4$	1562	(1417)	1272	(1127)
{[2]-[BSEEB]-[BBIPYBIXYCY]rotaxane}$[PF_6]_4$	1698	1553	1408	(1263)
{[2]-[BSEEEB]-[BBIPYBIXYCY]rotaxane}$[PF_6]_4$	1786	1641	1496	1351
{[2]-[BPP34C10]-[BBIPYBIXYCY]catenane}$[PF_6]_4$	1636	1491	1346	1201

[a] FABMS were obtained with a Kratos MS80RF mass spectrometer coupled to a DS90 data system. The atom gun (Ion Tech Limited) was operated at 7 keV with a tube current of 2 mA; the primary beam of atoms was produced from research grade xenon. Samples were dissolved in a small amount of 3-nitrobenzyl alcohol that had been coated onto a stainless steel probe, and spectra were recorded in the positive ion mode at a scan speed of 30 s per decade. [b] The molecular weight of the tetrakis(hexafluorophosphate). [c] The numbers in parentheses refer to peaks that were not observed.

Table III. Stability Constants (K_a) and Derived Free Energies of Complexation ($-\Delta G°$) for the 1:1 Complexes Formed Between $[BBIPYBIXYCY][PF_6]_4$ and 1/4DMB, BHEB, BHEEB, BHEEEB, and BHEEEEB in Acetonitrile at 25 °C

1:1 complex	K_a (M^{-1})	$-\Delta G°$ (kcal mol^{-1})
$[1/4DMB\cdot BBIPYBIXYCY][PF_6]_4$	17.2 ± 1.5[a]	1.7 ± 0.2
$[BHEB\cdot BBIPYBIXYCY][PF_6]_4$	257 ± 23[b]	3.3 ± 0.5
$[BHEEB\cdot BBIPYBIXYCY][PF_6]_4$	2220 ± 240[b]	4.6 ± 0.6
$[BHEEEB\cdot BBIPYBIXYCY][PF_6]_4$	2241 ± 250[b]	4.6 ± 0.6
$[BHEEEEB\cdot BBIPYBIXYCY][PF_6]_4$	2520 ± 320[b]	4.6 ± 0.7

[a] Determined by spectrophotometric titration at λ = 478 nm. [b] Determined by spectrophotometric titration at λ = 467 nm.

where R is the gas constant and T is the absolute temperature.

It is obvious from the data recorded in Table III that the addition and subsequent extension of polyether chains on to a hydroquinol ring leads to an appreciable enhancement of the binding of the substrate by the tetracationic macrocycle. However, a maximum is quickly reached at BHEEB, where diethylene glycol units are the appendages. It will be recalled that this was the first thread in the series to successfully template the synthesis (Scheme IV) of $[BBIPYBIXYCY][PF_6]_4$. Both the solid-state structures (Table I and Figures 5–7) from X-ray crystallographic studies and the solution-state structures (Table IV) from ^1H NMR spectroscopic investigations provide convincing structural evidence for the important role of the polyether chains in stabilizing the 1:1 complexes formed between $[BBIPYBIXYCY][PF_6]_4$ and the range of hydroquinol-derived threads that have been studied quantitatively. The data recorded in Table III indicate that electrostatic stabilization of the positively charged bipyridinium residues by the oxygen atoms in the polyether chains is slightly more important than the dispersive forces including charge-transfer interactions, which are common to all the 1:1 complexes, in contributing to the overall stabilities of the complexes. The same partitioning of the complexation strength probably also applies to the binding of $[PQT][PF_6]_2$ by BPP34C10. In this case, a charge-transfer band is observed at λ_{max} = 435 nm in acetone for

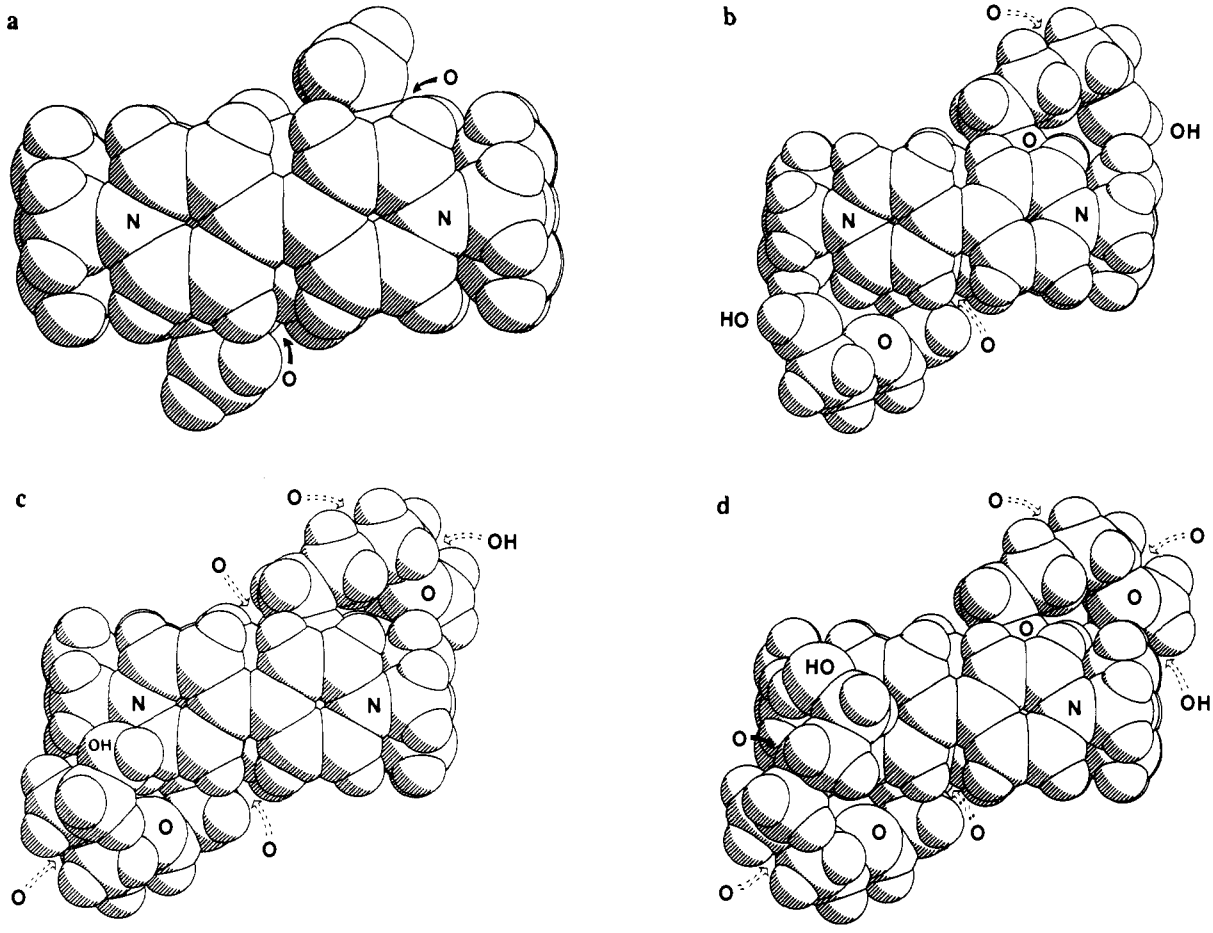

Figure 7. Side-on views of the space-filling representations of solid-state structures of (a) [1/4DMB·BBIPYBIXYCY]$^{4+}$, (b) [BHEEB·BBIPYBIXYCY]$^{4+}$, (c) [BHEEEB·BBIPYBIXYCY]$^{4+}$, and (d) [BHEEEEB·BBIPYBIXYCY]$^{4+}$.

the formation of a 1:1 complex, which has a K_a value of 730 M^{-1} and a corresponding $-\Delta G°$ value of 3.9 kcal mol^{-1} associated with it.

^{1}H NMR Spectroscopy. The ^{1}H NMR chemical shift data, which is listed in Table IV, indicates the formation of the inclusion complexes [PQT·BPP34C10][PF_6]$_2$, [1/4DMB·BBIPYBIXYCY][PF_6]$_4$, [BHEB·BBIPYBIXYCY][PF_6]$_4$, [BHEEB·BBIPYBIXYCY][PF_6]$_4$, [BHEEEB·BBIPYBIXYCY][PF_6]$_4$, and [BHEEEEB·BBIPYBIXYCY][PF_6]$_4$ with 1:1 stoichiometries in acetonitrile (CD_3CN) and with time-averaged supramolecular structures similar to those already characterized in the solid state. In these 1:1 complexes formed with the [BBIPYBIXYCY]$^{4+}$ tetracation, the most significant chemical shift changes are experienced by the β-protons ($\Delta\delta$ = −0.06 to −0.31 ppm) on the bipyridinium rings and the p-phenylene protons ($\Delta\delta$ = +0.06 to +0.28 ppm). The upfield shifts of the former and the downfield shifts of the latter are in accordance with the relative orientation of the hydroquinol rings inside the cavity of the tetracationic cyclophane. This conclusion is supported by the dramatic upfield shifts ($\Delta\delta$ = −0.64 to −2.89 ppm) of the hydroquinol ring protons, at least two of which are simultaneously involved on the average in stabilizing edge-to-face interactions[56] with the two p-phenylene rings in the tetracation. Also of interest is the fact that, whereas the signal for the α-OCH_2 protons is moved upfield ($\Delta\delta$ = −0.11 to −0.46 ppm) on complexation, the signal for the β-OCH_2 protons is moved downfield ($\Delta\delta$ = +0.13 to +0.14 ppm) on complexation. This implies that, on a time-averaged basis, the polyether chains in BHEB, BHEEB, BHEEEB, and BHEEEEB are wrapped around the tetracationic cyclophane in solution in a manner similar to the supramolecular structures observed in the solid state (Figures 5–7) for the 1:1 complexes formed between these threads and the [BBIPYBIXYCY]$^{4+}$ tetracation. The fact that all of the chemical shift changes observed (Table IV) for [1/4DMB·BBIPYBIXYCY][PF_6]$_4$ are a third to a quarter less than those for the threads where the hydroquinol rings carry polyether chains suggests that 1/4DMB is forming only a relatively weak complex with [BBIPYBIXYCY][PF_6]$_4$. This observation is amenable to quantitative assessment by calculating the chemical shift differences of selected protons in the vicinity of aromatic rings from X-ray data and comparing them with those values actually observed (Table IV) in the ^{1}H NMR spectrum. Using the equivalent dipole model[58] of an aromatic ring, it is possible to calculate the shielding effect ($\Delta\delta$) experienced by protons placed above the plane of the aromatic ring. This approach has been applied to some of the 1:1 complexes formed by [BBIPYBIXYCY][PF_6]$_4$ as well as to {[2]-[BSEEB]-[BBIPYBIXYCY]rotaxane}[PF_6]$_4$. In all cases, the protons of the hydroquinol rings, residing inside the cavity of the tetracationic cyclophane, serve as the ideal probe protons. From the equation,

$$\Delta\delta = k(1 - 3\cos^2\alpha)/r^3 \qquad (3)$$

where k is a constant, r is the distance (in angstroms) from the centroid of the aromatic ring to the probe proton, and α is the angle subtended to the normal to the plane of the aromatic ring by the probe proton–centroid vector (Table V), $\Delta\delta$ values can be calculated. The total shielding effect experienced by the hydroquinol protons (H_a and H_b), assuming the solid-state structures, is the sum of the contributions from the orthogonally facing p-xylylene residue and the parallelly aligned pyridinium units. Contributions to $\Delta\delta_a$ and $\Delta\delta_b$ from the other aromatic rings in the tetracationic cyclophane can be ignored since they are <0.005 ppm. However, in the solution state, H_a and H_b will be in fast exchange on the ^{1}H NMR time scale as the result of a "rocking"

(58) Abraham, R. J.; Fell, S. C. M.; Smith, K. M. *Org. Magn. Reson.* **1977**, *9*, 367–373.

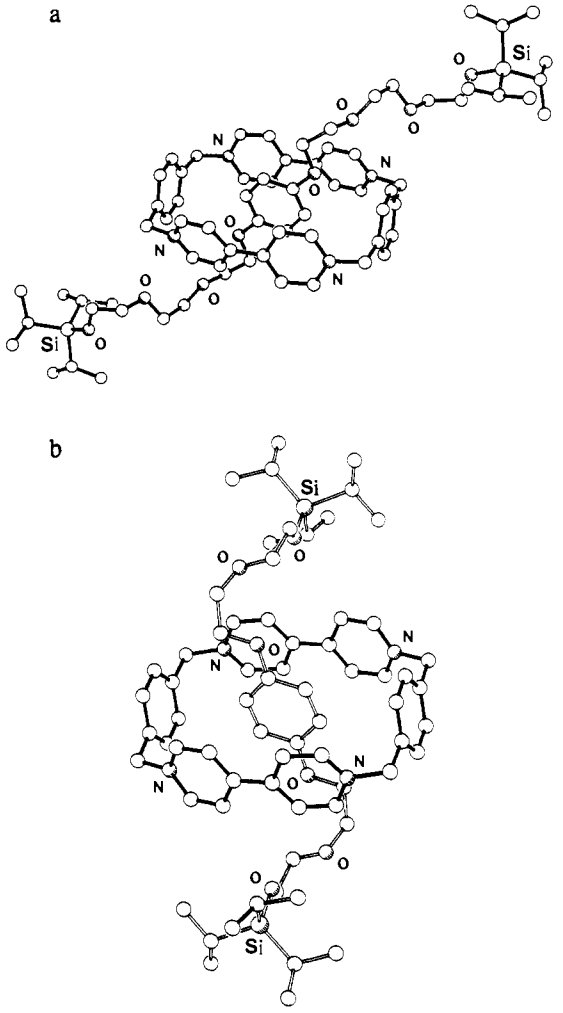

Figure 8. Ball-and-stick representations of the solid-state structures of (a) {[2]-[BSEEEB]-[BBIPYBIXYCY]rotaxane}$^{4+}$ and (b) {[2]-[BSEEB]-[BBIPYBIXYCY]rotaxane}$^{4+}$.

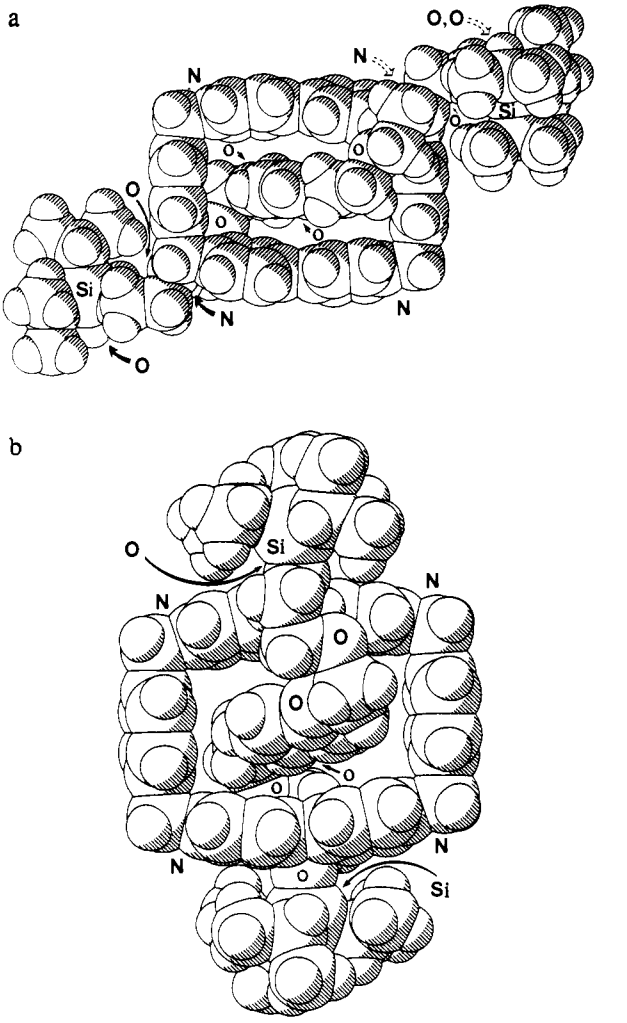

Figure 9. Plan views of the space-filling representations of the solid-state structures of (a) {[2]-[BSEEEB]-[BBIPYBIXYCY]rotaxane}$^{4+}$ and (b) {[2]-[BSEEB]-[BBIPYBIXYCY]rotaxane}$^{4+}$.

motion (Figure 15) of the hydroquinol ring inside the cavity of the tetracationic cyclophane. Because the occupancies of the two (degenerate) forms are 50%, the time-averaged shielding effect on H_a and H_b is given by

$$\Delta\delta(\text{calc 1}) = 0.5(\Delta\delta_a + \Delta\delta_b) \quad (4)$$

The value so obtained for $\Delta\delta$(calc 1) relates to a situation where the stability constant (K_a) is effectively infinite, which is, of course, the case for the [2]rotaxane. However, for the 1:1 complexes, K_a values are finite, and so we must adjust the shielding effect accordingly, making allowance for the fast complexation–decomplexation processes associated with the 1:1 complexes and defined by eqs 1 and 2. If we assume there is a fast exchange on the ^{1}H NMR time scale between bound (i.e., complexed) and unbound guest (G), then the chemical shift difference observed for a ^{1}H probe in G will be the weighted average of the unbound chemical shift difference ($\Delta\delta_u$) and the chemical shift difference ($\Delta\delta_c$) of the probe proton in the 1:1 complex. Although in principle the chemical shift difference, $\Delta\delta$(calc 2), which makes allowance for finite K_a values, can be derived from the fractional occupancies of the unbound (f_u) and complexed (f_c) states with $f_u + f_c = 1$ so that

$$\Delta\delta(\text{calc 2}) = f_u\Delta\delta_u + f_c\Delta\delta_c \quad (5)$$

In practice, since $\Delta\delta_u = 0$, this modified chemical shift difference is given by

$$\Delta\delta(\text{calc 2}) = f_c\Delta\delta_c \quad (6)$$

Using a standard[59] replacement for f_c in eq 6 and recognizing that $\Delta\delta_c$ can be equated with $\Delta\delta$(calc 1) in eq 4, one can derive

$$\Delta\delta(\text{calc 2}) = \frac{K_a[\text{H}]\Delta\delta(\text{calc 1})}{1 + K_a[\text{H}]} \quad (7)$$

Thus, starting from the solid-state structural data, we can obtain $\Delta\delta$(calc 1), and from it, using eq 7, deduce $\Delta\delta$(calc 2) for the hydroquinol protons in the 1:1 complexes. The results are summarized in Table VI and compared with the experimentally observed chemical shift differences, $\Delta\delta$(expt), recorded in Table IV. The comparison is not a good one, and this observation would suggest that the simple model used to obtain the $\Delta\delta$(calc 2) values needs to be modified to account for the additional upfield shifts of the hydroquinol probe protons. If it is assumed that the hydroquinol ring can undergo translation back and forth along the long axis of the tetracationic cyclophane between two preferred and degenerate states by means of a "rattling" process (Figure 15), then a much better match between the calculated and experimental shift differences can be achieved (Table VII). If the guest is allowed to oscillate between two equivalent positions inside the host, such that the center of the hydroquinol ring is displaced by a distance x from the centroid of the tetracationic macrocycle, then revised $\Delta\delta$(calc 1)′ and hence $\Delta\delta$(calc 2)′ values can be obtained. In Table VII, good matches (i.e., to within 10%) have been recorded for $\Delta\delta$(calc 2)′ with $\Delta\delta$(expt) for particular dis-

(59) Connors, K. A. *Binding Constants*; Wiley-Interscience: New York, 1987; pp 189–215.

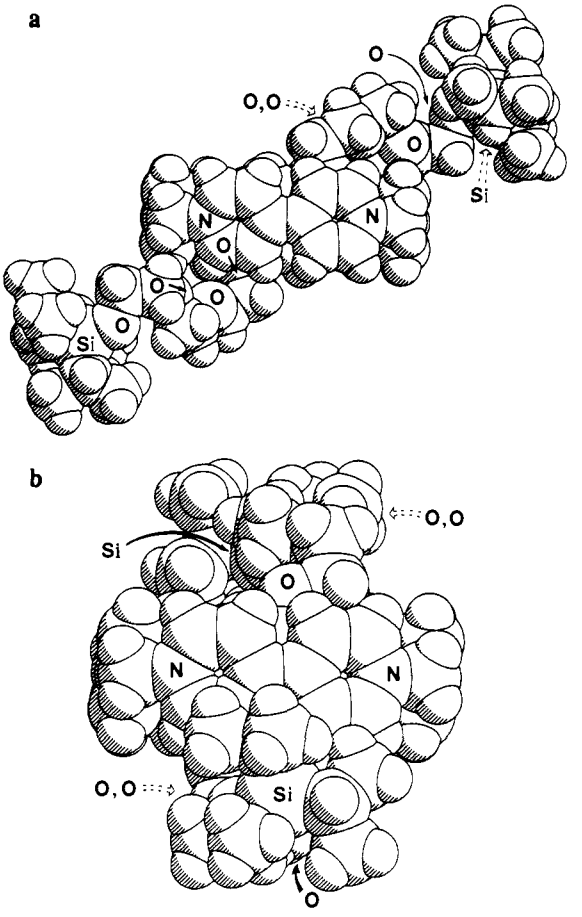

Figure 10. Side-on views of the space-filling representations of the solid-state structures of (a) {[2]-[BSEEEB]-[BBIPYBIXYCY]rotaxane}$^{4+}$ and (b) {[2]-[BSEEB]-[BBIPYBIXYCY]rotaxane}$^{4+}$.

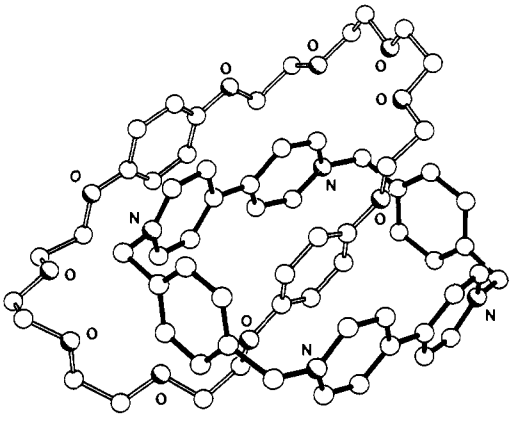

Figure 11. Ball-and-stick representation of the solid-state structure of {[2]-[BBP34C10]-[BBIPYBIXYCY]catenane}$^{4+}$.

placements x. It is therefore tempting to suggest[60] that, although in the solid state of the 1:1 complexes the hydroquinol rings occupy centrosymmetric positions in the cavity of the tetracationic cyclophane for obvious crystallographic reasons, in solution, the guest species are "rattling" as well as "rocking" (Figure 15). Thus, the

(60) It should be added that when the much tighter 1,5-naphtho ring is included inside the cavity of the tetracation, as in, for example, a [2]catenane formed between it and 1,5-dinaphtho-38-crown-10, a similar treatment of ^{1}H NMR chemical shift data revealed that there is a very close correspondence between solution- and solid-state structures, at least in the central zone of the tetracationic cavity comprising this particular [2]catenane. See: Ashton, P. R.; Brown, C. L.; Chrystal, E. J. T.; Goodnow, T. T.; Kaifer, A. E.; Parry, K. P.; Philp, D.; Slawin, A. M. Z.; Spencer, N.; Stoddart, J. F.; Williams, D. J. *J. Chem. Soc., Chem. Commun.* **1991**, 634–639.

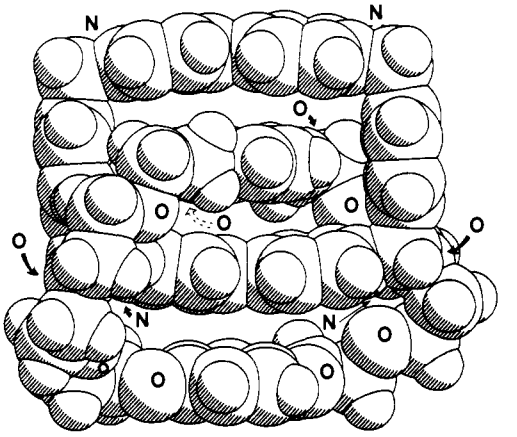

Figure 12. Plan view of the space-filling representation of the solid-state structure of {[2]-[BPP34C10]-[BBIPYBIXYCY]catenane}$^{4+}$.

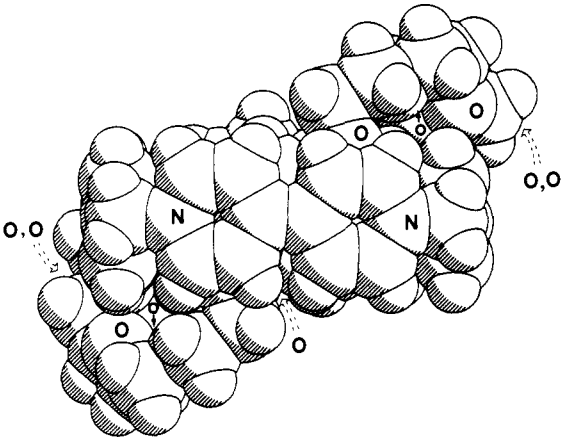

Figure 13. Side-on views of the space-filling representation of the solid-state structure of {[2]-[BPP34C10]-[BBIPYBIXYCY]catenane}$^{4+}$.

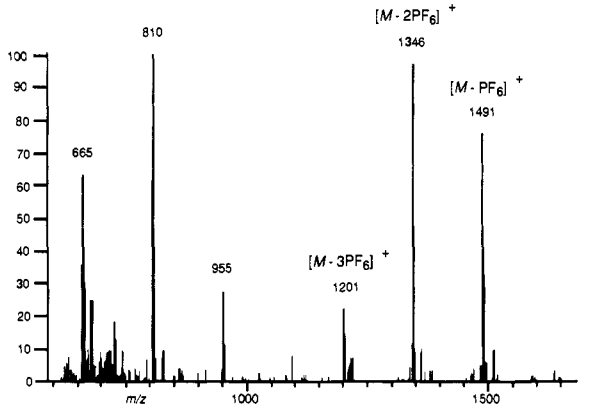

Figure 14. The FABMS of {[2]-[BPP34C10]-[BBIPYBIXYCY]catenane}$[PF_6]_4$.

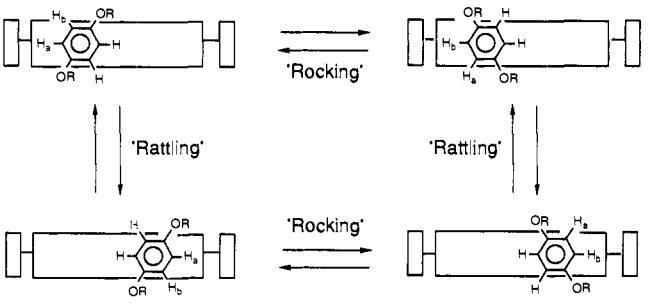

Figure 15. The proposed dynamic behavior within the supramolecular structures of the 1:1 complexes.

Table IV. ^{1}H NMR Chemical Shift Data [δ Values ($\Delta\delta$ Values)][a] for Compounds and Complexes in CD_3CN at Ambient Temperature

	polycationic component				neutral component						
	CH					OCH_2					
compound or complex	α	β	C_6H_4	CH_2N^+	ArH	α	β	γ	δ	ϵ	ζ
BPP34C10					6.73	3.95	3.73	3.59	3.59		
$[PQT][PF_6]_2$	8.83	8.35		4.38[b]							
$[PQT\cdot BPP34C10][PF_6]_2$	8.80	8.07		4.41[b]	6.44	3.69	3.69	3.66	3.66		
	(−0.03)	(−0.28)		(+0.03)[b]	(−0.29)	(−0.26)	(−0.04)	(+0.07)			
1/4DMB					6.84	3.72[c]					
$[BBIPYBIXYCY][PF_6]_4$	8.86	8.16	7.52	5.74							
$[1/4DMB\cdot BBIPYBIXYCY][PF_6]_4$	8.86	8.10	7.58	5.73	6.20	3.61[c]					
	(0.00)	(−0.06)	(+0.06)	(−0.01)	(−0.64)	(−0.11)[c]					
BHEB					6.85	3.95	3.76				
$[BHEB\cdot BBIPYBIXYCY][PF_6]_4$	8.98	7.92	7.72	5.71	4.78	3.71	3.89				
	(+0.03)	(−0.24)	(+0.20)	(−0.03)	(−2.07)	(−0.24)	(+0.13)				
BHEEB					6.85	4.03	3.74	3.58	3.53		
$[BHEEB\cdot BBIPYBIXYCY][PF_6]_4$	8.97	7.85	7.80	5.69	3.96	3.71	3.88	3.86	3.83		
	(+0.11)	(−0.31)	(+0.28)	(−0.05)	(−2.89)	(−0.32)	(+0.14)	(+0.28)	(+0.30)		
BHEEEB					6.84	4.02	3.74	3.58	3.58	3.58	3.48
$[BHEEEB\cdot BBIPYBIXYCY][PF_6]_4$	8.92	7.89	7.74	5.72	4.02	3.68	3.88	3.60	3.60	3.91	3.88
	(+0.06)	(−0.27)	(+0.22)	(−0.02)	(−2.82)	(−0.34)	(+0.14)	(+0.02)	(+0.02)	(+0.31)	(+0.40)
BHEEEEB[d]					6.84	4.05	3.73	3.58	3.58	3.58	3.58
$[BHEEEEB\cdot BBIPYBIXYCY][PF_6]_4$[e]	8.92	7.87	7.77	5.72	4.04	3.69	3.87				
	(+0.06)	(−0.29)	(+0.25)	(−0.02)	(−2.80)	(−0.46)	(+0.13)				
BSEEB					6.82	4.01	3.75	3.82	3.57		
{[2]-[BSEEB]-[BBIPYBIXYCY]-rotaxane}$[PF_6]_4$	8.87	7.83	7.79	5.70	3.56	4.11	3.94	3.94	3.60		
	(+0.01)	(−0.33)	(+0.27)	(−0.04)	(−3.26)	(+0.10)	(+0.19)	(+0.12)	(+0.30)		
BSEEEB					6.82	4.04	3.75	3.62	3.62	3.82	3.55
{[2]-[BSEEEB]-[BBIPYBIXYCY]-rotaxane}$[PF_6]_4$	8.94	7.81	7.80	5.69	3.56	3.64	3.89	3.94	3.94	3.86	3.72
	(+0.08)	(−0.35)	(+0.28)	(−0.05)	(−3.26)	(−0.40)	(+0.14)	(+0.32)	(+0.32)	(+0.04)	(+0.17)
{[2]-[BPP34C10]-[BBIPYBIXYCY]-catenane}$[PF_6]_4$[f]	8.85	7.66	7.79	5.67	3.45[g]	3.36[h]	3.61[h]	3.73[h]	3.88[h]		
	(−0.01)	(−0.50)	(+0.27)	(−0.07)	(−3.28)	(−0.59)	(−0.12)	(+0.14)	(+0.29)		

[a] The $\Delta\delta$ values indicated in parentheses under the respective δ values relate to the chemical shift changes experienced by probe protons in both the substrates (or threads) and the receptors (or beads) on 1:1 complexation or on rotaxane or catenane formation. The OCH_2 groups are labelled α, β, γ, etc starting with the group attached directly to the *p*-phenylene ring and proceeding away from it. They are identified on the structural formula for BPP34C10 in Figure 1. The α and β protons in the $[PQT]^{2+}$ dication and in the $[BBIPYBIXYCY]^{4+}$ tetracation are designated in Figure 2. [b] δ and $\Delta\delta$ values for NCH_3^+. [c] δ and $\Delta\delta$ values for OCH_3. [d] The η-OCH_2 and θ-OCH_2 protons all resonate at δ 3.46. [e] The protons other than the α-OCH_2 and β-OCH_2 protons cannot be assigned, even at 400 MHz. [f] In the [2]catenane, exchange between the "inside" and "alongside" hydroquinol rings is slow, resulting in all of the OCH_2 groups being anisochronous on the ^{1}H NMR time scale. Those OCH_2 groups emanating from the "inside" and "alongside" hydroquinol rings have been labelled α, β, γ, δ and α', β', γ', δ', respectively. [g] The protons on the "alongside" hydroquinol ring resonate at δ 6.16. At 7 °C, saturation transfer and difference spectroscopy show that the signal for the "inside" hydroquinol ring resonates at δ 3.45. [h] The α'-, β'-, γ'-, and δ'-OCH_2 groups resonate at 3.54, 3.83, 3.93, and 3.90, respectively.

time-averaged solution structures of the 1:1 complexes are *not* identical with the solid-state structures in the three cases investigated. In the {[2]-[BSEEB]-[BBIPYBIXYCY]rotaxane}$[PF_6]_4$, it would appear (Tables V and VI) that the "rattling" motion is accentuated, reflecting a looser fit between the hydroquinol ring and the cavity of the tetracationic cyclophane. It will be recalled that the solid-state structure (Figures 8b, 9b, and 10b) of this [2]rotaxane portrays some unique characteristics, probably as a result of steric interactions between the "walls" of the tetracationic cyclophane and the triisopropylsilyl groups at the ends of the relatively short "diethylene glycol" chains. In this regard, it is interesting that the $\Delta\delta$ value (Table IV) of +0.10 ppm for the α-OCH_2 protons contrasts with the negative values observed for these protons in all of the other compounds and complexes. This additional observation indicates that the solution-state structure, like the solid-state one, is the atypical structure in the series. The {[2]-[BPP34C10]-[BBIPYBIXYCY]catenane}$[PF_6]_4$ is a special case where the ^{1}H NMR spectrum also shows temperature dependence. However, before the dynamic ^{1}H NMR spectrum of the [2]catenane is analyzed, the evidence for the assignment of protons in the ^{1}H NMR spectrum will be presented.

In {[2]-[BPP34C10]-[BBIPYBIXYCY]-catenane}$[PF_6]_4$, the chemical shifts (Table IV) of the α-CH protons on the bipyridinium rings of the $[BBIPYBIXYCY]^{4+}$ tetracation were assigned by NOE difference spectroscopy following irradiation at the resonance for the benzylic methylene protons. At room temperature in CD_3CN solution, the BPP34C10 component of the [2]catenane is revolving slowly on the ^{1}H NMR time scale around the tetracationic macrocycle. This dynamic process, which allows a distinction to be made between the signals for the "inside" (δ 3.45) and the "alongside" (δ 6.16) hydroquinol ring protons, is reflected in the observation that all of the OCH_2 proton signals in each equivalent polyether chain, linking the two hydroquinol rings, are anisochronous and resonate between δ 3.30 and δ 4.00.

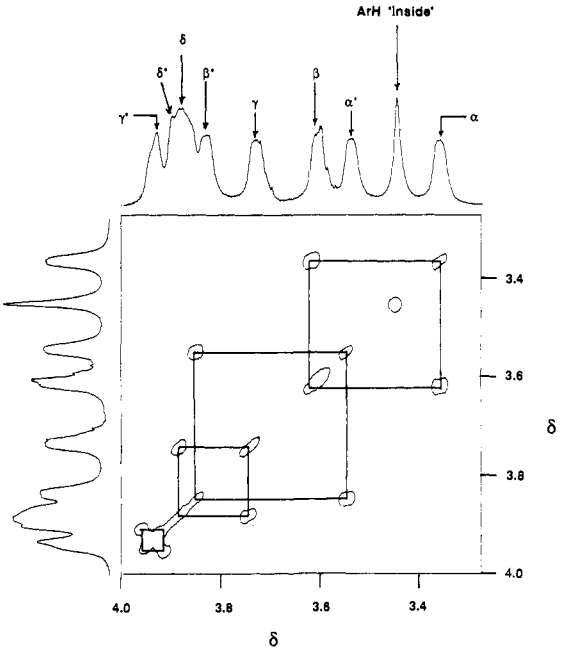

Figure 16. The 2D-COSY 45 spectrum for {[2]-[BPP34C10]-[BBIPYBIXYCY]catenane}$[PF_6]_4$ showing the OCH_2CH_2O connectivities.

Difference NOE spectroscopy performed by irradiating the "inside" hydroquinol ring protons at δ 3.45 at −20 °C allowed us to identify the signal at δ 3.36 as the resonance for the α-OCH_2 protons. The resonances for the β-, γ-, δ-, δ'-, γ'-, β'-, and α'-OCH_2 protons were assigned by coupling connectivity by 2D-COSY 45 (Figure 16) and by 2D-NOESY 45 (Figure 17), which

Table V. Values of r, α, $\Delta\delta_a$, and $\Delta\delta_b$ Obtained[a] from X-ray Data for the Probe Protons H_a and H_b, Respectively[b]

compound or complex	probe proton	aromatic ring[c]	r (Å)	α (°)	$\Delta\delta_a$ or $\Delta\delta_b$ (ppm)
[1/4DMB·BBIPYBIXYCY]-[PF_6]$_4$	H_a	1	3.36	11	−0.70
		2	2.90	8	−2.20
		3	3.46	16	−0.60
	H_b	1	4.35	36	−0.16
		2	5.05	25	−0.31
		3	4.33	40	−0.14
[BHEEEB·BBIPYBIXYCY]-[PF_6]$_4$	H_a	1	3.13	8	−0.88
		2	3.02	12	−1.86
		3	3.49	16	−0.59
	H_b	1	4.09	32	−0.24
		2	5.03	25	−0.32
		3	4.25	40	−0.14
[BHEEEEB·BBIPYBIXYCY]-[PF_6]$_4$	H_a	1	3.47	11	−0.64
		2	2.82	6	−2.43
		3	3.30	8	−0.76
	H_b	1	4.11	26	−0.29
		2	4.75	27	−0.36
		3	4.29	32	−0.21
{[2]-[BSEEB·BBIPYBIXYCY]-rotaxane}[PF_6]$_4$	H_a	1	3.60	24	−0.60
		2	3.27	34	−1.52
		3	3.64	19	−0.58
	H_b	1	4.27	5	−0.28
		2	3.49	9	−0.70
		3	3.58	6	−0.52

[a] Calculated from eq 3. [b] The model employed for the calculation is illustrated in diagram A, and r and α are defined in diagram B:

[c] The values of k used in eq 3 were 14.1 for the pyridinium units (aromatic rings 1 and 3) and 27.6 for the p-xylylene residue (aromatic ring 2).

allows sites linked (α and α', β and β', γ and γ', and δ and δ') by chemical exchange to be identified (Table IV). It is interesting to note that, while the chemical shift differences between the constitutionally related OCH_2 protons is in the range 0.18 to 0.22 ppm for the α/α', β/β', and γ/γ'-OCH_2 protons, it is much smaller (0.07 ppm) for the δ/δ'-OCH_2 protons.

Dynamic ^{1}H NMR spectroscopy reveals that an ordered arrangement of the molecular components (i.e., [BPP34C10] and [BBIPYBIXYCY]$^{4+}$) of the [2]catenane exists in solution. The ^{1}H NMR spectrum of {[2]-[BPP34C10]-[BBIPYBIXYCY]catenane}[PF_6]$_4$ shows temperature-dependent behavior both above (in CD_3CN or CD_3SOCD_3, shown in Figure 18) and below (in CD_3COCD_3, shown in Figure 19) room temperature. Clearly visible in Figure 18 are two equal-intensity singlets at δ 3.45 and 6.16 for the "inside" and "alongside" hydroquinol ring protons, respectively. On warming the solution up, these singlets coalesced at 81 °C to one singlet, which is centered on δ 4.57 in CD_3SOCD_3 solution. On cooling a CD_3COCD_3 solution of the [2]catenane

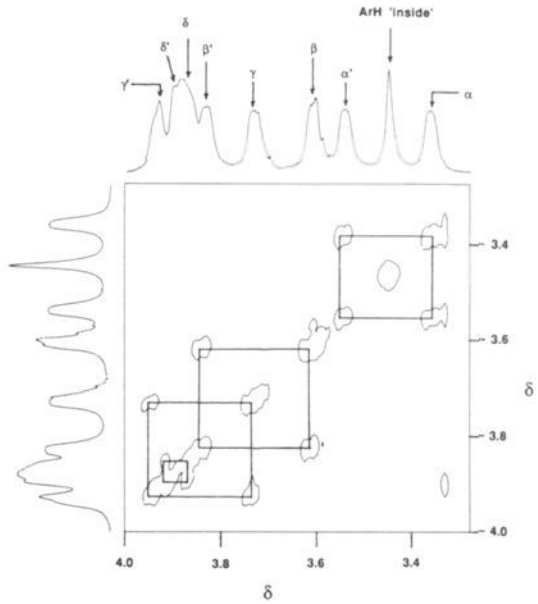

Figure 17. The 2D-NOESY 45 spectrum for {[2]-[BPP34C10]-[BBIPYBIXYCY]catenane}[PF_6]$_4$ showing the OCH_2CH_2O connectivities by virtue of chemical exchange.

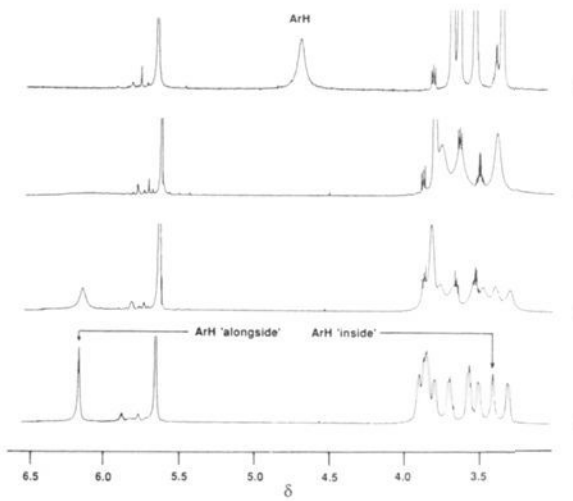

Figure 18. The partial temperature-dependent ^{1}H NMR spectra recorded in CD_3CN at (a) ambient temperature, (b) 40 °C, and (c) 75 °C and in CD_3SOCD_3 at (d) 150 °C.

down to −45 °C, the ^{1}H NMR spectrum (Figure 19) becomes considerably more complicated. In particular, two sets of signals are observed for the methylene protons at δ 5.93 and 6.04, as well as for the α and β protons on the bipyridinium rings at δ 9.23 and 9.41, and δ 8.23 and 8.31, respectively, of the [BBIPYBIXYCY]$^{4+}$ tetracation. Table VIII lists the kinetic and thermodynamic data obtained from approximate expressions[61] from the temperature-

Table VI. Comparison of the Experimental Chemical Shift Differences [$\Delta\delta$(expt)] and the Calculated Values [$\Delta\delta$(calc1) and $\Delta\delta$(calc2)] (Assuming the Solid-State Structures in the 1:1 Complexes and in the [2]Rotaxane are Adopted in Solution)

compound or complex	probe proton	$\Delta\delta_a$ and $\Delta\delta_b$ (ppm)	$\Delta\delta$(calc1) (ppm)	$\Delta\delta$(calc2) (ppm)	$\Delta\delta$(expt) (ppm)
[1/4DMB·BBIPYBIXYCY][PF_6]$_4$	H_a	−3.50	−2.05	−0.33	−0.55
	H_b	−0.61			
[BHEEEB·BBIPYBIXYCY][PF_6]$_4$	H_a	−3.33	−2.02	−1.85	−2.82
	H_b	−0.70			
[BHEEEEB·BBIPYBIXYCY][PF_6]$_4$	H_a	−3.83	−2.35	−2.24	−2.80
	H_b	−0.86			
{[2]-[BSEEB·BBIPYBIXYCY]rotaxane}[PF_6]$_4$	H_a	−2.70	−2.10		−3.26
	H_b	−1.50			

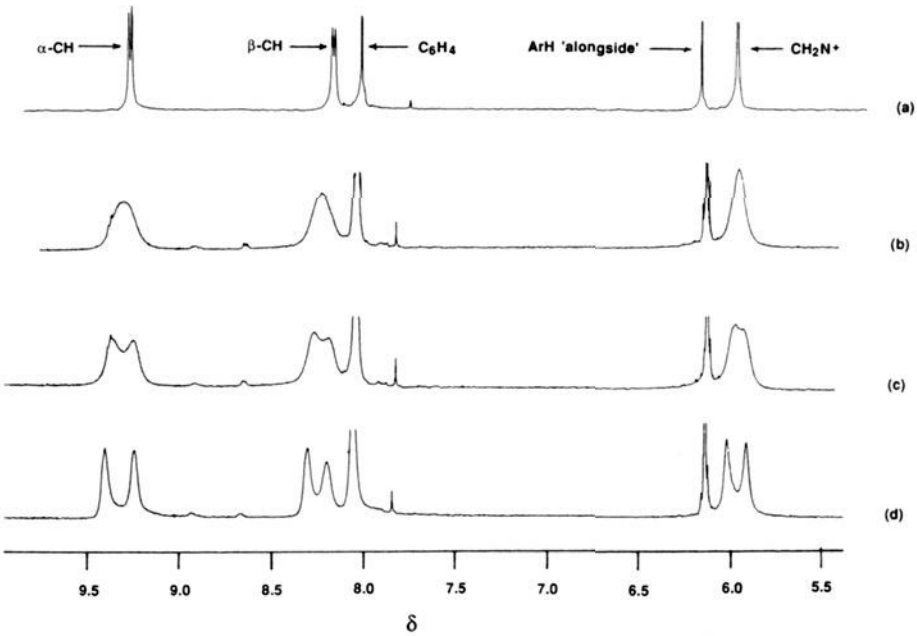

Figure 19. The partial temperature-dependent ^1H NMR spectra recorded in CD_3COCD_3 at (a) ambient temperature, (b) −23 °C, (c) −35 °C, and (d) −45 °C.

Table VII. Comparison of the Experimental Chemical Shift Differences [Δδ(expt)] and the Calculated Values [Δδ(calc1)′ and Δδ(calc2)′] (Assuming Equilibration Between Two Off-Center Degenerate States of the Hydroquinol Rings Inside the Tetracationic Cyclophane in Some 1:1 Complexes and a [2]Rotaxane)

compound or complex	x^a (Å)	Δδ(calc1)′ (ppm)	Δδ(calc2)′ (ppm)	Δδ(expt) (ppm)
[1/4DMB·BBIPYBIXYCY]-$[PF_6]_4$	0.60	−2.99	−0.49	−0.55
[BHEEEB·BBIPYBIXYCY]-$[PF_6]_4$	0.75	−2.93	−2.69	−2.82
[BHEEEEB·BBIPYBIXYCY]-$[PF_6]_4$	0.35	−2.90	−2.76	−2.80
{[2]-[BSEEB·BBIPYBIXYCY]-rotaxane}$[PF_6]_4$	0.80	−3.19		−3.26

[a] x is the distance that the center of the hydroquinol ring is displaced from the center of the tetracationic cyclophane in the degenerate equilibration:

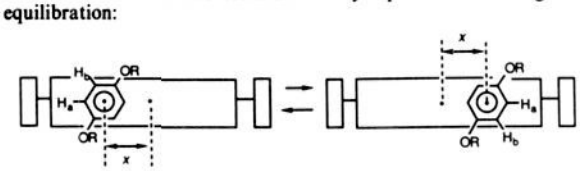

dependent behavior of the ^1H NMR spectra recorded on the [2]catenane. Clearly, there are two temperature-dependent processes occurring simultaneously within the [2]catenane in solution.

(61) Two methods were employed to obtain kinetic and thermodynamic data: (1) The *coalescence method*, where values for the rate constant k_c at the coalescence temperature (T_c) were obtained (Sutherland, I. O. *Annu. Rep. NMR Spectrosc.* **1971**, *4*, 71–235) from the approximate expression, $k_c = \pi(\Delta\nu)/(2)^{1/2}$, where $\Delta\nu$ is the limiting chemical shift difference (in hertz) between the signals observed below T_c for the protons undergoing site exchange. (2) The *exchange method*, where values of k were obtained (Sandström, J. *Dynamic NMR Spectroscopy*; Academic Press: London, 1982; Chapter 6) from the approximate expression $k = \pi(\Delta\nu)$, where $\Delta\nu$ is the difference (in hertz) between the line width at a suitable temperature T, where exchange of sites is occurring, and the line width in the absence of exchange. The Eyring equation was used to calculate $\Delta G^{\ddagger}_c$ of $\Delta G^{\ddagger}$ values at T_c or T, respectively.

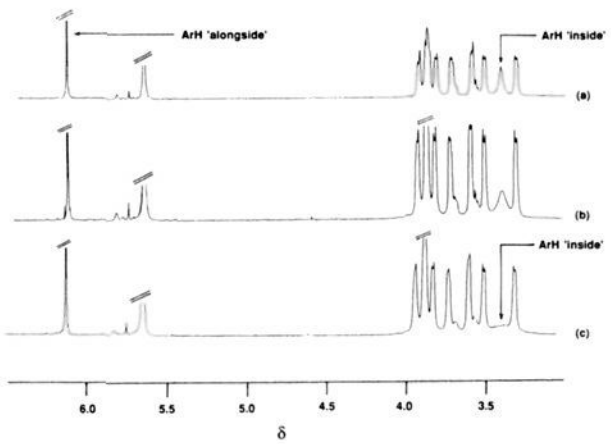

Figure 20. The partial temperature-dependent ^1H NMR spectra recorded in CD_3CN at (a) −5 °C, (b) −25 °C, and (c) −40 °C.

Scheme VII

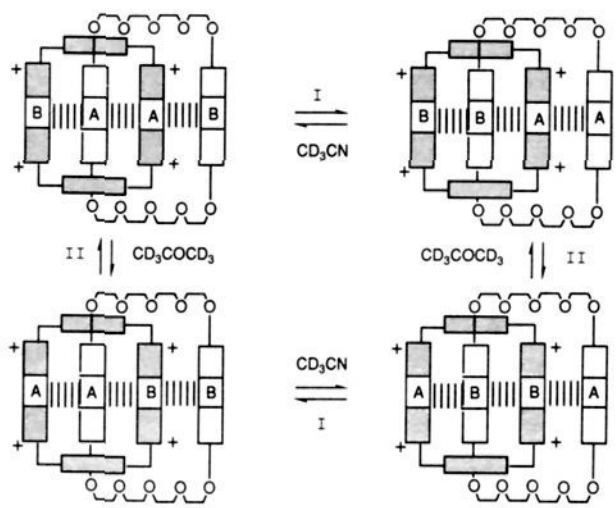

One process (I), which is associated with the higher activation barrier of 15.6 kcal mol^{-1}, almost certainly involves the loss of

Table VIII. Kinetic and Thermodynamic Parameters Obtained from the Temperature-Dependent ^1H NMR Spectra Recorded on {[2]-[BPP34C10]-[BBIPYBIXYCY]Catenane}$[PF_6]_4$

probe protons undergoing site exchange	$\Delta\nu^a$ (Hz) $(\Delta\nu)^b$	k_c^a (s^{-1}) $(k)^b$	T_c^a (°C) $(T)^b$	$\Delta G_c^{\ddagger a}$ (kcal mol^{-1}) $(\Delta G^{\ddagger})^b$
OC_6H_4O in [BPP34C10]	678[c]	1505	81[c]	15.6
	(19.0)[d]	(60)	(40)[d]	(15.7)
CH α to N^+ in $[BBIPYBIXYCY]^{4+}$	74.3[e]	165	−23[e]	12.0
	(26.9)[e]	(85)	−23[e]	12.3
CH β to N^+ in $[BBIPYBIXYCY]^{4+}$	34.3[e]	76	−26[e]	12.2
	(25.1)[e]	(79)	−26[e]	12.3
CH_2N^+ in $[BBIPYBIXYCY]^{4+}$	45.8[e]	102	−25[e]	12.1
	(30.7)[e]	(97)	−25[e]	12.2

[a] Data not in parentheses relates to the *coalescence method* (see ref 61). [b] Data in parentheses relates to the *exchange method* (see ref 61). [c] Data obtained at 250 MHz in CD_3CN. [d] Data obtained at 400 MHz in CD_3CN. [e] Data obtained at 400 MHz in CD_3COCD_3.

Table IX. ^{13}C NMR Chemical Shift Data (δ Values)[a] for {[2]-[BPP34C10]-[BBIPYBIXYCY]Catenane}$[PF_6]_4$ in CD_3CN at 0 °C

δ	no. of carbons	assignment
152.8	2	quat-ArH "alongside"
150.8	2	quat-ArH "inside"
146.5	4	quat-BIPY units
145.3	8	α-CH in BIPY units
137.5	4	quat-BIXY units
131.6	8	CH in BIXY units
126.2	8	β-CH in BIPY units
115.6	4	*tert*-ArH "alongside"
113.5	4	*tert*-ArH "inside"
71.5	2	γ'-OCH_2
71.2	2	δ-OCH_2
70.7	4	δ'-OCH_2/β'-OCH_2
70.3	2	β-OCH_2
69.8	2	γ-OCH_2
68.3	2	α-OCH_2
67.3	2	α'-OCH_2

[a] The δ values were obtained at 100.6 MHz by the JMOD sequence with a DI of 2 s.

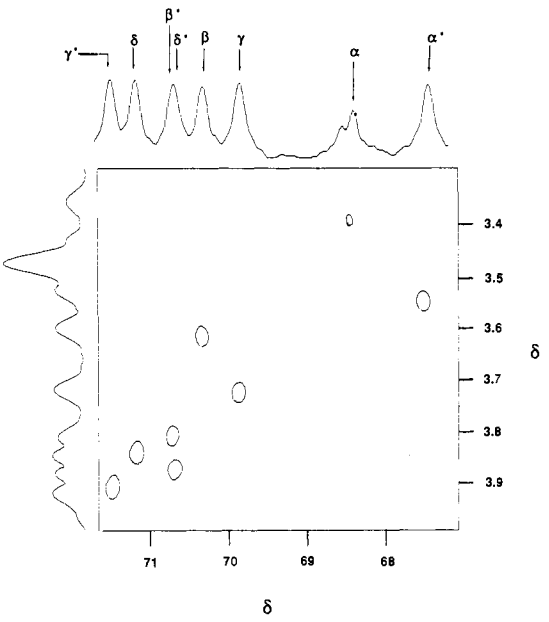

Figure 21. The ^{13}C–^1H correlation spectrum for {[2]-[BPP34C10]-[BBIPYBIXYCY]catenane}$[PF_6]_4$ in the OCH_2CH_2O region.

all the π-stacking interactions between the π-donors and the π-acceptors and can be interpreted (Scheme VII) in terms of the BPP34C10 ring revolving around the tetracationic macrocycle. This process exchanges hydroquinol rings A and B between "inside" and "alongside" environments with respect to the tetracationic cyclophane. The other process (II), which is associated with the lower activation barrier of ca. 12.2 kcal mol^{-1}, involves the exchange of the bipyridinium rings A and B between "inside" and "alongside" environments with respect to the BPP34C10 macrocycle. Only one hydroquinol ring needs to sacrifice its π-stacking interaction with a bipyridinium ring on the [BBIPYBIXYCY]$^{4+}$ tetracation as the other hydroquinol ring sweeps round the tetracationic cyclophane by pirouetting about the OC_6H_4O axis of the included hydroquinol ring. Interestingly, there is some evidence (Figure 20) that a third process is occurring at low temperatures in CD_3CN. Whereas the singlet at δ 6.16 for the "alongside" hydroquinol ring protons remains sharp, on lowering the temperature to −40 °C, i.e., close to the freezing point (−46 °C) of CD_3CN, the singlet at δ 3.45 for the "inside" hydroquinol ring protons broadens considerably. It is possible that the "rocking" process discussed in Figure 15 could account for this line broadening. The fact that the noncovalent bonding interactions responsible in the first place for the construction (Scheme VI) of the [2]catenane from its immediate precursors "live on" in the molecule afterward sets it apart from all its predecessors among the known catenanes.

The exchange processes I and II identified in Scheme VII can also be observed in the ^{13}C NMR spectrum recorded in CD_3CN. At 0 °C, while a single set of signals is observed for the [BBIPYBIXYCY]$^{4+}$ component, two sets of signals can be observed (Table IX) for all of the carbon atoms in the BPP34C10 component. On the basis of the fully assigned ^1H NMR spectrum, the carbon atoms bearing one proton were identified by selectively decoupling the proton-coupled ^{13}C NMR spectrum. The eight different OCH_2 carbon signals in the BPP34C10 component were identified (Figure 21) by ^{13}C–^1H correlation. On lowering the temperature below 0 °C, there is the expected line broadening of the signals for the [BBIPYBIXYCY]$^{4+}$ component.

Absorption Spectra, Luminescence Spectra, and Excited-State Lifetimes. The experiments were carried out in acetonitrile solution at room temperature and in a butyronitrile rigid matrix at 77 K. All compounds examined, including the {[2]-[BSEEEB]-[BBIPYBIXYCY]rotaxane}$[PF_6]_4$ and the {[2]-[BPP34C10]-[BBIPYBIXYCY]catenane}$[PF_6]_4$, were stable both in the dark and under the spectrophotometer and spectrofluorimeter lights, at least for the time periods of less than 30 min required to perform the experiments.

A summary of the absorption data is present in Table X. Figure 22 shows the absorption spectra of BSEEEB, BPP34C10, and [BBIPYBIXYCY]$[PF_6]_4$. The intense absorption band observed for [BBIPYBIXYCY]$[PF_6]_4$ with a maximum at 260 nm arises from the paraquat units, and the much less intense bands observed for BSEEEB and BPP34C10 with maxima at 290 nm are attributed to the hydroquinol units. The fact that the molar absorption coefficient of BPP34C10 is less than twice that of BSEEEB indicates that there is an interaction between the two hydroquinol units. On mixing equimolar amounts (4×10^{-5} M) of BPP34C10 and [BBIPYBIXYCY]$[PF_6]_4$, the absorption spectrum (curve a) shown in Figure 23 is obtained. It is exactly that expected from the summation of the two spectra (Figure 22) of BPP34C10 and [BBIPYBIXYCY]$[PF_6]_4$. Under the experimental conditions, there is no interaction between the crown ether and the tetracationic macrocycle. The absorption spectrum of the [2]catenane in which BPP34C10 and [BBIPYBIXYCY]$^{4+}$ are interlocked is shown by curve b in Figure 23. This spectrum

Table X. Absorption, Emission, and Lifetime Data for BSEEEB, BPP34C10, [BBIPYBIXYCY][PF_6]$_4$, {[2]-[BSEEEB]-[BBIPYBIXYCY]Rotaxane}[PF_6]$_4$, and {[2]-[BPP34C10]-[BBIPYBIXYCY]Catenane}[PF_6]$_4$ in Acetonitrile and, in Some Cases, in Butyronitrile

	absorption		emission						
			298 K			77 K[a]			
compound	λ_{max} (nm)	ϵ (M^{-1} cm^{-1})	λ_{max} (nm)	τ (ns)	I_{rel}[b] (AU)	λ_{max} (nm)	τ (ns)	λ_{max} (nm)	τ (s)
BSEEEB	290	3200	320	1	100	318	1	420	1
BPP34C10	290	5200	320	1	70	318	1	420	1
[BBIPYBIXYCY][PF_6]$_4$	260	40700							
{[2]-[BSEEEB]-[BBIPYBIXYCY]rotaxane}[PF_6]$_4$	262	36800	320		<2				
	470	350							
{[2]-[BPP34C10]-[BBIPYBIXYCY]catenane}[PF_6]$_4$	263	36500	320	1	5	318	1		
	478	700							

[a] Butyronitrile solution. [b] Relative luminescence intensity.

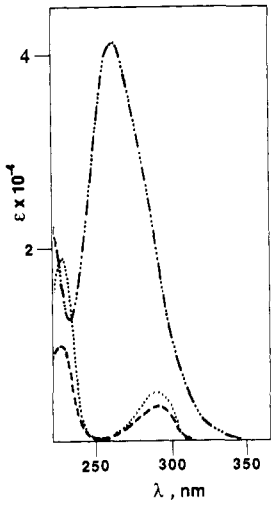

Figure 22. Absorption spectra in acetonitrile of [BBIPYBIXYCY][PF_6]$_4$ (—···—), BPP34C10 (···), and BSEEEB (- - -).

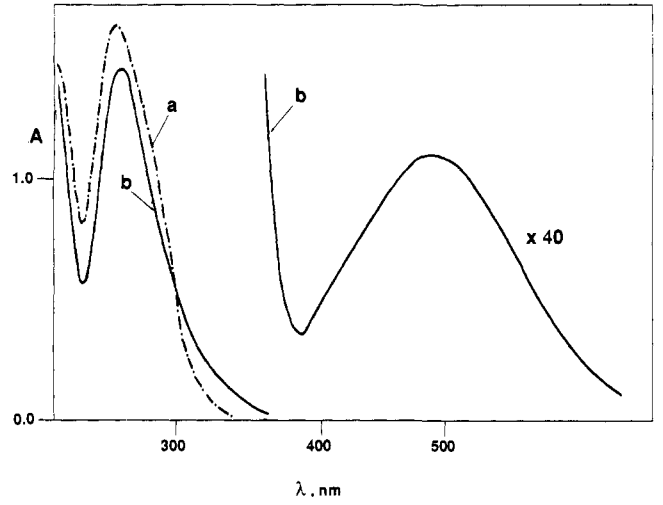

Figure 23. Absorption spectra in acetonitrile (c = 4.0 × 10^{-5} M) for (a) a solution containing equimolar amounts of [BBIPYBIXYCY][PF_6]$_4$ and BPP34C10 (-·-) and (b) {[2]-[BPP34C10]-[BBIPYBIXYCY]catenane}[PF_6]$_4$ (—).

is noticeably different from that exhibited by curve a in Figure 23. The intense band for the paraquat units with λ_{max} = 260 nm not only undergoes a small red shift (λ_{max} = 263 nm) but it also displays a noticeable decrease in intensity. Furthermore, a tail appears in the 300–380-nm region, and a broad weak band is present in the visible region with λ_{max} = 478 nm (ϵ = 700 M^{-1} cm^{-1}).

Of the two components present in the [2]catenane, the [BBIPYBIXYCY]$^{4+}$ tetracation is not luminescent, whereas

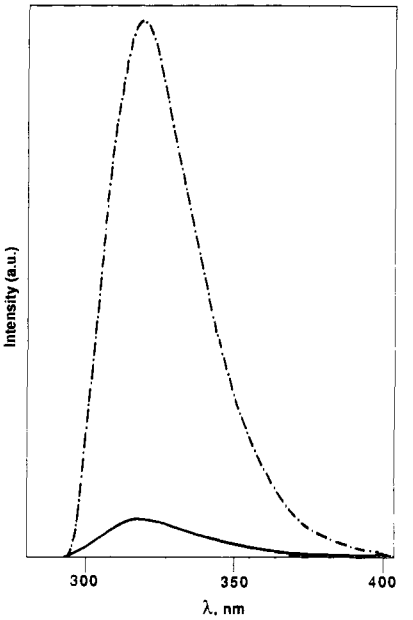

Figure 24. Emission spectra in acetonitrile (c = 4.0 × 10^{-5} M) for (a) a solution containing equimolar amounts of [BBIPYBIXYCY][PF_6]$_4$ and BPP34C10 (-·-) and (b) {[2]-[BPP34C10]-[BBIPYBIXYCY]catenane}[PF_6]$_4$ (—).

BPP34C10 exhibits a fluorescence emission at room temperature with λ_{max} = 320 nm and τ = 1 ns. By contrast, in the rigid matrix at 77 K, the fluorescence is accompanied by a very weak phosphorescence with λ_{max} = 420 nm and $\tau \approx$ 1 s (Table X). An equimolar mixture of BPP34C10 and [BBIPYBIXYCY][PF_6]$_4$ shows (Figure 24) exactly the same luminescence properties as those of BPP34C10 alone. However, when BPP34C10 and the [BBIPYBIXYCY]$^{4+}$ tetracation are interlocked in the [2]catenane, the fluorescence at room temperature and both the fluorescence and phosphorescence at 77 K of BPP34C10 are strongly quenched. In particular, at room temperature on excitation at the isosbestic point at 300 nm (Figure 23), the residual fluorescence of BPP34C10, when it is interlocked with the [BBIPYBIXYCY]$^{4+}$ tetracation in the [2]catenane, is (Figure 24) about 7% that of BPP34C10 in the equimolar mixture of BPP34C10 and [BBIPYBIXYCY][PF_6]$_4$. This conclusion is based on the reasonable assumption (Figure 23) that the fraction of 300-nm light absorbed by BPP34C10 is the same in the [2]catenane as in the equimolar mixture of the components. The excitation spectrum of the residual fluorescence of the [2]catenane coincides with that of BPP34C10.

The results obtained for {[2]-[BSEEEB]-[BBIPYBIXYCY]rotaxane}[PF_6]$_4$ are rather similar to those just described in detail for the [2]catenane. Figure 25 shows the absorption spectra of an equimolar mixture (4 × 10^{-5} M) of BSEEEB and [BBIPYBIXYCY][PF_6]$_4$ (a) and of the [2]rotaxane (b). The spectral changes obtained on interlocking the two components are clear.

Table XI. Electrochemical Parameters for $[PQT][PF_6]_2$, $[BBIPYBIXYCY][PF_6]_4$, $[BHEEEB\cdot BBIPYBIXYCY][PF_6]_4$, {[2]-[BSEEEB]-[BBIPYBIXYCY]Rotaxane}$[PF_6]_4$, and {[2]-[BPP34C10]-[BBIPYBIXYCY]Catenane}$[PF_6]_4$

compound or complex	reduction potential			peak[a] half-width	ΔE^b	
	E_1 (mV)	E_1' (mV)	E_2 (mV)	(mV)	(mV)	K_D
$[PQT][PF_6]_2$	−428		−837			
$[BBIPYBIXYCY][PF]_6]_4$	−283		−709	59.7	40.2	0.21
$[BHEEEB\cdot BBIPYBIXYCY][PF_6]_4$	−292		−709	60.6	41.8	0.20
{[2]-[BSEEEB]-[BBIPYBIXYCY]rotaxane}$[PF_6]_4$	−327		−802	80.3	61.1	0.09
{[2]-[BPP34C10]-[BBIPYBIXYCY]catenane}$[PF_6]_4$	−310	−437	−845	180.6	148.9	0.003

[a] Calculated from $E_p - E_p/2$ as described in ref 67. [b] Potential difference between the $[PQT]^{4+}/[PQT]^{3+}$ and $[PQT]^{3+}/[PQT]^{2+}$ couples, obtained as described in ref 67.

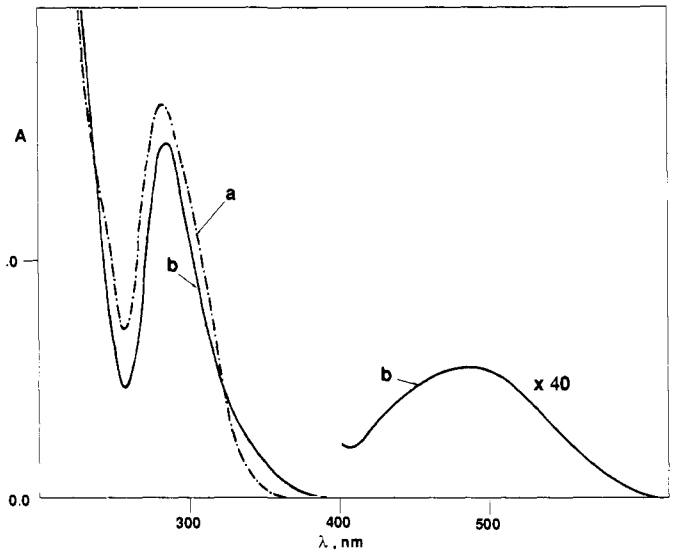

Figure 25. Absorption spectra in acetonitrile ($c = 4.0 \times 10^{-5}$ M) for (a) a solution containing equimolar amounts of $[BBIPYBIXYCY][PF_6]_4$ and BSEEEB (−·−) and (b) {[2]-[BSEEEB]-[BBIPYBIXYCY]rotaxane}$[PF_6]_4$ (—).

The fluorescence emission of the hydroquinol moiety is not present in the [2]rotaxane within the limits (≤2%) of experimental detection. The data obtained from the experiments are gathered in Table X.

In summary, the results obtained show that in both the [2]-catenane and the [2]rotaxane, an electronic interaction[62-64] occurs between the π-electron-rich hydroquinol units of BSEEEB and BPP34C10 and the π-electron-deficient bipyridinium residues of the $[BBIPYBIXYCY]^{4+}$ tetracation. Such a charge-transfer interaction causes (Figures 23–25 and Table X) (i) some modification in the intense $\pi \rightarrow \pi^*$ band of $[BBIPYBIXYCY][PF_6]_4$, (ii) the appearance of broad and weak bands in the visible region, and (iii) the quenching of the luminescence of the hydroquinol units. The maxima for the visible bands of the [2]rotaxane and [2]catenane coincide as expected because of the identical nature of the interacting chromophores in the two closely related molecular assemblies. Furthermore, the extinction coefficient (at $\lambda_{max} = 478$ nm) of the [2]catenane is practically twice that (at $\lambda_{max} = 470$ nm) of the [2]rotaxane, suggesting that, in the [2]-catenane, both hydroquinol units in BPP34C10 interact with a bipyridinium residue. The result is consistent with the almost complete quenching of the fluorescence of the hydroquinol units in both the [2]rotaxane and the [2]catenane.

Electrochemistry. The electrochemistry of paraquat derivatives is characterized by two consecutive monoelectron reduction processes. If a bis-paraquat compound $[BBIPY]^{4+}$ contains a pair of identical bipyridinium subunits, then the electrochemistry will

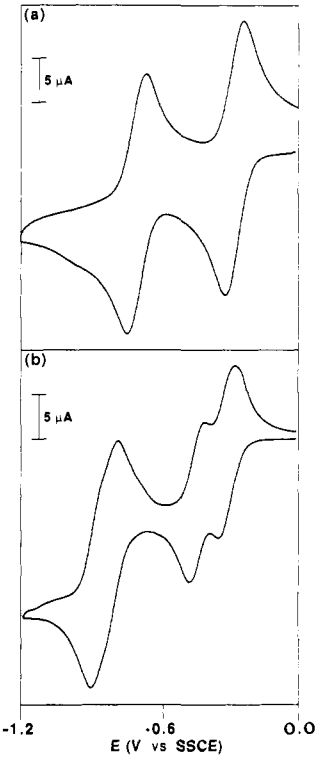

Figure 26. Cyclic voltammograms obtained at 25 °C of 0.5 mM solutions of (a) $[BBIPYBIXYCY][PF_6]_4$ and (b) {[2]-[BPP34C10]-[BBIPYBIXYCY]catenane}$[PF_6]_4$ in 0.1 M $TBAPF_6$/MeCN. Scan rate: 50 mV/s.

display two sets of redox waves corresponding to the following processes:

$$[BBIPY]^{4+} + 2e \rightleftarrows [BBIPY]^{2+} \quad (8)$$

$$[BBIPY]^{2+} + 2e \rightleftarrows [BBIPY] \quad (9)$$

It has been shown by Nicholson and Shain[65] that it is possible to determine the half-wave potential for overlapping voltammetric waves in multistep charge-transfer reactions. By using cyclic voltammetry to obtain the peak half-width and the working curves of Myers and Shain,[66] which were extended later by Richardson and Taube,[67] the potential differences between the individual monoelectron reductions of the bis-paraquat derivatives were determined and are shown in Table XI. Additional equilibria can exist in solution and affect the shape of the voltammogram, such as the disproportionation reaction,

$$2[BBIPY]^{3+} \rightleftarrows [BBIPY]^{4+} + [BBIPY]^{2+} \quad (10)$$

Disproportionation constants may be obtained from the relationship, $K_D = \exp[(\Delta E_0)n_1n_2F/RT]$, where ΔE_0 is the standard potential difference between the successive monoelectron reduction steps. The disproportionation constants (K_D) determined for bis-paraquat compounds and complexes are shown in Table XI.

(62) Foster, R. *Organic Charge-Transfer Complexes*; Academic Press: London, 1969.
(63) Ferguson, J. *Chem. Rev.* **1986**, *86*, 957–982.
(64) Jones, G. In *Photoinduced Electron Transfer*; Fox, M. A., Chanon, M., Eds.; Elsevier: New York, 1988; Part A, pp 245–304.
(65) Nicholson, R. S.; Shain, I. *Anal. Chem.* **1964**, *36*, 706–723.
(66) Myers, R. L.; Shain, I. *Anal. Chem.* **1969**, *41*, 980.
(67) Richardson, D. E.; Taube, H. *Inorg. Chem.* **1981**, *20*, 1278–1285.

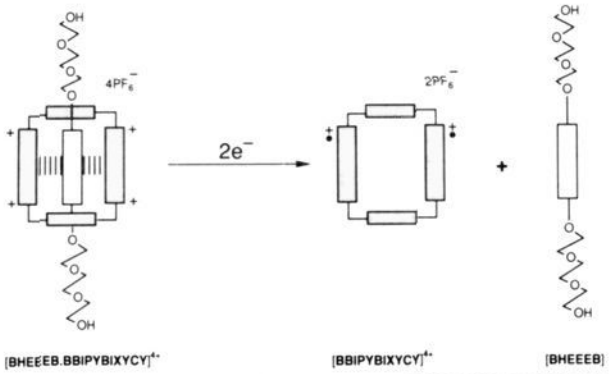

Figure 27. The unthreading of the 1:1 complex [BHEEEB·BBIPYBIXYCY]$^{4+}$ upon reduction.

The voltammetry of the bis-paraquat cyclophane {BBIPYBIXYCY}$[PF_6]_4$ exhibits, as expected for a symmetrical two-site molecule, two sets of redox waves (Figure 26a). The first apparent redox couple at −0.283 V vs SSCE corresponds to the reduction of both paraquat units within the cyclophane from the +2 to the +1 state. The second at −0.709 V corresponds to the reduction of both subunits to yield the neutral molecule. Complete electrochemical reversibility is noted in the voltammogram, indicating that the integrity of both the monoreduced and direduced species is retained in solution. On comparing the formal potentials of the bis-paraquat cyclophane [BBIPYBIXYCY]$[PF_6]_4$ with the well-known [PQT]$[PF_6]_2$ standard, we observe a shift in the first and second reductions to a less negative potential. The increased ability of the cyclophane to accept the electron can be rationalized if one considers that the electrostatic repulsion between the two charged $[PQT]^{2+}$ units is significantly decreased upon reduction.

The cyclic voltammetry of the [2]rotaxane model, [BHEEEB·BBIPYBIXYCY]$[PF_6]_4$, and {[2]-[BSEEEB]-[BBIPYBIXYCY]rotaxane}$[PF_6]_4$ is similar to that of the bis-paraquat cyclophane [BBIPYBIXYCY]$[PF_6]_4$, except that the first reductions are 9 and 44 mV, respectively, more negative than the parent cyclophane. Significantly, however, the second reduction potentials for the [2]rotaxane model and the bis-paraquat cyclophane are identical. This implies that, in the former, the bead unthreads spontaneously (Figure 27) after the first reduction, leaving the bis-paraquat cyclophane completely free of its original substrate. The observed peak half-widths also begin to broaden in these two cases, indicating a separation in the overlapping voltammetric waves. The voltammetry of {[2]-[BPP34C10]-[BBIPYBIXYCY]catenane}$[PF_6]_4$ is remarkably different, with three well-resolved current peaks being observed (Figure 26b). The primary redox couple ($[PQT]^{2+}/[PQT]^{+}$) is resolved into two distinct reductions, which exhibit E_0' values some 149 mV apart. The voltammetry of the [2]catenane can be rationalized by observing that the environmental homogeneity is lost between the two paraquat subunits. The "alongside" subunit exhibits a reversible redox couple at −0.310 V. The "inside" paraquat moiety reduction potential is at −0.437 V as a result of the fact that the "inside" subunit is stabilized by charge-transfer interactions with two adjacent hydroquinol units. The positional differences between the two otherwise identical subunits creates an electrochemical gradient within the molecule. The second redox process ($[PQT]^{+}/[PQT]^{0}$) is observed to occur at −0.845 V as a single-step reduction. Closer inspection of the second current peak does indicate a broadened curve with a slight shoulder. This shape means that the potential difference between the "inside" and "alongside" paraquat subunits is reduced significantly in this state. This decrease in potential differences arises from the diminished acceptor character of $[PQT]^{+}$ subunits with the neighboring hydroquinol rings.

As the progression is made (Table XI and Figure 28) from the bis-paraquat cyclophane to the [2]rotaxane model, to the [2]rotaxane, and, finally, to the [2]catenane, a systematic trend develops in the reduction potentials of the compounds. As the series is traversed through situations when paraquat subunits are further

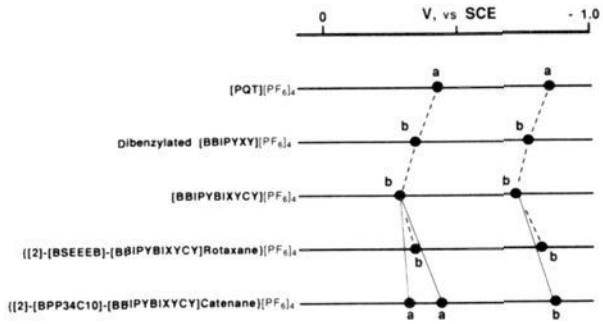

Figure 28. Reduction potentials in acetonitrile of {[2]-[BPP34C10]-[BBIPYBIXYCY]catenane}$[PF_6]_4$, {[2]-[BSEEEB]-[BBIPYBIXYCY]rotaxane}$[PF_6]_4$, and related compounds: a, monoelectronic wave; b, bielectronic wave.

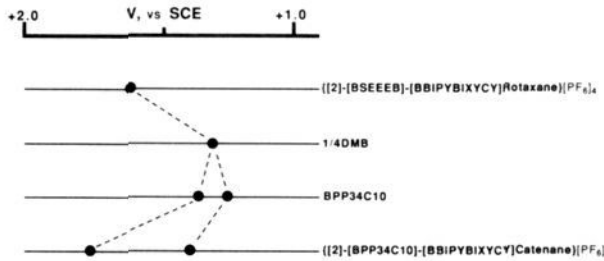

Figure 29. Oxidation potentials in acetonitrile of {[2]-[BPP34C10]-[BBIPYBIXYCY]catenane}$[PF_6]_4$, {[2]-[BSEEEB]-[BBIPYBIXYCY]rotaxane}$[PF_6]_4$, and related compounds.

and further stabilized by charge-transfer interactions, they exhibit a decrease in electron affinity. As more π-donors are locked into place, the stabilization upon reduction, which results from the relief of electrostatic repulsions between two paraquat subunits, decreases. In the [2]rotaxane model and in the [2]rotaxane, the "inside" hydroquinol ring can be thought of as an insulator to electronic communication between paraquat subunits. This pattern culminates with the [2]catenane, which shows a completely distinct redox couple for the "inside" and "alongside" paraquat subunits.

The behavior (Figure 29) of {[2]-[BSEEEB]-[BBIPYBIXYCY]rotaxane}$[PF_6]_4$ on electrochemical oxidation can be easily rationalized on the basis of the behavior of the parent reference compounds, 1/4DMB and BPP34C10. Oxidation of 1/4DMB occurs at +1.31 V. In the [2]rotaxane, where the hydroquinol unit is constrained to spend a lot of its time inside the [BBIPYBIXYCY]$^{4+}$ tetracationic macrocycle, the oxidation potential becomes much more positive (+1.60 V), as expected, because of the electron donation to the paraquat units. On passing to BPP34C10, two distinct oxidation waves can be observed (+1.28 and +1.37 V), showing that there is some interaction between the equivalent hydroquinol units in agreement with the absorption and emission properties. In the [2]catenane, both of the oxidation waves are displaced toward more positive potentials (+1.42 and +1.72 V), and their splitting is much larger than in BPP34C10. This is indeed expected behavior because (i) the interaction with π-electron-acceptor paraquat units makes the hydroquinol units more difficult to oxidize and (ii) the two hydroquinol units are not topologically equivalent for the same reason discussed above for the two paraquat units in the same molecule. Thus, the "alongside" hydroquinol unit, which interacts with only one paraquat unit, is the first to be oxidized, and the "inside" hydroquinol unit, which interacts with two paraquat units, is oxidized only at a much higher potential.

ESR Spectroscopy. The electron spin density delocalization within some of the paraquat derivatives was evaluated by ESR spectroscopy. The room temperature spectrum of the reduced +3 form bis-paraquat cyclophane [BBIPYBIXYCY]$[PF_6]_3$ is shown in Figure 30. A broadened, rather featureless spectrum results from the fast electron exchange between the paraquat subunits. The ESR line broadening is observed to change as the

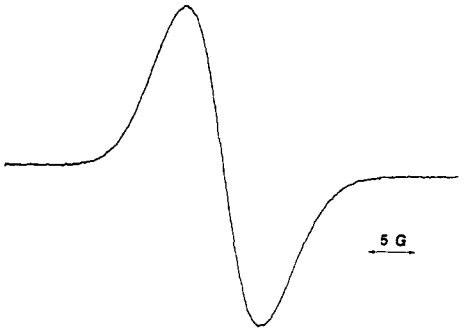

Figure 30. ESR spectrum of the reduced +3 form of bis-paraquat cyclophane [BBIPYBIXYCY][PF_6]$_3$ in acetonitrile at 25 °C.

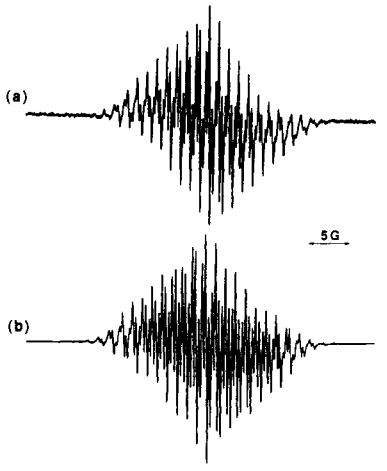

Figure 31. (a) ESR spectrum of {[2]-[BPP34C10]-[BBIPYBIXYCY]-catenane}[PF_6]$_3$ in acetonitrile at 25 °C. (b) Digital simulation of this spectrum using the coupling constants given in the text.

inverse of the mean lifetime of the electron in each subunit.[68] The overall S shape of the spectrum can be understood by the realization that there are 50 625 different possible hyperfine frequency transitions in this complex. It is evident that the reduced species exhibits a spectrum that is characteristic of the intermediate exchange region.[69] Essentially, the frequency of electron transfer between the two subunits is at least the same as the hyperfine intervals, leading to the observed broadening. The ESR spectrum (Figure 31a) of the reduced +3 form of the [2]catenane is completely different from the +3 form of the bis-paraquat cyclophane spectrum and distinct from that[70] of [PQT][PF_6]. Digital simulation of the spectra (Figure 31b) with the determined coupling constants of a_{2N} = 4.16 G, a_{4H} = 1.85 G, and a_{8H} = 1.43 G clearly reveals that the charge is positioned only within one paraquat subunit. The observed spectral shape implies that the electron exchange frequency for this compound falls in the slow exchange region (<106 s^{-1}), and therefore broadening of the spectra is not evident. Analysis of the spectra of the reduced rotaxane model, [BHEEEB·BBIPYBIXYCY][PF_6]$_3$, shows a rather nondescript spectrum with a small degree of hyperfine superimposed on a broadened background. Similarly, the ESR spectrum of {[2]-[BSEEEB]-[BBIPYBIXYCY]rotaxane}[PF_6]$_3$ shows slightly more hyperfine—relative to the spectrum of the rotaxane model—also, superimposed on the broadened background. These spectra fall intermediately between the featureless bis-paraquat cyclophane [BBIPYBIXYCY][PF_6]$_3$ and the hyperfine-rich {[2]-[BPP34C10]-[BBIPYBIXYCY]catenane}[PF_6]$_3$ spectra. These shapes are expected if one rationalizes that the overall spin

Scheme VIII

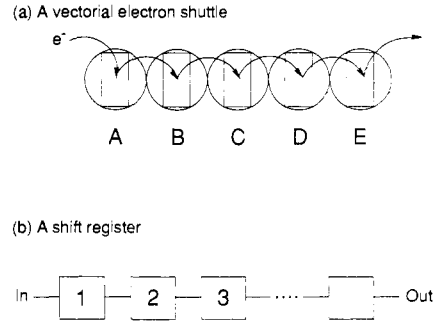

distribution will be approximately the same in all complexes containing the same bis-paraquat backbone. What will vary from molecule to molecule will be the rate of intramolecular electron transfer. As the "inside" hydroquinol ring is forced more and more tightly in between the paraquat subunits, the degree of insulation increases, yielding progressively slower intramolecular transfer. This is perhaps a surprising result since it is well-known that the stacking of segregated donor and acceptor aromatic groups yields organic solids with appreciable electronic conductivity. However, the electrochemical and ESR results described above were obtained in solution, where, of course, the stacking of aromatic donor and acceptor moieties is limited by the dimensions of the individual molecules. Under these conditions, the interlocking of the donor and the acceptor groups in {[2]-[BPP34C10]-[BBIPYBIXYCY]catenane}[PF_6]$_4$ breaks the equivalence of the two paraquat subunits. When this molecule undergoes monoelectronic reduction, intramolecular electron transfer is slower than in [BBIPYBIXYCY][PF_6]$_3$ because there is a sizable energy difference between the two possible electronic sites. In contrast, both sites are equivalent in [BBIPYBIXYCY][PF_6]$_3$ and that increases the rate of intramolecular electron transfer in this species. Therefore, the relative degree of insulation observed between the paraquat subunits in the [2]catenane results from the energy difference between the two electronic sites, which increases the energetic barrier for the intramolecular electron-transfer process.

Conclusion. In this first paper of a new series, we have outlined a general approach to establishing the concept of self-assembly[71]

(68) Ward, R. L.; Weissman, S. I. *J. Am. Chem. Soc.* **1957**, *79*, 2086–2090.
(69) Williams, D. J.; Pearson, J. M.; Levy, M. J. *J. Am. Chem. Soc.* **1971**, *93*, 5483–5489.
(70) Kosower, E. M.; Cotter, J. L. *J. Am. Chem. Soc.* **1964**, *86*, 5524–5527.

(71) Some recent examples of self-assembly in chemical systems include the following. (a) Curcurbituril: Freeman, W. A.; Mock, W. L.; Shih, N.-Y. *J. Am. Chem. Soc.* **1981**, *103*, 7367–7368. (b) Cavitands: Cram, D. J. *Science (Washington, D.C.)* **1983**, *219*, 1177–1183. Bryant, J. A.; Blanda, M. T.; Vincenti, M.; Cram, D. J. *J. Chem. Soc., Chem. Commun.* **1990**, 1403–1405. (c) Carcerands: Cram, D. J.; Karbach, S.; Kim, Y. H.; Baczynskyj, L.; Marti, K.; Sampson, R. M.; Kalleymeyn, G. W. *J. Am. Chem. Soc.* **1988**, *110*, 2554–2560. (d) Surfaces: Bain, C. D.; Troughton, E. B.; Tao, Y. T.; Evall, J.; Whitesides, G. M.; Nuzzo, R. G. *J. Am. Chem. Soc.* **1989**, *111*, 321–335. (e) Bibraccial lariat ethers carrying side arms terminated by nucleic acid bases: Gokel, G. W.; Echegoyen, L.; Kim, M.; Hernandez, J. C.; de Jesus, M. *J. Inclusion Phenom.* **1989**, *7*, 73–81. (f) Transition metal chelates: Saalfrank, R. W.; Stark, A.; Bremer, M.; Hummel, H.-U. *Angew. Chem., Int. Ed. Engl.* **1990**, *29*, 311–314. (g) Ordered supramolecular strands: Lehn, J.-M.; Mascal, M.; DeCian, A.; Fischer, J. *J. Chem. Soc., Chem. Commun.* **1990**, 479–481. (h) A self-replicating system: Tjivikua, T.; Ballester, P.; Rebek, J., Jr. *J. Am. Chem. Soc.* **1990**, *112*, 1249–1250. (i) Threaded cyclodextrin molecular loop: Rao, T. V. S.; Lawrence, D. S. *J. Am. Chem. Soc.* **1990**, *112*, 3614–3615. See also: Manka, J. S.; Lawrence, D. S. *J. Am. Chem. Soc.* **1990**, *112*, 2440–2442. (j) Hydrogen-bonded molecular tapes: Zerkowski, J. A.; Seto, C. T.; Wierda, D. W.; Whitesides, G. M. *J. Am. Chem. Soc.* **1990**, *112*, 9025–9026. See also: Seto, C. T.; Whitesides, G. M. *J. Am. Chem. Soc.* **1990**, *112*, 6409–6411. *J. Am. Chem. Soc.* **1991**, *113*, 712–713. (k) Micelles: Bachmann, P. A.; Walder, P.; Luisi, P. L.; Lang, J. *J. Am. Chem. Soc.* **1990**, *112*, 8200–8201. (l) Hydrogen bond directed cocrystallization: Etter, M. C.; Urbanczyk-Lipkowska, Z.; Zia-Ebrahimi, M.; Panunto, T. W. *J. Am. Chem. Soc.* **1990**, *112*, 8415–8426. (m) Supramolecular liquid crystalline polymers: Fouquey, C.; Lehn, J.-M.; Levelut, A.-M. *Adv. Mater.* **1990**, *2*, 254–257. (n) Lipid bilayers: Tien, H. T. *Adv. Mater.* **1990**, *2*, 316–318. Ulman, A. *Adv. Mater.* **1990**, *2*, 573–582. (o) Bisubstrate reaction templates: Kelly, T. R.; Bridger, G. J.; Zhao, C. *J. Am. Chem. Soc.* **1990**, *112*, 8024–8034. (p) Multichromophore structures: Tecilla, P.; Dixon, R. P.; Slobodkin, G.; Alavi, D. S.; Waldeck, D. H.; Hamilton, A. D. *J. Am. Chem. Soc.* **1990**, *112*, 9408–9410. (q) Discotic liquid crystalline polymers: Green, M. M.; Ringsdorf, H.; Wagner, J.; Wüstefeld, R. *Angew. Chem., Int. Ed. Engl.* **1990**, *29*, 1478–1481. (r) Cyclic porphyrin oligomers: Anderson, H. L.; Sanders, J. K. M. *Angew. Chem., Int. Ed. Engl.* **1990**, *29*, 1400–1403.

in the making of [2]rotaxanes and a [2]catenane. It is dependent on rather precise stereoelectronic matching of the various different types of noncovalent bonding interactions between their molecular components. The syntheses rely upon the use of template-directed methods.[72] Not only does this mean that the synthetic methods are efficient but it also dictates that the order responsible for the production of the 1:1 complexes leading to rotaxane and catenane formation "lives on" in the products after they have been made. The fact that the separate components of these molecular assemblies interact so intimately and precisely with each other conjures up the prospect of molecules that have machine-like properties[73] to them, in so far as the components move with respect to each other in a related and interdependent manner. It is for this reason that we can look forward to constructing supramolecular structures in a modular fashion and then studying their mechanical properties—that is, we are engaged in the development of a kind of *molecular meccano*.

Making molecular machines that could function as information-processing systems by a "bottom-up" approach presents a considerable challenge to the chemical community. Let us consider here two examples (Scheme VIII) of how the properties of the compounds and the supramolecular structures reported in this paper could be elaborated into slightly more complicated molecular machines.

(a) The [2]catenane shows an intramolecular electrochemical gradient that causes the constituent bipyridinium units to undergo reduction at distinct potential values. This is a consequence of the distinctly different environment of each reducible subunit. These differences can be easily extended and utilized to build a *vectorial electron shuttle*; i.e., a molecular device capable of efficient unidirectional electron transport through identical redox sites. The electrochemical gradient driving the unidirectional electron flow could be created by the gradual variation in the environments (A, B, C, D, and E in Scheme VIII) to which the identical redox sites are exposed. This type of molecular electronic device could find important applications in artificial photosynthetic schemes or electrocatalysis.

(b) The [2]rotaxanes and the [2]catenane may be regarded as prototypes for the construction of photochemical molecular devices, i.e., ordered assemblies of molecular components designed to achieve specific photoinduced functions such as energy or electron migration.[4b] The various applications of such devices include the antenna effect, i.e., absorption of light energy by several components and migration of the resulting electronic energy to a single, specific component, and developments in the field of molecular electronics, e.g., the recently described *molecular shift register*.[74]

For these two specific reasons and more, it is important to establish how supramolecular structures can be self-assembled in a spontaneous manner so that information can be written into them, stored in them, processed in them, transferred between them, and eventually read back out of them; i.e., the molecular-scale computer will start to become a reality. The late George Pimentel predicted[75] in 1985 that it is no longer a matter of *whether* there will be man-made molecular-scale computers but *when* they will come into existence and *who* will be leading in their development. He went on to add, "The *when* question will be answered on the basis of fundamental research in chemistry; the *who* question will depend on which countries commit the required resources and creativity to the search."

Experimental Section

General Methods. Chemicals were purchased from Aldrich and used as received, with the exception of tetrabutylammonium hexafluorophosphate ($TBAPF_6$), which was purchased from Fluka (Purum). Solvents were dried [THF (from Na/benzophenone ketyl), DMF (from CaH_2), and MeCN (from P_2O_5)] according to literature procedures. Tetraethylene glycol bis(*p*-toluenesulfonate) and 2-[2-[2-[2-(benzyloxy)ethoxy]ethoxy]ethoxy]ethyl *p*-toluenesulfonate were prepared according to published procedures. Thin-layer chromatography (TLC) was carried out on aluminum sheets coated with silica gel 60 (Merck 5554) or with neutral alumina 60 (Merck 5550). Column chromatography was performed on silica gel 60 (Merck 9385, 230–400 mesh) or neutral alumina 90 (Merck 1077, 70–230 mesh). Melting points were determined on a Reichert hot-stage apparatus and are uncorrected. Microanalyses were performed by the University of Sheffield Microanalytical Service. Low-resolution mass spectra were obtained on a Kratos MS 25 or a Kratos MS80 mass spectrometer. Fast atom bombardment mass spectrometry (FABMS) using argon or xenon was performed on the Kratos MS80 instrument. UV–visible spectra were measured on a Perkin-Elmer 559 or on a Philips PU8720 spectrometer. ^1H NMR spectra were recorded on either a Bruker WH400 (400 MHz) or a Bruker AM250 (250 MHz) spectrometer. ^{13}C NMR spectra were recorded on the Bruker WH400 (100 MHz) spectrometer. ESR spectra were recorded with the X-band of an IBM ER200D SRC spectrometer.

1,11-Bis[4-(benzyloxy)phenoxy]-3,6,9-trioxaundecane (BBPTU). A solution of 4-(benzyloxy)phenol (8.7 g, 43.5 mmol) in dry DMF (70 mL) was added over 20 min to a suspension of NaH (2.16 g, 50% in mineral oil, washed previously with pentane, 45 mmol) in dry DMF (60 mL) stirred in a nitrogen atmosphere. After an additional 15 min, tetraethylene glycol bistosylate (11.4 g, 22.7 mmol) dissolved in dry DMF (100 mL) was added over 2.5 h and the temperature was raised to 80 °C. Stirring and heating were continued for 24 h. After the reaction was cooled to room temperature, the slight excess of NaH was quenched by the addition of a few drops of H_2O. The solvent was removed in vacuo, and the residue was partitioned between CH_2Cl_2 (150 mL) and H_2O (70 mL). The organic phase was washed with H_2O and dried ($MgSO_4$). Evaporation of the solvent in vacuo afforded a residue, which was purified by column chromatography [silica gel, EtOAc–light petroleum (1:1), then EtOAc-CH_2Cl_2–light petroleum (5:3:2)] to yield BBPTU as a pale yellow oil that quickly solidified (10.3 g, 85%): mp 78–80 °C; MS 558 (M^+); ^1H NMR ($CDCl_3$) δ 3.66–3.75 (8 H, m), 3.80–3.85 (4 H, m), 4.04–4.09 (4 H, m), 5.00 (4 H, s), 6.81–6.91 (8 H, m), 7.28–7.44 (10 H, m). Anal. ($C_{34}H_{38}O_7$) C, H.

1,11-Bis(4-hydroxyphenoxy)-3,6,9-trioxaundecane (BHPTU). A solution of BBPTU (10 g, 17.9 mmol) in $CHCl_3$–MeOH (1:1, v/v, 160 mL) was subjected to hydrogenolysis over 10% palladium on charcoal (1.0 g). After filtration of the catalyst, the solvent was evaporated to give BHPTU as a viscous pale yellow oil (6.8 g, 99%), which was employed in the following step without further purification: MS 378 (M^+); ^1H NMR (CD_3COCD_3) δ 3.57–3.66 (8 H, m), 3.73–3.77 (4 H, m), 3.98–4.03 (4 H, m), 5.61 (2 H, s), 6.70–6.80 (8 H, m).

1,4-Bis[2-(2-hydroxyethoxy)ethoxy]benzene (BHEEB). A solution of 1/4DHB (4.0 g, 36.4 mmol) in dry DMF (75 mL) was added over 30 min to a stirred suspension of K_2CO_3 (40.3 g, 291.2 mmol) in dry DMF (75 mL) under nitrogen. After an additional 30 min, a solution of 2-(2-chloroethoxy)ethanol (18.1 g, 145.6 mmol) in dry DMF (60 mL) was added over 30 min, and the temperature was raised to 75 °C. Stirring and heating were continued for 7 days. After cooling to room temperature, the reaction mixture was filtered and the residue was washed with DMF (20 mL). The solvent was removed in vacuo and the

(72) (a) Stoddart, J. F. In *Chirality in Drug Design and Synthesis*; Brown, C., Ed.; Academic Press: London, 1990; pp 53–81. In *Frontiers in Supramolecular Organic Chemistry and Photochemistry*; Schneider, H.-J.; Dürr, H., Eds.; VCH: Weinheim, Germany, 1991; pp 251–263. In *Host-Guest Interactions from Chemistry to Biology*; Ciba Foundation Symposium 158; Wiley: Chichester, England, 1991; pp 5–22. *Chem. Br.* **1991**, *27*, 714–718. (b) Reddington, M. V.; Spencer, N.; Stoddart, J. F. In *Inclusion Phenomena and Molecular Recognition*; Atwood, J. L., Ed.; Plenum Press: New York, 1990; pp 41–48. (c) Goodnow, T. T.; Reddington, M. V.; Stoddart, J. F.; Kaifer, A. E. *J. Am. Chem. Soc.* **1991**, *113*, 4335–4337. (d) Anelli, P. L.; Spencer, N.; Stoddart, J. F. *J. Am. Chem. Soc.* **1991**, *113*, 5131–5133. (e) Philp, D.; Stoddart, J. F. *Synlett.* **1991**, 445–458. (f) Brown, C. L.; Philp, D.; Stoddart, J. F. *Synlett.* **1991**, 459–461 and 462–464. (g) Reddington, M. V.; Slawin, A. M. Z.; Spencer, N.; Stoddart, J. F.; Vicent, C.; Williams, D. J. *J. Chem. Soc., Chem. Commun.* **1991**, 630–634. (h) Ashton, P. R.; Brown, C. L.; Chrystal, E. J. T.; Goodnow, T. T.; Kaifer, A. E.; Parry, K. P.; Philp, D.; Slawin, A. M. Z.; Spencer, N.; Stoddart, J. F.; Williams, D. J. *J. Chem. Soc., Chem. Commun.* **1991**, 634–639. (i) Anelli, P. L.; Ashton, P. R.; Spencer, N.; Slawin, A. M. Z.; Stoddart, J. F.; Williams, D. J. *Angew. Chem., Int. Ed. Engl.* **1991**, *30*, 1036–1039. (j) Ashton, P. R.; Brown, C. L.; Crystal, E. J. T.; Goodnow, T. T.; Kaifer, A. E.; Parry, K. P.; Slawin, A. M. Z.; Spencer, N.; Stoddart, J. F.; Williams, D. J. *Angew. Chem., Int. Ed. Engl.* **1991**, *30*, 1039–1042. (k) Ashton, P. R.; Brown, C. L.; Chrystal, E. J. T.; Parry, K. P.; Pietraskiewicz, M.; Spencer, N.; Stoddart, J. F. *Angew. Chem., Int. Ed. Engl.* **1991**, *30*, 1042–1045. (l) Ashton, P. R.; Philp, D.; Spencer, N.; Stoddart, J. F. *Makromol. Chem.*, in press.

(73) (a) *Artificial Life*; Langton, C. G., Ed.; Addison-Wesley: Redwood City, CA, 1989. (b) Drexler, K. E. *Engines of Creation*; Fourth Estate: London, 1990.

(74) Hopfield, J. J.; Onuchic, J. N.; Beratan, D. N. *Science* **1988**, *241*, 817–820. *J. Phys. Chem.* **1989**, *93*, 6350–6357.

(75) Pimentel, G. C. *Opportunities in Chemistry*; National Academy Press: Washington, DC, 1985.

residue was partitioned between CH_2Cl_2 (150 mL) and H_2O (70 mL) with addition of NaCl. The pH was adjusted to ca. 2 with 2 N HCl, and the aqueous phase was washed with CH_2Cl_2 (2 × 50 mL). The combined organic solutions were washed with H_2O (80 mL), dried ($MgSO_4$), and concentrated in vacuo. Recrystallization of the residue from CH_2Cl_2–*n*-pentane afforded BHEEB as a white solid (6.7 g, 60%): mp 75–77 °C; MS 286 (M^+); ^1H NMR ($CDCl_3$) δ 2.28 (2 H, br s), 3.65–3.70 (4 H, m), 3.73–3.81 (4 H, m), 3.83–3.87 (4 H, m), 4.07–4.12 (4 H, m), 6.86 (4 H, s). Anal. ($C_{14}H_{22}O_6$) C, H.

1,4-Bis[2-(2-hydroxyethoxy)ethoxy]benzene Bis(4-methylbenzenesulfonate) (BTEEB). A solution of tosyl chloride (2.65 g, 13.9 mmol) in dry CH_2Cl_2 (15 mL) was added at room temperature over 30 min to a solution of BHEEB (1.33 g, 4.6 mmol) and triethylamine dried over KOH (1.64 g, 16.2 mmol) in CH_2Cl_2 (15 mL). After stirring for 15 h, the reaction mixture was extracted with 2 N HCl (10 mL) and H_2O (2 × 10 mL). The organic phase was dried ($MgSO_4$) and the solvent was removed in vacuo. Column chromatography (SiO_2, 50% light petroleum–$CHCl_3$ then $CHCl_3$) afforded BTEEB as a white solid (2.5 g, 88%): mp 96–97 °C; MS 594 (M^+); ^1H NMR ($CDCl_3$) δ 2.42 (6 H, s), 3.74–3.79 (8 H, m), 3.98–4.02 (4 H, m), 4.17–4.22 (4 H, m), 6.82 (4 H, s), 7.29–7.34 (4 H, m), 7.77–7.83 (4 H, m). Anal. ($C_{28}H_{34}S_2O_{10}$) C, H.

1,4,7,10,17,20,23,26,28,32-Decaoxa[13.13]paracyclophane (BPP34C10). Method A. A solution of BHPTU (7.0 g, 18.5 mmol) in dry THF (200 mL) and a solution of tetraethylene glycol bistosylate (9.5 g, 18.9 mmol) in dry THF (250 mL) were added simultaneously over 2 h to a stirred suspension of NaH (2.66 g, 50% in mineral oil, washed previously with *n*-pentane, 55.6 mmol) in refluxing dry THF (250 mL) under nitrogen. The mixture was refluxed for 5 days beforre being cooled down to room temperature. Excess NaH was quenched by the addition of a few drops of H_2O, and then the solvent was removed in vacuo and the residue was partitioned between CH_2Cl_2 (150 mL) and H_2O (100 mL). The organic phase was washed with 2 N HCl (80 mL) and H_2O (80 mL), dried ($MgSO_4$), and then concentrated in vacuo. Column chromatography [SiO_2, Et_2O–$CHCl_3$–MeOH (68:30:2)] afforded BPP34C10 as a white solid (2.42 g, 25%): mp 87–88 °C (lit.[76] mp 93–94 °C); MS 536 (M^+); ^1H NMR (CD_3COCD_3) δ 3.58–3.66 (16 H, m), 3.76–3.80 (8 H, m), 3.94–3.99 (8 H, m), 6.77 (8 H, s); ^{13}C NMR (CD_3COCD_3) δ 69.0, 70.4, 71.4, 71.5, 116.3, 154.1. Anal. ($C_{28}H_{40}O_{10}$) C, H. Single crystals, suitable for X-ray crystallography were grown by slow evaporation of a solution of BPP34C10 in acetone.

Method B. A solution of BHEEB (2.3 g, 8 mmol) in dry THF (200 mL) was added over 15 min to a stirred suspension of NaH (1.2 g, 50% in mineral oil, washed previously with *n*-pentane, 24 mmol) in dry THF (200 mL) under nitrogen. After 1 h, a solution of BTEEB (5.0 g, 8.4 mmol) in dry THF (200 mL) was added over 15 min. The reaction mixture was then heated under reflux for 4 days. Workup according to Method A afforded BPP34C10 (1.21 g, 28%).

[BPP34C10·PQT][PF_6]$_2$. Single crystals, suitable for X-ray crystallography, were grown by vapor diffusion of *n*-pentane into an equimolar solution of BPP34C10 and [PQT][PF_6]$_2$ in acetone.

1,4-Bis[2-[2-(2-hydroxyethoxy)ethoxy]ethoxy]benzene (BHEEEB). A solution of 1/4DHB (5.5 g, 50 mmol) in dry *tert*-butyl alcohol (50 mL) was added to a solution of potassium *tert*-butoxide (12.3 g, 110 mmol) in dry *tert*-butyl alcohol (50 mL) under nitrogen. The mixture was refluxed for 2 h, and then 2-[2-(2-chloroethoxy)ethoxy]ethanol (18.5 g, 110 mmol) was added over 15 min and refluxing was maintained for 65 h. After cooling down to room temperature, the reaction mixture was filtered and the solid residue was washed with CH_2Cl_2 (50 mL). The combined organic solutions were evaporated in vacuo, and the residue, dissolved in CH_2Cl_2 (100 mL), was washed with 2 N HCl (30 mL) and H_2O (2 × 30 mL). The organic phase was dried ($MgSO_4$) and the solvent was evaporated in vacuo. Purification of the residue by column chromatography (SiO_2, 5% MeOH–EtOAc) gave BHEEEB as a white solid (14.6 g, 78%): mp 48–51 °C; ^1H NMR (CD_3CN) δ 2.77 (2 H, br s), 3.45–3.51 (4 H, m), 3.53–3.64 (12 H, m), 3.71–3.76 (4 H, m), 4.00–4.05 (4 H, m), 6.84 (4 H, s). Anal. ($C_{18}H_{30}O_8$) C, H.

1,4-Bis[2-[2-[2-(benzyloxy)ethoxy]ethoxy]ethoxy]ethoxy]benzene (BBEEEEB). A solution of 1/4DHB (1.65 g, 15 mmol) in dry *tert*-butyl alcohol (40 mL) was added to a solution of potassium *tert*-butoxide (3.70 g, 33 mmol) in dry *tert*-butyl alcohol (30 mL) under nitrogen, and the mixture was refluxed for 2 h. A solution of 2-[2-[2-[2-(benzyloxy)ethoxy]ethoxy]ethoxy]ethyl 4-methylbenzenesulfonate (13.8 g, 31.5 mmol) in dry *tert*-butyl alcohol–THF (2:3, v/v, 50 mL) was added over 30 min and refluxing was maintained for 65 h. After cooling to room temperature, the reaction mixture was filtered, and the residue was washed with CH_2Cl_2 (50 mL). The combined organic solutions were evaporated in vacuo, and the residue was purified by column chromatography (SiO_2, Et_2O) to afford BBEEEEB (7.06 g, 73%) as a colorless oil: ^1H NMR ($CDCl_3$) δ 3.50–3.70 (24 H, m), 3.70–3.89 (4 H, m), 3.92–4.12 (4 H, m), 4.54 (4 H, s), 6.82 (4 H, s), 7.25–7.40 (10 H, m). Anal. ($C_{36}H_{50}O_{10}$) C, H.

1,4-Bis[2-[2-[2-(2-hydroxyethoxy)ethoxy]ethoxy]ethoxy]benzene (BHEEEEB). A solution of BBEEEEB (6.77 g, 10.5 mmol) in 10% CH_2Cl_2–MeOH (70 mL) was subjected to hydrogenolysis at room temperature in the presence of 10% palladium on charcoal (700 mg) for 1 h. The reaction mixture was filtered, and the solvent was removed in vacuo to yield BHEEEEB (4.58 g, 94%) as a thick colorless oil: ^1H NMR (CD_3CN) δ 2.77 (2 H, br s), 3.44–3.49 (4 H, m), 3.52–3.64 (20 H, m), 3.70–3.75 (4 H, m), 4.00–4.05 (4 H, m), 6.84 (4 H, s).

1,4-Bis[2-[2-[[tris(1-methylethyl)silyl]oxy]ethoxy]ethoxy]benzene (BSEEB). A solution of triisopropylsilyl triflate (4.59 g, 15 mmol) in CH_2Cl_2 (10 mL) was added over 10 min to a solution of BHEEB (1.43 g, 5 mmol) and imidazole (1.15 g, 16.9 mmol) in CH_2Cl_2 (15 mL) cooled at 0–5 °C. The reaction mixture was stirred at room temperature for 2 h and was then washed with H_2O (2 × 10 mL). After drying ($MgSO_4$), the solvent was removed in vacuo, and the residue was purified by column chromatography (SiO_2, light petroleum then 10% Et_2O–light petroleum) to yield BSEEB (1.66 g, 55%) as a colorless oil: ^1H NMR (CD_3CN) δ 0.98–1.14 (42 H, m), 3.55–3.58 (4 H, m), 3.74–3.77 (4 H, m), 3.80–3.83 (4 H, m), 4.00–4.03 (4 H, m), 6.82 (4 H, s). Anal. ($C_{32}H_{62}O_6Si_2$) C, H.

1,4-Bis[2-[2-[2-[[tris(1-methylethyl)silyl]oxy]ethoxy]ethoxy]ethoxy]-benzene (BSEEEB). The disilyl ether BSEEEB was prepared in 94% yield from BHEEEB, employing the same procedure as that described for BSEEB. Colorless oil: ^1H NMR (CD_3CN) δ 1.00–1.14 (42 H, m), 3.49–3.53 (4 H, m), 3.57–3.62 (8 H, m), 3.71–3.74 (4 H, m), 3.77–3.81 (4 H, m), 3.99–4.02 (4 H, m), 6.82 (4 H, s). Anal. ($C_{36}H_{70}O_8Si_2$) C, H.

1,1′-[1,4-Phenylenebis(methylene)]bis-4,4′-bipyridinium Bis(hexafluorophosphate) ([BBIPYXY][PF_6]$_2$). A solution of 1,4-bis(bromomethyl)benzene (22.0 g, 83.3 mmol) in dry MeCN (400 mL) was added over 6 h to a solution of 4,4′-bipyridine (31.2 g, 200 mmol) in dry MeCN (300 mL), which was heated under reflux. Heating was continued for 18 h. After the solution was cooled to room temperature, the yellow precipitate was filtered off and washed with MeCN (50 mL) and Et_2O (50 mL) before being dissolved in H_2O (3 L). The aqueous solution was washed with Et_2O (4 × 500 mL), and then H_2O was removed in vacuo to leave a solid residue, which was recrystallized three times from H_2O. The solid was then dissolved in hot water, and a saturated aqueous solution of NH_4PF_6 was added until no further precipitation was observed. The precipitate was filtered off and washed with H_2O (50 mL), MeOH (50 mL), and Et_2O (50 mL). Finally, it was recrystallized from Me_2CO–H_2O to afford [BBIPYXY][PF_6]$_2$ as a white solid (42.2 g, 71%): mp 145 °C dec [lit.[49b] mp 130 °C dec]; FABMS 561 ($M - PF_6$)$^+$; ^1H NMR (CD_3COCD_3) δ 6.16 (4 H, s), 7.80 (4 H, s), 7.94–7.98 (4 H, m), 8.64–8.69 (4 H, m), 8.83–8.88 (4 H, m), 9.31–9.36 (4 H, m). Anal. ($C_{28}H_{24}N_4F_{12}P_2$) C, H, N.

5,12,19,26-Tetraazoniaheptacyclo[24.2.2.2^{2,5}.2^{7,10}.2^{12,15}.2^{16,19}.2^{21,24}]-tetraconta-2,4,7,9,12,14,16,18,21,23,26,28,29,31,33,35,37,39-octadecaene Tetrakis(hexafluorophosphate) ([BBIPYBIXYCY][PF_6]$_4$). Method A. A solution of 1,4-bis(bromomethyl)benzene (0.52 g, 2.0 mmol) and [BBIPYXY][PF_6]$_2$ (1.40 g, 2.0 mmol) in dry MeCN (300 mL) was heated under reflux for 18 h. More 1,4-bis(bromomethyl)benzene (0.2 g, 0.8 mmol) was added and the reaction mixture was refluxed for an additional 24 h. After the solution was cooled down to room temperature, the yellow precipitate was filtered off and washed with MeCN (20 mL) and Et_2O (20 mL). The precipitate was dissolved in H_2O to give an aqueous solution, which was then filtered. After evaporation of the H_2O in vacuo, the residue was subjected to chromatography [SiO_2, MeOH–H_2O–saturated aqueous NH_4Cl solution (6:3:1)]. The cyclophane-containing fractions were combined, and the solvent was removed in vacuo. The residue was dissolved in H_2O, and a saturated aqueous solution of NH_4PF_6 was added until no further precipitation was observed. After filtration, the precipitate was washed with H_2O (10 mL), MeOH (20 mL), and Et_2O (20 mL). It was then recrystallized from acetone–H_2O to give [BBIPYBIXYCY][PF_6]$_4$ as a white solid that becomes bluish in the presence of light (271 mg, 12%): mp > 275 °C; FABMS 955 ($M - PF_6$)$^+$, 810 ($M - 2PF_6$)$^+$; ^1H NMR (CD_3CN) δ 5.74 (8 H, s), 7.52 (8 H, s), 8.14–8.18 (8 H, m), 8.84–8.88 (8 H, m); ^{13}C NMR (CD_3CN) δ 65.7, 128.3, 131.4, 137.0, 146.2, 150.4. Anal. ($C_{36}H_{32}N_4F_{24}P_4$) C, H, N. Single crystals, suitable for X-ray crystallography, were grown by vapor diffusion of *i*-Pr_2O into a solution of [BBIPYBIXYCY][PF_6]$_4$ in MeCN.

Method B. A solution of 1,4-bis(bromomethyl)benzene (0.26 g, 1.0 mmol), [BBIPYXY][PF_6]$_2$ (0.71 g, 1.0 mmol), and BHEEB (0.86 g, 3.0 mmol) in dry MeCN (30 mL) was stirred at room temperature for 9

(76) Helgeson, R. C.; Tarnowski, T. L.; Timko, J. M.; Cram, D. J. *J. Am. Chem. Soc.* **1977**, *99*, 6411–6418.

days. The orange precipitate was filtered, washed with MeCN (5 mL), and then dried under vacuum to give a red solid (5.9 g), which was dissolved in hot H_2O (40 mL). The aqueous solution was extracted continuously with CH_2Cl_2 for 5 days. During this time, the aqueous solution changed from deep orange to very pale yellow. It was concentrated and the residue was dissolved in the minimum amount of hot H_2O. This aqueous solution was passed through a short column of silica gel with MeOH–H_2O–saturated aqueous NH_4Cl solution (6:3:1) as the eluant. Fractions containing the cyclophane were evaporated, and the residue was partitioned between $MeNO_2$ (10 mL) and a saturated aqueous solution (10 mL) of NH_4PF_6. The organic phase was washed with the saturated aqueous NH_4PF_6 solution (10 mL) before being concentrated in vacuo. The residue was suspended in H_2O (10 mL), filtered, and washed with H_2O (3 × 10 mL). Recrystallization of the residue from acetone–H_2O afforded [BBIPYBIXYCY][PF_6]$_4$ (385 mg, 35%). The filtrate (MeCN solution) from the reaction mixture was evaporated in vacuo and the residue was suspended in CH_2Cl_2 (50 mL). After filtration, the organic solution was combined with the CH_2Cl_2 solution obtained from the continuous extraction, and the solvents were evaporated in vacuo. Recrystallization of the residue from EtOAc afforded 770 mg (90%) of BHEEB. Use of the diol BHEEEB, instead of BHEEB, as a template gave [BBIPYBIXYCY][PF_6]$_4$ in 23% yield. 1/4DMB and the diol BHEB were totally ineffective as templates for the formation of [BBIPYBIXYCY][PF_6]$_4$; i.e., the yields obtained were 12% in both cases.

Method C. 1,4-Bis(bromomethyl)benzene (26.4 mg, 0.1 mmol), [BBIPYXY][PF_6]$_2$ (70.6 mg, 0.1 mmol), and BHEEB (85.8 mg, 0.3 mmol) were dissolved in dry DMF (5 mL). NaI (5 mg) was added to the clear solution and it was stirred at room temperature. A red precipitate started to appear after 90 min. After 5 days, THF (15 mL) was added and the crude product (86.2 mg) was filtered off and dried in vacuo. Decomplexation was effected by continuous extraction of an aqueous solution (5 mL) of the crude product with CH_2Cl_2 as described under Method B. Treatment of the almost colorless aqueous solution with NH_4PF_6 caused a precipitate to form. The product, which was filtered off, was pure [BBIPYBIXYCY][PF_6]$_4$ (49.5 mg, 45%).

Method D. The same starting materials (without NaI) in the same quantities as were employed in method C were dissolved in dry DMF (10 mL). The reaction mixture was transferred to a high-pressure-reaction Teflon tube, which was then compressed (10 kbars) at room temperature for 24 h. After decompression of the reaction vessel, the reaction mixture was reclaimed and treated with Et_2O (50 mL). The precipitate, which was produced, was filtered off, washed with THF, and dried in vacuo to give a crude product (88.8 mg). Treatment of this material, as described for the crude product in Method C, afforded pure [BBIPYBIXYCY][PF_6]$_4$ (68 mg, 62%).

[1/4DMB·BBIPYBIXYCY][PF_6]$_4$, [BHEEB·BBIPYBIXYCY][PF_6]$_4$, [BHEEEB·BBIPYBIXYCY][PF_6]$_4$, and [BHEEEEB·BBIPYBIXYCY][PF_6]$_4$. In all cases, single crystals, suitable for X-ray crystallography, were grown by vapor diffusion of *i*-Pr_2O into an equimolar solution of the two appropriate components in MeCN.

{[2]-[BSEEB]-[BBIPYBIXYCY]rotaxane}[PF_6]$_4$. Triisopropylsilyl triflate (321 mg, 1.05 mmol) was added to a solution of [BBIPYBIXYCY][PF_6]$_4$ (154 mg, 0.14 mmol), BHEEB (119 mg, 0.42 mmol), and 2,6-dimethylpyridine (112 mg, 1.05 mmol) in dry MeCN (5 mL). After the solution was stirred for 1 h at room temperature, the solvent was removed in vacuo without heating. The residue was suspended in CH_2Cl_2–Et_2O (1:1, v/v, 10 mL), transferred into a tube, and centrifuged. After decantation of the solvent, the procedure was repeated three times. The residue was dissolved in $MeNO_2$ (5 mL) before adding CH_2Cl_2 (10 mL) to precipitate a white solid, which was separated by centrifugation, suspended in CH_2Cl_2–$MeNO_2$ (2:1, v/v, 6 mL), and centrifuged again. The combined organic solutions were evaporated in vacuo without heating, and the residue was purified by column chromatography [SiO_2, MeOH–2 N aqueous NH_4Cl–$MeNO_2$ (7:2:1)]. The rotaxane-containing fractions were combined and evaporated in vacuo without heating. The residue was partitioned between $MeNO_2$ (10 mL) and H_2O (5 mL), and saturated aqueous NH_4PF_6 (5 mL) was added. The organic phase was washed with saturated aqueous NH_4PF_6 (2 × 5 mL), the solvent was removed in vacuo without heating, and the residue was suspended in H_2O (5 mL), filtered, and finally washed with H_2O (2 × 5 mL) and MeOH (2 × 5 mL). After drying under vacuum (0.5 mbar, 70 °C, 15 h), {[2]-[BSEEB]-[BBIPYBIXYCY]rotaxane}[PF_6]$_4$ was recovered as an orange solid (53 mg, 22%): mp > 280 °C; FABMS 1553 $(M - PF_6)^+$, 1408 $(M - 2PF_6)^+$; ^{1}H NMR (CD_3CN) δ 1.07–1.21 (42 H, m), 3.56 (4 H, s), 3.58–3.63 (4 H, m), 3.91–3.97 (8 H, m), 4.08–4.13 (4 H, m), 5.70 (8 H, s), 7.79 (8 H, s), 7.80–7.85 (8 H, m), 8.84–8.89 (8 H, m); ^{13}C NMR (CD_3COCD_3) δ 12.8, 18.4, 64.2, 66.0, 67.8, 71.1, 74.2, 114.2, 127.1, 132.0, 137.8, 145.8, 148.0, 151.2. Anal. ($C_{68}H_{94}N_4O_6F_{24}P_4Si_2$) C, H, N. Single crystals, suitable for X-ray crystallography, were grown by vapor diffusion of *i*-Pr_2O into a solution of the rotaxane in MeCN.

{[2]-[BSEEEB]-[BBIPYBIXYCY]rotaxane}[PF_6]$_4$. Method A. This rotaxane was prepared from BHEEEB and [BBIPYXYCY][PF_6]$_2$ in 22% yield according to the procedure outlined above for {[2]-[BSEEB]-[BBIPYBIXYCY]rotaxane}[PF_6]$_4$. Orange solid: mp > 280 °C; FABMS 1641 $(M - PF_6)^+$, 1496 $(M - 2PF_6)^+$, 1351 $(M - 3PF_6)^+$; ^{1}H NMR (CD_3CN) δ 0.96–1.08 (42 H, m), 3.56 (4 H, s), 3.62–3.65 (4 H, m), 3.70–3.73 (4 H, m), 3.84–3.87 (4 H, m), 3.87–3.90 (4 H, m), 5.94 (8 H, s), 7.69 (8 H, s), 7.80–7.83 (8 H, d), 8.92–8.96 (8 H, d); ^{13}C NMR (CD_3COCD_3) δ 12.6, 18.2, 63.7, 65.7, 67.5, 70.9, 71.8, 73.6, 114.0, 127.0, 131.9, 137.8, 145.9, 147.8, 151.1. Anal. ($C_{72}H_{102}N_4O_8F_{24}P_4Si_2$) C, H, N. Single crystals, suitable for X-ray crystallography, were grown by vapor diffusion of *n*-pentane into a solution of the rotaxane in acetone.

Method B. A solution of [BBIPYXY][PF_6]$_2$ (706 mg, 1 mmol), 1,4-bis(bromomethyl)benzene (264 mg, 1 mmol), BSEEEB (2.06 g, 3 mmol), and silver hexafluorophosphate (632 mg, 2.5 mmol) in dry MeCN (50 mL) was stirred at room temperature for 7 days. After filtration of the precipitate (AgBr), the solvent was evaporated off and the residue was suspended in CH_2Cl_2 (20 mL) and centrifuged. After decantation of the solvent, the procedure was repeated three times. The residue was dissolved in $MeNO_2$ (10 mL) before adding CH_2Cl_2 (20 mL) to precipitate a white solid, which was separated by centrifugation, suspended in CH_2Cl_2–$MeNO_2$ (2:1, v/v, 10 mL), and then centrifuged again. The combined organic solutions were evaporated, and the residue was purified by column chromatography [SiO_2, MeOH–2 N NH_4Cl–$MeNO_2$ (7:2:1)]. The rotaxane-containing fractions were combined and evaporated in vacuo without heating. The residue was partitioned between $MeNO_2$ (10 mL) and H_2O (5 mL), and saturated aqueous NH_4PF_6 (5 mL) was added. The organic phase was washed with saturated aqueous NH_4PF_6 (2 × 5 mL). The solvent was removed in vacuo without heating, and the residue was suspended in H_2O (2 × 5 mL) and MeOH (2 × 5 mL) and finally dried to yield {[2]-[BSEEEB]-[BBIPYBIXYCY]rotaxane}[PF_6]$_4$ (154 mg, 14%). The method was not successful in the attempted preparation of the smaller rotaxane.

{[2]-[BPP34C10]-[BBIPYBIXYCY]-catenane}[PF_6]$_4$. A solution of [BBIPYXY][PF_6]$_2$ (140 mg, 0.2 mmol) in dry MeCN (5 mL) was added to a stirred solution of BPP34C10 (280 mg, 0.52 mmol) in dry MeCN (5 mL) under nitrogen. A deep yellow color was formed immediately, and a solution of 1,4-bis(bromomethyl)benzene (56 mg, 0.2 mmol) in dry MeCN (5 mL) was added. After 4 h, the reaction became a deep red color, which preceded the precipitation of a red solid. After the reaction was stirred at room temperature for 48 h, the precipitate was filtered off, washed with $CHCl_3$ (10 mL), dissolved in H_2O (30 mL), and filtered to remove a small amount of insoluble material. An aqueous solution of NH_4PF_6 was added until no further precipitation occurred. The precipitate was filtered off, washed with H_2O (10 mL), and dried. Recrystallization from MeCN–H_2O gave {[2]-[BPP34C10]-[BBIPYBIXYCY]catenane}[PF_6]$_4$ as a pure compound (230 mg, 70%): mp > 280 °C; FABMS 1491 $(M - PF_6)^+$, 1347 $(M - 2PF_6)^+$; ^{1}H NMR (CD_3CN) 3.32–3.39 (4 H, m), 3.43–3.48 (4 H, br s), 3.52–3.57 (4 H, m), 3.59–3.65 (4 H, m), 3.70–3.77 (4 H, m), 3.81–3.86 (4 H, m), 3.86–3.92 (8 H, m), 3.92–3.97 (4 H, m), 5.67 (8 H, s), 6.16 (4 H, s), 7.66 (8 H, d), 7.79 (8 H, s), 8.85 (8 H, d); ^{13}C NMR (CD_3COCD_3) 65.5, 67.3, 68.4, 70.0, 70.5, 70.8, 70.9, 71.4, 71.5, 113.8, 115.8, 126.4, 131.7, 137.7, 145.6, 146.9, 151.1, 153.0. Single crystals, suitable for X-ray crystallography, were grown by vapor diffusion of *i*-Pr_2O into a solution of the catenane in MeCN.

Absorption and Emission Spectra. Absorption spectra were recorded at room temperature (ca. 25 °C) with a Kontron Uvikon 860 spectrophotometer. Luminescence experiments were performed both at room temperature and at 77 K. Uncorrected emission spectra were recorded with a Perkin-Elmer 650-40 spectrofluorimeter. Corrected excitation spectra were obtained with a Perkin-Elmer LS 5 spectrofluorimeter that was also used to obtain luminescence lifetimes in the 5 μs–10 ms time region; an Edinburgh single-photon-counting apparatus was used for shorter lifetimes. In all cases, the experimental error on the lifetime values is estimated to be ±10%. In the Edinburgh system, the flash lamp was filled with H_2, and a monochromator was used to select the excitation wavelength. The instrument response function was deconvoluted from the emission data to obtain an undisturbed decay, which was then fitted by a least-squares method on an IBM PC. In each case a single-exponential decay was observed.

Electrochemistry. The electrochemical reduction experiments were performed with a Princeton Applied Research (PAR) Model 175 universal programmer, a Model 173 potentiostat, and a Model 179 digital coulometer. Cyclic voltammograms were recorded at 25 °C on a Houston Model 200 X-Y recorder. These cyclic voltammetry experiments were performed under a purified nitrogen atmosphere. Nitrogen gas was also used to purge all solutions prior to experimentation. The solutions for electrochemistry were routinely held at a constant concen-

tration of 5×10^{-4} M electroactive species. 0.1 M $TBAPF_6$ was included as a supporting electrolyte. Measurements were taken in a standard single-compartment electrochemical cell. A glassy carbon electrode (0.08 cm^2, Bioanalytical Systems) was used as the working electrode; its surface was routinely polished with a 0.05 μm alumina–water slurry on a felt surface immediately prior to use. All potentials were recorded against a sodium chloride saturated calomel electrode (SSCE), and a platinum flag was utilized as a counter electrode. The potential range was cycled from 0 to −1.2 V (vs SSCE) for all samples. In the electrochemical oxidation experiments, cyclic voltammetry was performed with an Amel 448/XA oscillographic polarograph in Ar-purged acetonitrile solution containing 0.1 M $TBABF_4$ as the supporting electrolyte. The working electrode was a platinum microelectrode, the counter electrode was a platinum wire, and a standard calomel electrode (SCE) was the reference electrode. All of these experiments were performed at room temperature.

ESR Spectroscopy. ESR spectra were acquired under vacuum conditions, with the reduced samples being generated either electrochemically or chemically with Zn granules (20 mesh). Bulk electrolysis was performed in an evacuated dual-compartment electrochemical cell with a 12-cm^2 platinum foil as the working electrode and a platinum flag counter electrode. All potentials were referenced to a silver/silver chloride electrode. The reduction was realized in a controlled potential format (generally at −0.45 V vs Ag/AgCl). The chemical reduction was also completed under vacuum. The solvent in both cases was acetonitrile, with 0.1 M $TBAPF_6$ included as a supporting electrolyte for the electrochemical reductions. Prior to reduction, the solution was always degassed via three freeze–pump–thaw cycles. After the reduction, the solution was transferred under vacuum to a 1-mm (i.d.) sample tube, which was then flame sealed and detached from the cell for spectroscopic analysis. The spectra obtained from the electrochemical reduction or the chemical reduction were observed to be essentially identical in control experiments. The extent of reduction was monitored by obtaining the concentration of ESR active species in the partially reduced samples. This was done by comparing the double integral value of the overmodulated ESR spectra with that of a standard sample containing a known concentration of the methyl viologen cation radical.

NMR Spectroscopy. Saturation-transfer experiments were performed on the catenane in a manner similar to NOE experiments with standard Bruker software. During irradiation, saturation is transferred by chemical exchange, and the site to which this occurs is identified as an additional irradiation point. The resulting difference spectrum contains NOEs generated both by the actual irradiated resonance and by that which has been saturated by exchange. The temperature for the experiment was chosen by careful judgment of the onset of line broadening as a result of chemical exchange in the signal of interest. In the two-dimensional experiment (2D-NOESY 45), a mixing time of 200 ms was used. Standard Bruker software was used to perform 2D-COSY 45 and ^{13}C–^1H-shift correlation experiments. The latter featured H–H decoupling in the proton domain (F1).

Stability Constant Determinations by Spectrophotometric Titration Procedures. The methods employed in this investigation were based on observing changes in optical densities of solutions where the relative concentration of one component (the substrate or the thread) is increased with respect to the other component (the receptor or the bead). All stability constants were determined in dry acetonitrile solutions at 25 °C. In a typical experiment, a solution of the receptor was made up in a graduated flask and its optical density was recorded. The solution was then transferred back into a graduated flask, and the sample cell and transferring pipette were washed. The washings were added to the graduated flask. A known quantity of the substrate was added to the solution. Excess solvent was evaporated off from the thermostated (25 °C) solution with a stream of nitrogen. The optical density of the solution of the complex was recorded, and the procedure was repeated until no significant changes in optical density were observed on further addition of substrate. The initial concentrations of the receptors were in the range 4×10^{-4} mol L^{-1} to 3×10^{-3} mol L^{-1}. Molar ratios of substrates to receptors used were in the range 0.1:1 to 30:1 for relatively strong 1:1 complexes, and in the range 5:1 to 300:1 for relatively weak 1:1 complexes. The data were treated on the nonlinear curve-fitting program EUREKA[77] on an IBM Vanilla Microcomputer.

X-ray Crystallography. X-ray diffraction measurements were performed on a Nicolet R3m diffractometer with graphite-monochromated Cu Kα radiation with ω scans. Crystal data and data collection parameters are given in Table XII. Lattice parameters were determined by least-squares fits from 18 to 22 centered reflections. Intensities were corrected for the decay of two control reflections, measured every 50

(77) EUREKA: Borland International Inc., 4585 Scotts Valley Drive, Scotts Valley, CA, 95066. We thank Dr. B. F. Taylor for assistance in the use of this program.

Table XII. Crystal Data and Data Collection Parameters

data	A[a]	B[a]	C[a]	D[a]	E[a]	F[a]	G[a]	H[a]	I[a]	J[a]
formula	$C_{28}H_{40}O_{10}$	$C_{46}H_{66}N_2O_{12}P_2F_{12}$	$C_{42}H_{41}N_7P_4F_{24}$	$C_{48}H_{48}N_6O_2P_4F_{24}$	$C_{50}H_{54}N_4O_8P_4F_{24}$	$C_{62}H_{77}N_8O_8P_4F_{24}$	$C_{62}H_{76}N_6O_{10}P_4F_{24}$	$C_{71}H_{97}N_5O_6Si_2P_4F_{24}$	$C_{79.5}H_{117}N_4O_{10.5}Si_2P_4F_{24}$	$C_{74}H_{87}N_9O_{10}P_4F_{24}$
solvent		$2Me_2CO$	3MeCN	2MeCN	4MeCN	4MeCN	2MeCN	$2[MeCN{\cdot}C_2]$[a]	$2.5Me_2CO$	5MeCN
formula weight	536.7	1129	1224	1238.7	1551.1	1642.2	1645.2	1752.6	1932.9	1842.4
lattice type	monoclinic	triclinic	monoclinic	monoclinic	triclinic	triclinic	monoclinic	triclinic	triclinic	triclinic
space group	$P2_1/c$	$P\bar{1}$	$P2_1/n$	$P2_1/n$	$P\bar{1}$	$P\bar{1}$	$I2/d$[b]	$P\bar{1}$	$P\bar{1}$	$P\bar{1}$
T, K	293	293	293	293	293	293	293	293	293	293
cell dimensions										
a, Å	10.890 (2)	10.204 (2)	10.805 (1)	10.948 (4)	11.725 (2)	12.570 (5)	23.623 (10)	12.173 (5)	11.268 (3)	13.847 (6)
b, Å	21.450 (6)	11.562 (2)	19.819 (2)	19.869 (8)	13.090 (2)	13.231 (6)	11.653 (5)	18.261 (6)	12.197 (3)	13.998 (4)
c, Å	12.361 (4)	13.835 (5)	14.027 (2)	13.886 (6)	13.462 (3)	13.808 (4)	26.595 (17)	20.705 (6)	20.622 (7)	26.584 (15)
α, deg		105.59 (2)			62.02 (1)	64.77 (3)		106.45 (2)	95.96 (2)	84.36 (14)
β, deg	106.31 (2)	98.70 (2)	109.36 (1)	110.55 (3)	81.16 (2)	65.02 (3)	93.58 (4)	100.70 (3)	101.80 (3)	80.91 (4)
γ, deg		115.47 (1)			76.35 (1)	73.60 (3)		90.74 (3)	114.20 (2)	60.79 (3)
V, Å^3	2771	1350	2834	2828	1771	1868	7307	4327	2474	4440
Z	4	1	2	2	1	1	4	2[c]	1	2
D_c, g cm^{-3}	1.29	1.39	1.43	1.55	1.45	1.46	1.50	1.35	1.30	1.38
$F(000)$	1152	590	1236	1340	794	865	3384	1820	1010	1900
μ, mm^{-1}	0.67	1.61	2.31	2.43	2.3	2.0	2.0	2.0	1.8	1.7
θ range, deg	2–49	2–49	2–49	2–56	2–58	2–55	2–55	2–50	2–48	2–49
no. of unique reflections										
measd	2849	2679	2867	3812	4776	4400	4599	8875	5075	9103
obsd	2638	2369	2027	2935	3828	3522	3756	7036	3528	5188
no. of variables	344	344	416	386	462	491	489	1046	596	1058
R, %	5.2	8.0	10.0	10.1	8.5	11.4	8.7	13.1[d]	9.8	14.1
R_w, %	6.0	9.5	8.7	11.0	10.0	11.9	9.3	13.2	10.7	13.6
weighting factor p	0.0013	0.0013	0.0002	0.0005	0.00178	0.00040	0.0010	0.00050	0.0020	0.00050
extinction g	0.0058 (9)	0.009 (2)	0.0034 (4)	0.0001 (2)	0.006 (1)	0.012 (2)	0.0009 (1)	0.0025 (4)	0.0011 (5)	0.0011 (2)

[a] In addition to the two partial-occupancy ordered MeCN molecules, there is a third unidentified solvent fragment allowed for as two partial-weight carbon atoms. [b] Body-centered cell chosen because the C-face-centered cell had β = 137°. [c] Two crystallographic-independent centrosymmetric half-molecular units. [d] Because of computational limitations (there were significantly in excess of 200 atoms in the asymmetric unit) the refinement does not include the contribution of the hydrogen atoms. [e] A = [BPP34C10]; B = [BPP34C10·PQT][PF_6]$_2$; C = [BBIPYBIXYCY][PF_6]$_4$; D = [1/4DMB·BBIPYBIXYCY][PF_6]$_4$; E = [BHEEB·BBIPYBIXYCY][PF_6]$_4$; F = [BHEEEB·BBIPYBIXYCY][PF_6]$_4$; G = [BHEEEEB·BBIPYBIXYCY][PF_6]$_4$; H = {[2]·[BSEEB]·[BBIPYBIXYCY]rotaxane}[PF_6]$_4$; I = {[2]·[BSEEEB]·[BBIPYBIXYCY]rotaxane}[PF_6]$_4$; J = {[2]·[BPP34C10]·[BBIPYBIXYCY]catenane}[PF_6]$_4$.

reflections, and for Lorentz and polarization factors but not for absorption.

The structures were solved by direct methods and refined by full-matrix least-squares. Reflections with $|F_o| > 3\sigma(|F_o|)$ were considered to be observed and were included in the refinements (based on F_o). A weighting function of the form $w^{-1} = \sigma^2(F) + pF^2$ was applied. Where possible, hydroxyl hydrogen atoms were located from ΔF maps and refined isotropically. Leading hydrogen atoms on methyl groups attached to sp^2 carbon atoms were located from ΔF maps where possible. All methyl groups were refined as idealized rigid bodies. Depending on data quality and the data:parameter ratio, hydrogens were either included in the refinement or placed in calculated positions (C-H distance 0.96 Å) and allowed to ride on their parent C atoms ($U(H) = 1.2U_{eq}(C)$).

Parameters refined were the overall scale factor, isotropic extinction parameter g (correction of F_c where $F^* = F_c[1.0 + 0.002gF^2/\sin(2\theta)]^{0.25}$), positional and anisotropic thermal parameters for non-H atoms, and positional and isotropic thermal parameters for hydroxyl hydrogen atoms where located. Refinements converged with shift:error ratios less than unity for all variables, except occasionally for disordered atoms. Final difference Fourier maps showed no significant features. All calculations were carried out using the SHELXTL program system.[78]

Acknowledgment. This research was supported by the Agricultural and Food, and Science and Engineering Research Councils, The Royal Society, ICI Agrochemicals, Shell Research, and the University of Sheffield in the United Kingdom, by the National Economic Development Organization in Japan, and by Consiglio Nazionale delle Richerche in Italy.

Supplementary Material Available: Tables listing atomic coordinates, temperature factors, bond lengths and angles, and torsion angles (64 pages). Ordering information is given on any current masthead page.

(78) Sheldrick, G. M. SHELXTL, *An Integrated System for Solving, Refining and Displaying Crystal Structures from Diffraction Data*; Revision 5.2, University of Göttingen, Germany, 1985.

X-ray Structural Analysis and Thermal Decomposition of 1-Aza-2-silacyclobutanes: A New Route to Silanimine Species

Kohei Tamao,* Yoshiki Nakagawa, and Yoshihiko Ito*

Contribution from the Department of Synthetic Chemistry, Faculty of Engineering, Kyoto University, Kyoto 606, Japan. *Received March 11, 1991. Revised Manuscript Received July 29, 1991*

Abstract: X-ray structural analysis of a 1-aza-2-silacyclobutane derivative, *trans*-1-(*tert*-butyldimethylsilyl)-2,2,4-triphenyl-3-isopropyl-1-aza-2-silacyclobutane (**1**), has been carried out for the first time. The 1-aza-2-silacyclobutane skeleton is of small angle strain, being nonplanar in relation to the nearly planar nitrogen atom, and has normal bond lengths, aside from the considerably long C-N bond. 1-Aza-2-silacyclobutanes undergo thermal decomposition around 200 °C in toluene to form a silanimine species, $R_2Si{=}NR$, and an olefin. The formation of silanimine has been confirmed by quantitative formation of the dimer and a 1:1 adduct with Me_3SiOEt in the copyrolysis. The 3,4-trans and -cis isomers form trans and cis olefins, respectively. The decomposition rates obey the first-order rate law and decrease in the order 3,4-trans > 3,4-cis > 3,3,4-trisubstituted derivatives. The results are analyzed by the concerted $[2_s + 2_a]$ cycloreversion mechanisms.

Of the numerous silicon-containing double bond species, silanimines, $R_2Si{=}NR$, have not been extensively studied. Five synthetic routes have been developed so far.[1] We now report a new route to silanimines, i.e., the thermal decomposition of 1-aza-2-silacyclobutanes. In principle, there are two routes, A and B, for [2 + 2] cycloreversion of the 1-aza-2-silacyclobutane skeleton, as shown in Scheme I. While route A has been postulated by Sommer involving the copyrolysis of a silacyclobutane and an imine to form a silanimine intermediate and an olefin,[2] route B has recently been developed by Wiberg to generate a silene and an imine from a 3,3-bis(trimethylsilyl)-1-aza-2-silacyclobutane derivative.[1b,3] Formation of 1-aza-2-silacyclobutane from a stable silanimine and an olefin by [2 + 2] cycloaddition, the reverse reaction of route A, has also been observed by Wiberg.[4] Our present observations clearly demonstrate that route A is the principal decomposition mode of 1-aza-2-silacyclobutanes containing less-crowded substituents, affording the first experimental evidence for Sommer's proposal.

Scheme I

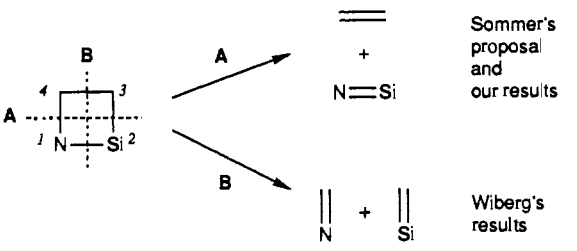

Results and Discussion

X-ray Structural Analysis. All 1-aza-2-silacyclobutanes were prepared by the intramolecular hydrosilation of allylamines, which we recently developed.[5] In order to obtain structural aspects of the four-membered-ring skeleton, we carried out the X-ray structural analysis of *trans*-1-(*tert*-butyldimethylsilyl)-2,2,4-triphenyl-3-isopropyl-1-aza-2-silacyclobutane (**1**). To our knowl-

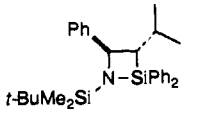

(**1**)

(1) (a) Raabe, G.; Michl, J. In *The Chemistry of Organic Silicon Compounds*; Patai, S., Rappoport, Z., Eds.; John Wiley: Chichester, England, 1989; Chapter 17. (b) Wiberg, N. *J. Organomet. Chem.* **1984**, *273*, 141.

(2) Golino, C. M.; Bush, R. D.; Sommer, L. H. *J. Am. Chem. Soc.* **1974**, *96*, 614.

(3) (a) Wiberg, N.; Preiner, G.; Schieda, O. *Chem. Ber.* **1981**, *114*, 3518. (b) Wiberg, N.; Preiner, G.; Schurz, K. *Chem. Ber.* **1988**, *121*, 1407 and their works cited therein.

(4) Wiberg, N.; Schurz, K.; Fischer, G. *Angew. Chem., Int. Ed. Engl.* **1985**, *24*, 1053.

(5) Tamao, K.; Nakagawa, Y.; Ito, Y. *J. Org. Chem.* **1990**, *55*, 3438.

0002-7863/92/1514-218$03.00/0